The Pennsylvania State University

The Graduate School

A NEW PERSPECTIVE OF UNDERSTANDING COMPACTION OF PARTICULATE ASPHALT MIXTURES: MECHANISM AND AUTOMATED ASSESSMENT

A Dissertation in

Civil Engineering

by

Shuai Yu

Submitted in Partial Fulfillment
of the Requirements
for the Degree of

Doctor of Philosophy

May 2024

The dissertation of Shuai Yu was reviewed and approved by the following:

Shihui Shen
Professor
Dissertation Advisor
Chair of Committee

Tong Qiu
Professor
in the Department of Civil and Environmental Engineering

Mansour Solaimanian
Research Professor
in the Department of Civil and Environmental Engineering

Tieyuan Zhu
Associate Professor
in the Department of Geosciences

Farshad Rajabipour
Professor
Interim Department Head of Civil and Environmental Engineering

ABSTRACT

Effective compaction is crucial for the performance and durability of asphalt pavement. Traditional field compaction, relying heavily on engineers' experience and test strips, sometimes could be problematic to achieve a unified pavement with a desirable density, especially with new materials. To address these challenges, Intelligent Compaction (IC) has been developed to equip the vibratory rollers with GPS, accelerometers, onboard computers, and infrared thermometers to facilitate the quality control of pavement compaction. This technology allows for real-time monitoring and visualization of pavement responses and temperatures, significantly improving compaction uniformity. However, accurately predicting pavement density remains challenging due to the multilayered pavement structure and the complex interactions between the roller drum and the viscoelastic asphalt mixture.

To understand the compaction mechanism and improve the compaction quality of the asphalt pavement, a Microelectromechanical System (MEMS) sensor, SmartKli® was employed to study the asphalt mixture compaction at the mesoscale. It was found that the compaction characteristics at the macroscale are closely related to the behavior of coarse aggregates at the mesoscale level. The particle rotation plays a critical role in the densification of the asphalt specimens. Utilizing the Discrete Element Model (DEM), the impact of mix design and particle property on kinematic behaviors was examined. The mixture gradation and particle size also greatly affect the aggregates' behavior during compaction.

Based on the developed compaction mechanism, a new method for evaluating asphalt mixture workability was proposed, incorporating workability parameters, compaction curves, and statistical analysis of compaction data. By verifying with different asphalt types including Hot Mix Asphalt (HMA), Warm Mix Asphalt (WMA), and Recycled Plastic Modified Asphalt (RPMA), this method could effectively assess the influence of various factors like asphalt content,

compaction temperature, and additives on mixture workability, aiding in optimizing mix design and construction conditions. Moreover, an innovative compaction monitoring system was developed to accurately predict the compaction conditions of the asphalt pavement. This system uses a wireless particle size sensor for data acquisition and a machine learning model for density prediction. Linking laboratory gyratory and field roller compaction data through particle kinematic behaviors, the system achieved high precision in density prediction with a prediction error of less than 0.7%. The results demonstrate that integrating AI and sensing data is effective for predicting asphalt mixture compaction. This system could significantly enhance the compaction quality of asphalt pavement and contribute to the comprehensive quality control and assurance of pavement construction.

Keywords: asphalt mixture, MEMS sensor, particle rotation, compaction mechanism, artificial intelligence, sensing technology, density prediction.

TABLE OF CONTENTS

LIST OF FIGURES

LIST OF TABLES

ACKNOWLEDGEMENTS

As I near the conclusion of my Ph.D. journey, I reflect on the years of research and personal life. There are countless individuals to whom I owe a debt of gratitude. The support from professors and friends has made my Ph.D. experience immensely rich and meaningful.

Foremost, I extend my sincere gratitude to my advisor, Dr. Shihui Shen. She is the person who led me to the world of research in civil engineering and has been training me to be a confident and professional researcher. She is a knowledgeable, caring, and thoughtful professor, who provides invaluable advice for my career and personal life. I truly appreciate it! Moreover, I want to thank the professors: Dr. Tong Qiu, Dr. Mansour Solaimanian, Dr. Tieyuan Zhu, and Dr. Hai Huang for their support in my Ph.D. journey. I am grateful for them serving as a member of my Ph.D. committee and providing valuable advice to my research. Their support was critical in facilitating the smooth progression of my research.

My Ph.D. research was funded by the Center for Integrated Asset Management for Multi-modal Transportation Infrastructure Systems (CIAMTIS) University Transportation Center (UTC) and Ingevity company. Their support is greatly acknowledged. My thanks also extend to Railroad Technology & Services, LLC, New Enterprise Stone & Lime Co. Inc., HRI, Inc., and Brooks Construction Company, Inc. for providing the technical, material, and field support. Special acknowledgments go to Mr. Richard Steger, Mr. Mark Moyer, and Mr. Jeff Austin. Their assistant made my project complete more smoothly. In addition, any opinions, findings, conclusions, or recommendations expressed in this publication are those of the authors and do not necessarily reflect the views of the funding agencies.

The research in my Ph.D. was challenging and collaborative. During this period, my peers, Cheng Zhang, Xue Wang (both), Jubair Ahmad Musazay, Yuliang Zhou, Kun Zeng, Pengsen Hu, and friends from Penn State and other institutes, provided immense support in both research and

personal aspects. Their help was crucial and greatly contributed to the success of my research. The shared leisure activities also brought great joy and added meaning to my life.

Finally, I would like to express my deepest love and gratitude to my parents. During my nearly five years in the United States, I have only been able to get home once, staying for just a few weeks, and I feel profoundly guilty for that. Despite the physical distance, they never stop loving me with all their heart. The unwavering support and boundless love from my parents have been the bedrock and the most powerful force in my life. This Ph.D. is as much your achievement as it is mine!

Chapter 1

Introduction

Background and Motivation

Compaction is a critical construction step that directly impacts the performance and service life of asphalt pavement. The reduced volume of the asphalt mixture during compaction leads to aggregate interlocking, and material densification and eventually achieves a stable structure to sustain the external traffic (U.S. DOT, 2000). Although the performance is greatly dependent on the mix design, the compaction quality has a direct impact on the volumetric and mechanical properties of the paving materials (Al-Shamsi and Mohammad, 2007) (Chen et al., 2013). Compaction issues, such as under-compaction, over-compaction, or lack of uniformity would weaken the performance and reduce the service life of the asphalt pavement. According to the study by Linden et al. (Linden et al., 1999), for asphalt pavement with a 7% base air voids, a 1% increase in air voids can lead to about a 10% loss in pavement life. 3% or less air void would not provide enough room for thermal expansion and the mixture would become plastic and unstable. Therefore, a desirable level of compaction is the foundation of the durability and long-term performance of the asphalt pavement.

The satisfactory pavement density is realized by a combined application of roller compactors, such as static rollers, vibratory rollers, etc. (Wang et al., 2018). Currently, the most prevailing compaction method is based on the engineers' experiences with the aid of the density measurement devices at the selected spots. These measurements include nuclear or non-nuclear density gauges or taking pavement cores for laboratory density verification. Some construction agencies are using intelligent devices and methods to compact asphalt pavement, such as the continuous compaction

control (CCC) method or the Intelligent Compaction (IC) technology. These technologies equip the GPS, accelerometers, onboard computer reporting systems, and infrared thermometers on the vibratory rollers for real-time data collection and compaction monitoring (U.S. DOT, 2013). This information, like the precise construction location, compaction passes, surface temperature, and the Intelligent Compaction Measurement Value (ICMV) can evaluate the compaction condition and uniformity of the asphalt pavement. Engineers can make appropriate and in-time strategies accordingly to improve the compaction quality of the asphalt pavement.

However, limitations still exist for both conventional and intelligent compaction methods. For the conventional compaction method, the compaction quality is greatly dependent on the engineers' judgments and experiences, which are subjective and with high variance. The process of collecting pavement cores can destroy the asphalt pavement, introducing potential concerns for future distress. The measurement at limited spots lacks representation of the compaction conditions for the whole pavement section. Moreover, the density measurement gauges are the post-compaction method, which cannot provide in-time feedback for compaction improvement. These measurement devices, such as the nuclear density gauge, need to be calibrated beforehand to establish the correlations between the pavement density and the compaction patterns (passes, speed, vibration amplitude, mode, etc.). The correlation is hardly adjusted once the compaction pattern is determined, the compaction quality of the entire pavement construction thus cannot be guaranteed. For intelligent compaction, the compaction uniformity can be greatly improved with the assistance of GPS and various sensors. However, a critical concern for IC technology lies in the monitoring of the compaction degree of the asphalt pavement. Multiple researchers tried to establish the correlation between the pavement density and the ICMV collected by the IC equipment. This correlation can be verified in laboratory configuration but is hard to obtain a consistent relationship in the field compaction when the multilayered pavement structure and environmental effects are considered (Chen and McDowell, 2014) (Chang et al., 2014). In field compaction, the responses collected by

the IC system are from the entire pavement structure, so it is difficult to correlate the IC responses with the density of the sole asphalt layer (Chang et al., 2014). Moreover, the coupling effects between the viscoelastic materials and the vibratory drum, especially at high temperatures, make the prediction of the compaction degree more complicated. All of these resulted in inconsistent correlations between the ICMV and the pavement density (Chang et al., 2014; Hu et al., 2017; Nieves, 2014).

Despite extensive efforts in pavement construction, the compaction mechanism of the asphalt material is still unclear, preventing the development of compaction techniques and automation in pavement construction. Meanwhile, the industry is seeking methodologies to assess the properties quantitatively and efficiently of the asphalt pavement during compaction, so that the in-situ compaction quality can be monitored in real-time. These knowledge gaps in both theoretical and practical aspects have thus motivated this research.

Objectives

The objective of this research is to propose a comprehensive understanding of the compaction mechanisms of asphalt mixture from mesoscale and create an innovative system to predict the compaction degree qualitatively and quantitively to prompt automation in pavement construction. To achieve this goal, two specific objectives are developed as follows:

Specific objective 1: Compaction mechanism of the asphalt mixture from mesoscale.

The mechanisms of compaction will consist of both theoretical and practical meanings. Theoretically, this study will discover the relationships between the mesoscale characteristics (i.e., particle kinematic behavior) and the mixture's bulk properties (i.e., volumetric properties) during the process of compaction. Such dynamic relationships will be evaluated at different compaction

stages, temperature and mixture types, etc. Different sizes of the aggregate will be investigated so that a comprehensive understanding of the compaction mechanism for the particulate asphalt mixture can be captured. Practically, this study will explain the influence of different compaction modes (laboratory and field) on the particle mesoscale characteristics during compaction, and discuss their impact on the density, internal structure, and mechanical properties of asphalt mixture. With a clear understanding of the compaction mechanisms from both theoretical and practical perspectives, it is possible to reasonably adjust the compaction strategies and realize automatic compaction and assessment to achieve high-quality compaction.

Specific Objective 2: Develop an intelligent system to predict the compaction qualitatively and quantitively.

With the understanding of the compaction mechanism of asphalt materials, the second objective of the study is to develop an intelligent compaction monitoring system utilizing sensing technology and Artificial Intelligence (AI). The model can collect real-time compaction data and qualify or quantify the pavement compaction condition based on significant variables, such as the internal particle mesoscale characteristics, compaction energy, material design, and environmental information. This system can improve the compaction quality by accurately predicting the real-time compaction degree of the asphalt pavement. Such a system can be integrated with Intelligent Compaction (IC) technology so that full-coverage data collection, compaction uniformity monitoring, and compaction degree prediction can be achieved, which is a significant step toward automation in pavement construction.

Thesis Layout

The layout of this thesis will be elaborated as follows:

Chapter 1 is the introduction to this dissertation. The background, motivation, objective, and contribution of the research will be introduced in this chapter.

Chapter 2 will summarize the state-of-the-art asphalt pavement compaction, including the current understanding of the compaction mechanism and the compaction techniques.

Chapter 3 will introduce the methodology and the scope of this research.

Chapter 4 will provide the basic information about the materials, the devices, and the experiments used in this study.

Chapter 5 will investigate the compaction mechanism of the viscoelastic asphalt mixture. The compaction mechanism will be unfolded from (1) the compaction experiments (at both the laboratory and field) with the assistance of the sensor; and (2) the compaction simulation using the Discrete Element Method (DEM). Various effects on the compaction will be evaluated, including the gradation, particle size, and angularity. Eventually, a comprehensive mesoscale explanation of the compaction mechanism for the particulate asphalt mixture will be given, and this concept will serve as the foundation for the following compactability evaluation and compaction prediction.

Chapter 6 will evaluate the compactability (workability) of various asphalt mixtures based on the compaction mechanism. A new test method for determining the workability of asphalt mixture will be proposed based on particle kinematic behaviors during compaction. Utilizing this test method, different compaction scenarios and various effects on the workability of the asphalt mixture will be evaluated, including asphalt content, compaction temperature, WMA additives, plastic content, and different plastic processing methods.

Chapter 7 will focus on compaction prediction. An innovative system will be established in this chapter, containing the remote data collection, and a compaction predictive model based on

the machine learning algorithm. The two predive models, compaction condition prediction, and pavement density prediction, will both be built and verified using the laboratory and field compaction project.

Chapter 8 will summarize the main findings and conclusions of this research and provide several perspectives to continue this research in the future.

Chapter 2

Literature Review

Compaction Mechanism

Compaction is an important step during the construction of the asphalt pavement, which can significantly affect its performance and service life. Adequate compaction increases the strength, stability, and fatigue life of the asphalt mixture, decreasing its permanent deformation, moisture damage, and low-temperature cracking (U.S. DOT, 2000). On the contrary, an asphalt mixture with the desirable mix design could perform poorly if the proper level of compaction is not achieved. During compaction, the aggregate particles transit from the initial static state to the dynamic state under compaction loadings. In this process, the shearing stress plays a critical factor in material densification (Zheng et al., 2007). The asphalt particles would only move and rearrange if the shear stress generated in the mixture is greater than its tolerant shear strength, as explained by the Mohr-Coulomb theory as follows. In the equation, c is the cohesion, σ is the normal stress and φ is the internal friction angle.

$$\tau > \tau_f = c + \sigma * tan\varphi \qquad (2\text{-}1)$$

Therefore, applying adequate shearing stress is essential for achieving the target density of the asphalt pavement. Meanwhile, the hot asphalt binder reduces the friction between particles, allowing the shearing stress to rearrange particles more effectively. Since the viscosity of the asphalt binder is temperature-dependent, maintaining a relatively high temperature is also crucial during the compaction of the asphalt pavement.

Based on this theory, two possible approaches can be performed to improve the compaction effectiveness: increasing the shearing stress or reducing the tolerant strength. To achieve this, different roller compactors with varying loadings, stress types, force direction, and speed were utilized, including static roller, vibratory roller, oscillatory roller, and pneumatic tire roller, as shown in Figure 2-1. The static rollers normally weigh between 3 to 14 tons and use their weight/gravity to increase the shear stress between the particles to overcome cohesion and friction. It was usually used at the beginning and last stage of the compaction. Pneumatic tire rollers are operated in the middle stage of the compaction. Compared with the static roller, pneumatic rollers can produce a kneading effect on the asphalt mixture, so that the particles can horizontally move and rotate to reach a stable structure (Wang et al., 2021). The vibratory roller is the most common roller compactor in field compaction. It can apply two types of compaction effort to pave materials: static weight caused by the drums and the frame, and the dynamic force produced by a rotating eccentric weight located inside the drum. Unlike traditional vibratory rollers that use vertical vibrations, oscillatory rollers involve the drum moving back and forth in the direction the roller is moving. This horizontal vibration could create the shearing or kneading effect on the material being compacted (Pistrol and Adam, 2018). During compaction, the vibration imparted by the roller compactor reduces the internal friction between the particles and thus decreases the tolerant shear strength. The drum weight, on the other side, raises the particle shear stress. The combined effects made the mixture more prone to move and rotate and formed a stable and interlocked structure.

Figure 2-1 Static roller (left), pneumatic tire roller (middle), and vibratory roller (right)

Under different amounts of compaction weights and vibratory frequency, asphalt materials would experience several stages to attain a durable structure and smooth surface: breakdown stage, intermediate compaction stage, and finish stage (Linden et al., 1989). Breakdown compaction is the first stage immediately after the asphalt mixture is laid. Static rollers and heavy vibratory rollers are typically used in this stage. The dynamic load generated by the vibratory roller and the static roller weight can help to rearrange the aggregate particles and reduce air voids. The highly flowable asphalt binder facilitates the aggregates to move and settle into a dense structure. Following the breakdown compaction, the intermediate stage further compresses the asphalt to a smoother surface. This stage aims to reach the desired density and remove small remaining irregularities. Vibratory rollers and sometimes pneumatic tire rollers are used in this stage. The high-frequency vibration by the vibratory roller and the kneading effect generated by the pneumatic tire roller can help to further compact the asphalt pavement. The particles continue to rearrange, but the focus shifts towards eliminating smaller air voids and enhancing the bond between the aggregates and the binder. The finish compaction stage is to achieve the required surface smoothness and final density. Non-vibratory rollers are used to avoid disturbing the already compacted layers. Particle movement is minimal at this stage to ensure a uniform surface layer (Jiang et al., 2019). The lower temperature would also reduce the material's plasticity thereby stabilizing the overall structure.

The laboratory compaction experiences a similar process of material densification and particles interlocking but with different compactors. The laboratory compaction holds equivalent importance since the mix design and properties verification are all performed in the lab. Current laboratory compaction methods mainly encompass impact compaction, kneading compaction, gyratory compaction, and rolling wheel compaction (Roberts et al., 2002). The development of each compaction method is usually along with the revolution of the asphalt mix design. Among

these methods, Marshall compaction and Superpave Gyratory Compaction (SGC) are the most prevalently utilized methods.

The Marshall method was introduced by Bruce G. Marshall and further developed by U.S. Air Force engineers. It provides a pivotal laboratory compaction technique for determining optimal asphalt content (Harold et al., 1988). Utilizing a compaction hammer, the Marshall method applies vertical impacts to interlock aggregates and densify mixtures. However, the premature damage and accelerated rutting that occurred on these pavements revealed limitations of the Marshall design method, especially under heavy traffic. This led engineers to question the field relevance of Marshall hammer compaction compared to roller compaction. To address these concerns, the U.S. initiated the Strategic Highway Research Program (SHRP), aiming to advance asphalt mix design and compaction methods (Roberts et al., 2002). The Superpave design method emerged from this program, including asphalt binder specifications, aggregate procedures, and a comprehensive asphalt mixture design. The Superpave system pivots on the Superpave gyratory compactor, an evolution of the Texas gyratory compactor. The gyratory compactor applies both vertical pressure and horizontal shear force to specimens, effectively simulating the kneading effect during compaction. Superpave gyratory compaction offers several advantages compared with Marshall impact method, including the integration of traffic considerations into mix design, and the ability to monitor height and mechanical properties during compaction. These features have led to its widespread adoption in the U.S. and globally.

Laboratory compaction and field measurements can assess the particle arrangement, compaction condition, and properties of the asphalt mixture. Obtaining this information is vital to understanding the compaction mechanism of the asphalt mixture and ensuring the pavement meets the required performance and durability. To investigate the material's properties of the field cores and laboratory specimens, the National Cooperative Highway Research Program (NCHRP) (Harold et al., 1988) conducted the project "Asphalt-Aggregate Mixture Analysis System" to

evaluate different laboratory compaction procedures, including the Marshall hammer, the California kneading compactor, the Texas gyratory compactor, the Arizona vibratory/kneading compactor, and the Mobil wheel simulator. By comparing the field cores and laboratory specimens on the indirect tensile test, uniaxial compression test, etc., the gyratory shear compactor was found to more consistently match the engineering properties of the field cores. The ranking of the compaction devices that simulate the engineering properties of field cores more consistently is the gyratory shear compactor, California kneading compactor and mobile wheel simulator, Arizona vibratory or kneading compactor, and Marshall hammer. Button al. et (Button and Little, 1994) conducted a similar work by comparing the mechanical and volumetric properties of the field cores with four laboratory compaction samples. Analyses indicated that the gyratory method most often produced specimens like pavement cores (73%). The Marshall compactor had the least probability of producing specimens like pavement cores (50%). The gyratory compactor can more closely simulate the roller compaction process according to the volumetric and mechanical properties. The gyratory compactor can also provide more reproducible and consistent results compared to other lab compaction methods (Harold et al., 1988).

The advancement of digital image technology, such as X-ray, Computed Tomography (CT), and digital cameras made it possible to explore the internal structure of asphalt mixtures. Numerical research confirmed the feasibility of using digital image technology to evaluate the gradation, shape, and orientation of coarse aggregates in mixtures. Masad et al. (1999) pointed out that the porosity distribution of the asphalt mixture greatly impacts its performance. They established a method to quantitatively evaluate the internal structural characteristics of asphalt mixtures, including porosity distribution, aggregate orientation, and aggregate contact. Their team (Eyad et al., 1999) further studied the characteristics of the SGC compaction and found that the internal porosity distribution of SGC specimens is uneven, with a higher degree of compaction in the middle than at the top and bottom. Their research also compared the porosity distribution between the field cores and SGC

specimens. The result indicated that the porosity of SGC specimens is closest to that of field cores at the 20th gyration, but the aggregate orientation of laboratory specimens is closest to the 100th gyration. Additionally, researchers have studied the impact of gyratory compactor parameters on the internal structure of the asphalt mixture. Tashman et al. (2002, 2001) and Peterson et al. (2004) found that the gyratory compaction could better simulate the field roller compaction by adjusting its compaction parameters, such as the tilting angle and specimen height. The mechanical properties and aggregate orientation are closest to the field cores when using a 1.50° gyratory angle for the specimen with a height between 50mm and 75mm. Partl et al. (2003, 2007) studied the internal uniformity of three lab-compacted mixtures using CT technology, including Marshall compaction, Superpave gyratory compaction, and wheel rolling compaction. The findings confirmed the porosity distribution of the gyratory compacted specimens with a higher compaction level in the middle than at the top and bottom. The porosity of the Marshall specimens shows differences between the center and edges, while the wheel-compacted specimens have the most uniform porosity distribution.

Recently, researchers have realized the importance of the particle kinematic behaviors on the compaction of the asphalt mixture. The mineral aggregates consist of about 95% weight of the asphalt mixture, and most external loads are borne and transmitted by the skeleton of the mineral aggregates (Zhu and Nodes, 2000). The behavior of the particulate aggregates should be related to the densification of the mixtures. With the development of microelectromechanical sensing (MEMS) devices, the particles' behaviors can be monitored during the entire process of compaction. With the aid of the wireless particle size sensor, SmartRock, Wang, et al. (2018) pioneered studying the rotation characteristics of the particulate asphalt mixture during the SGC compaction. A curve of particle rotation was recorded during the SGC compaction. Based on the particle behaviors, the SGC compaction can be divided into three stages: initial compaction stage, transition stage, and plateau stage. Wang et al. (2019) further compared the particle movement characteristics between

the laboratory compaction and various roller compactors. Three laboratory compactions, including Superpave gyratory compaction, Marshall compaction, and rolling wheel compaction, and three roller compactions, involving static roller, vibratory roller, and pneumatic tire roller were studied in their research. The differences in the particle kinematic behaviors were identified, and none of the laboratory compaction methods can consistently simulate the field compaction. However, a certain identical particle movement was discovered. The Superpave gyration compaction and the rolling wheel compaction can simulate the kneading effect as the field pneumatic-tire roller. The Marshall hammer compaction can generate vibrating effects on the asphalt material as the vibratory roller did. In addition, the particle's mechanical responses during compaction were also evaluated, and certain relationships were identified. Polaczyk et.al (2018) correlated the particle acceleration of the Marshall hammer compaction with the compaction condition of the aggregates. The intensity and duration of the particle's acceleration respond differently at different compaction stages, which can evaluate the locking condition of the aggregate particles. Jia et al. (2019) confirmed similar conclusions by investigating the compactability of aggregates through the Superpave Gyratory Compactor, the Marshall impacting hammer, and a vibratory compacting machine. A consistent relationship was identified between the material stiffness and the dynamic vibration responses, which can characterize the compaction of different paving materials. Cheng et al. (2022) and Zhang et al. (2022) studied the contract stress of the asphalt particles during compaction. The contact stress was found to be correlated with skeleton formation and mixture densification, which can be used to determine the mixture's locking point. All these studies validate the feasibility of using particle behaviors, including kinematic or mechanical characteristics, to evaluate the compactability of the asphalt mixture.

The compaction of the asphalt mixture is a complicated process, which is dominated by the relationship between the particle stress and their tolerant strength. Different compaction devices varying in loading weight, stress types, and vibration frequency, have been performed to interlock

the aggregate particles, densify the materials, and eventually attain a desirable compaction condition. To figure out the compaction mechanism of the asphalt mixture, the volumetrics, mechanical properties, porosity distribution, and particle compaction behaviors have been investigated by utilizing experimental tests, digital image technology, MEMS sensors, etc. The correlation between the lab-compacted specimen and field cores has also been investigated. All projects provided valuable findings to help us understand the compaction of asphalt mixtures. However, the mechanism of the asphalt mixture compaction is still elusive, including: How did the mechanical or kinematic properties change during compaction? What properties can indicate the material density during compaction? What is the relationship between the different methods of compaction? Are there any parameters that can link the lab and field compaction methods? Answering these questions can help us comprehensively understand the compaction mechanism of the asphalt mixture and improve the laboratory compaction to better simulate the field compaction. A clear compaction concept can also improve the control assurance (QA) and quality control (QC) of the asphalt pavement compaction, and further facilitate the automation in pavement construction.

Compaction Simulation

Experimental testing and numerical simulation are the two predominant approaches to examining the mechanical and volumetric properties of asphalt mixtures. Experiments are straightforward, but they often entail significant costs and labor, particularly when adapting to various scenarios. It is also challenging for operators to access the mesoscale or microscale properties of the material. In contrast, numerical simulations offer a practical alternative, which can overcome some limitations inherent in experimental tests. These benefits are: (1) It is cost-effective and versatile as most test scenarios can be simulated repeatably. (2) Numerical simulations can perform extreme situations that are difficult to achieve in experiments. (3) Numerical simulation

can analyze the mesoscale and micro properties (e.g., stress, strain, rotation, translation) at selected points or areas (Ding et al., 2019). However, several aspects still need to be paid attention to ensure the accuracy of the simulation, including (1) appropriate simplifications and assumptions are needed to capture the materials' properties at certain conditions. (2) validation and calibration are required to obtain a reasonable simulation. (3) maintain a trade-off between the simulation accuracy and the computational efficiency (Yao et al., 2022).

Focusing on the methodologies, the Finite Element Method (FEM) and Discrete Element Method (DEM) are primarily utilized in numerical simulations. FEM is a computational technique, providing approximate solutions to boundary value problems in engineering. By dividing a continuum into a finite set of elements, FEM estimates the characteristics of the entire domain based on the properties of these individual elements. This method excels in addressing continuum problems but is less effective for large, discontinuous deformations (Sawan, 2018). On the other hand, DEM is commonly employed in engineering fields to analyze the interactions between individual particles. This method is more appropriate for simulating the behavior of granular materials, like sand, gravel, and powders (Yao et al., 2022). Therefore, most researchers tend to use the DEM to simulate the stress-strain relationships, damage situations, fracture processing, and the compaction process of the asphalt mixtures from the macro, mesoscale, and micro perspectives (Collop et al., 2004, Dai and You, 2007, You and Liu, 2010, Wang et al., 2023).

The Discrete Element Method (DEM) was first introduced by Professor Cundall in 1971 to analyze granular materials in geotechnical engineering (Cundall, 1971). 2D models were initially favored due to their rapid computational speed and satisfactory simulation quality. DEM has since been extensively applied in various research areas, including the prediction of dynamic modulus, creep properties, and fracture behavior in materials. Buttlar and You (2001) applied the DEM method to predict creep strains of a 2D asphalt specimen in the Superpave indirect tension test. Their research highlighted the potential of micromechanical modeling to significantly reduce the

costs of the experimental tests on the material characterization. Collop et al. (2004, 2006) used DEM to simulate the behavior of the asphalt mixture under the creep test under compression conditions. Their findings indicated a reasonable correlation between the DEM predictions and experimental data, underscoring its suitability for asphalt mixture analysis. You and Buttlar (2005) utilized a 2D clustered discrete element modeling to simulate the hollow cylinder tensile test. The simulation results aligned well with experimental data across different test temperatures and loading frequencies, further validating the effectiveness of DEM. Dai and You (2007) developed 2D discrete element models to predict the viscoelastic creep stiffness of asphalt mixtures. Their simulation successfully achieved reasonable creep stiffness across various loading times. Kim (2008) utilized the DEM to investigate fracture mechanisms in asphalt concrete at low temperatures. The DEM simulation provided more details of the fracture process and the particle movement under the dynamic loads. Liu et al. (2009) investigated the viscoelastic properties of asphalt mixtures with the burger model by establishing a 2D model. Their DEM simulations successfully predicted the dynamic modulus and phase angle of the asphalt mixtures under sinusoidal loading.

Compared with the 2D model, 3D simulation can provide a more accurate representation of the physical particulate systems, the simulation is thereby more reliable and consistent with the real condition. Initially, the 3D model uses the spherical element to model the aggregates for its high efficiency. You et al. (2010) conducted the 3D DEM to predict the dynamic modulus and phase angle of asphalt mixtures, they found that the relative errors between the laboratory and simulation results were within an acceptable range. You et al. (2011) further established a 3D DEM model to simulate the creep test of the asphalt mixture, the prediction of the DEM model is similar but lower value compared with the experiment results. Liu et al. (2012) compared the experiment results and DEM simulation and discovered that the element size affected the predicted mechanical performance of the asphalt mixture. Adhikari and You (2011) established 3D models of hollow cylindrical asphalt concrete specimens and found that the 3D models yielded a better dynamic

modulus prediction than 2D models. Although extensive DEM simulations have been performed on the asphalt mixture, most of them were to investigate the mechanical behavior. Little research focused on the compaction behavior of hot loose mixtures. Chen et al. (2013) used the DEM model to simulate the process of the Superpave gyratory compaction and vibratory compaction of asphalt mixture. The impact of Burger's contact model, compactor parameters, and aggregate properties on the porosity of the compacted specimens has been investigated in the DEM simulation. The simulation results of the porosity distribution at different compaction cycles were consistent with the findings using digital image methods, demonstrating the reliability and reasonability of the DEM simulation. Wang et al. (2023) establish a DEM model to simulate the compaction process of the asphalt mixture using the spherical element. The simulation confirmed the effect of the mixture's gradation on the compaction easiness from the mesoscale. The ratio of the fine aggregates greatly affects the compaction behavior of the aggregates. The results also revealed the significance of the particle rotation on the compaction of the asphalt mixture.

The advancement of digital image technology makes it possible to further modify the DEM model by simulating the morphological features (shape, texture, angularity) of the particulate aggregates. Since 95% weight of the asphalt mixtures are aggregates, modeling aggregate morphological features is important in understanding their mechanical behaviors in the asphalt mixture. Yu et. al (2012) modified the aggregates clump approach by introducing an image-aided 3D ball-clumping approach. Reasonable prediction of the dynamic modulus has been achieved in the new 3D DEM model. Gong et al. (2018) analyzed the movement characteristic of different shapes of aggregates during the SGC compaction through DEM simulation, the results revealed that three main stages of particle movement took place in the SGC compaction; The shape of the coarse aggregates have a great influence on the particle movement. Rounded and flat coarse aggregates were more likely to form horizontal displacement but less likely to cause rotation during compaction. Liu et. al (2017) model the angularity of the aggregates through a MATLAB-based

imaging process. The aggregate clump proved to be a more accurate approach for evaluating the particulate asphalt mixture but with reduced compactional efficiency. Song et al. (2021) investigated the skeleton behaviors of the open-graded friction course (OGFC) from the mesoscale by performing the DEM simulation. The penetration load was found to be strongly related to the gradation of the asphalt mixture. The penetration strength was larger for the coarse mixture, affirming the significance of the gradation and skeleton on the performance and strength of the asphalt mixture. With the aid of the 3D blue-ray scanner, Zhu et al. (2022) obtained the morphology of the coarse aggregates and simulated the compaction process of the Marshall impact compaction. The DEM model effectively simulated the process of the Marshall impact compaction of asphalt mixture by calibrating the trend of the air void and specimen height. It was found that the displacement and the unbalanced force of the coarse aggregates played a vital role in the Marshall impact compaction of the asphalt mixture.

The DEM model is capable of simulating the compaction process of the discrete particle under loadings. The motion and stress of the particulate can also be monitored from the micro or mesoscale perspective, which makes it possible to evaluate the relationship between the particle characteristic and the material's properties. The simulation results can help us comprehensively understand the compaction mechanism of the asphalt mixture under various scenarios. The appropriate selection of the particle contacts model and the accurate modeling of the particle’s morphological features using the imaging-aided approach make the DEM simulation more reasonable and reliable for simulating the asphalt mixture compaction and studying its compaction mechanisms. However, the trade-off between simulation accuracy and compactional efficiency is also important to consider.

Intelligent Compaction

The conventional compaction is based on the “point type” and spot tests for the compaction quality assessment. This method, such as the nuclear density gauges, or taking the pavement core for the laboratory measurement is problematic because of its randomness, destructiveness, or regional limitations. The measured density cannot guide the compaction practice in real-time (Xu et al. 2019) (Xu and Chang, 2019). Intelligent Compaction (IC, as shown in Figure 2-2) thereby originates from continuous compaction control. IC technology usually refers to the vibratory rollers equipped with an integrated measurement system that consists of a highly accurate GPS, accelerometers, onboard computer reporting system, and infrared thermometers for compacted material feedback control (Transportation and Administration, 2013). The essential concept of the IC is that the control system persistently gathers information on compaction quality throughout the rolling process.

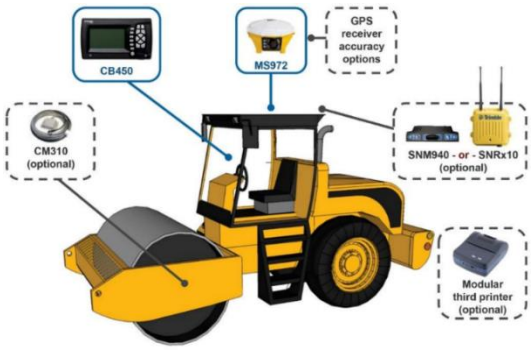

Figure 2-2 Intelligent Compaction Technology

To achieve intelligent compaction, the IC system needs to be advanced in implementing and analyzing the dynamic responses at four fundamental criteria: (1) The roller needs to be outfitted with a "brain," encompassing a control system, a measurement setup, control software, and algorithm software (Ma et al., 2022). (2) The Intelligent Compaction Measurement Values (ICMV)

must be technically accurate and valid, crucially reflecting reliable compaction quality control. (3) The control system should be capable of automatically perceiving, learning, analyzing, making decisions, and issuing feedback control instructions. (4) The roller should have the capability to adjust its parameters, thereby achieving intelligence in both performance and functionality. Conclusively, IC is defined based on the essential characteristics of "perception, analysis, decision-making, execution" (Xu et al., 2022).

Perceiving compaction information is the first step in intelligent compaction. Back in 1974, Dr. Heinz Thurner conducted field soil compaction using a vibratory roller equipped with an accelerometer to collect the soil responses during compaction. A correlation was discovered between the materials' compaction degree with the acceleration of the vibratory roller (Thurner and Sandström, 1980). A compaction documentation system (CDS) was then developed in the 1980s, which can provide a conceptual system to monitor the compaction process (Compaction, 1985). With the invention of the global positioning system (GPS), the technology of automated real-time positioning has improved tremendously. IC technology has been rapidly developing in soil and flexible pavement compaction by perceiving the precise compaction location using GPS. Nowadays, with the aid of various sensors, such as accelerometers, sensors, thermometers, GPS, etc., the response of the pavement, the compaction site, the temperature of the pavement, and the movement of the compaction equipment can be captured during compaction. Due to the mobility of the roller compactor, the current system primarily measured the response signals of the vibrating drum. One of the problems is that the responses are the combined signals from both the paved materials and the support conditions (U.S. DOT, 2013).

The analysis of the perceived responses is to provide the basis for decision-making. It is to establish the correlation between the response signals and the compaction quality to obtain the density or modulus of the compacted materials (Yu et al., 2023). To guarantee the compaction quality of the materials, three aspects are necessary to be assessed: compaction degree, compaction

stability, and compaction uniformity (Xu et al., 2018, Xu et al., 2022). The IC can decide whether to continue rolling, adjust the compaction process, or issue control instructions based on these three matrices. IC technology can greatly enhance the compaction uniformity of the soil or asphalt pavement compaction. By continuously monitoring the full coverage of the pavement, including the surface temperature, and the responses of the roller drum during the compaction, continuous color-coded plots can be displayed on the screen to indicate the compaction status of the paved materials. Therefore, the compaction strategies can be adjusted accordingly to improve the uniformity of the asphalt pavement. For the compaction stability and compaction degree, the system can calculate the intelligent compaction measurement value (ICMV) based on the collected vibration (Ling et al., 2018). Currently, most ICMVs are established based on the similar assumption that the stiffness of the compacted soil increases as the progress of compaction, which will in turn affect the dynamic roller drum behavior. Compaction Meter Value (CMV) is a widely used parameter among various ICMVs (Mokwa and Cuelho, 2008). The relationship between the CMV and materials compactability as an example will be mainly investigated. By calculating the relative ratio of the high-order harmonic components to the fundamental frequency component of the acceleration data, the compaction quality of the material can be characterized. Therefore, a ratio between the amplitude of the fundamental frequency and various frequency components could indicate the properties of paved materials, as presented in equation (2-2).

$$CMV = 300 \times \frac{A_{2\Omega}}{A_{\Omega}} \qquad (2\text{-}2)$$

where A_{Ω} = acceleration amplitude of the fundamental component of the vibration; $A_{2\Omega}$ = acceleration amplitude of the first harmonic component of the vibration.

CMV is an empirical parameter, and it lacks the support of mechanical principles. Researchers found that a good correlation between the CMV and the compaction quality only exists in the specific compaction stage (Yu et al., 2014). In soil compaction, the vibration roller may undergo multiple different operation modes, including continuous contact mode, partial uplift mode, double jump mode, and chaos mode (Fang et al., 2022, Yu et al., 2014, Liu et al., 2015). Different modes indicate different drum motion behaviors and dynamic response characteristics. In continuous contact mode, the drum provides consistent and even compaction. The drum maintains continuous contact with the soil surface during compaction. This mode only occurs when the soil is uncompacted or in soft condition. In the partial uplift mode, the vibratory drum partially loses contact with the soil cyclically, causing a slight lift-off and then re-contact. This mode allows for better compaction than continuous contact, as the impact when the drum recontacts the soil aids in densification. As the compaction continues, the drum experiences a more pronounced lift-off from the soil surface, resulting in a "double jump" effect during each vibration cycle. This results in a higher compaction energy being delivered to the soil, suitable for more demanding compaction tasks. However, it also leads to less uniform compaction if not properly controlled. Partial uplift and double jump are the most frequent operation conditions. The difference between these two modes consists of the number of excitation cycles, and the motion behavior of the drum repeats itself. As the soil stiffness increases further, the motion of the drum axis is no longer vertical, the drum starts rocking and enters its chaos mode. The drum's motion at this stage was unpredictable, with irregular contact and lift-off patterns. Chaos motion is generally undesirable as it leads to very uneven compaction and potential damage to the drum. Neither compaction nor continuous compaction control is possible in this mode (Yu et al., 2014).

CMV is highly dependent on the interaction between the vibrating drum and compacted materials. It is an effective indicator of soil density in the continuous contact and partial uplift modes when no or limited lift-offs or jumps occur during compaction (Adam and Brandl, 1997).

CMV values are more reliable for assessing soil density at that time because the contact is steady, and the vibration energy is consistently applied. In contrast, in the more aggressive modes of "double jump" and "chaos motion", the drum's inconsistent contact with the soil surface can result in CMV values that do not accurately represent the soil's density, as the compaction energy is not uniformly transmitted into the soil. To detect the desirable mode in the compaction monitoring, an auxiliary value, Resonant Meter Value (RMV) was created to consider the operation conditions of the drum. RMV is the ratio of the amplitude of the half frequency of the acceleration signal to the amplitude of the exciting frequency. If RMV is different from zero, the operation mode of the drum is that of a double jump (Adam and Brandl, 1997).

$$RMV = \frac{A_{0.5\Omega}}{A_{\Omega}} \qquad (2\text{-}3)$$

Many research projects have investigated the relationship between the CMV and the compaction parameter of the soil. Brandl and Adam (1997) have compared the CMV and the plate loading test (PLT) results in the field compaction, but the soil type was not specified in this project. A strong linear correlation was established between these two parameters with an $\boldsymbol{R^2}$=0.9 and $\boldsymbol{R^2}$=0.6 at the partial lift mode and double jump mode, respectively. Nohse et al. (1999) conducted the field compaction of the clayey gravel and observed strong linear relationships between the average dry soil density and CMV with an $\boldsymbol{R^2}$=0.9. White et al. (2008) also found a linear correlation between the CMV and material density with an $\boldsymbol{R^2}$=052 for the compaction of the well-graded sand with silt. Similar projects have been performed by Liu et al. (2014) with several soil materials. They discovered the linear correlation between the CMV and dry density with an $\boldsymbol{R^2}$=0.68 for the earth-rock fill. Further projects have continued on the lime-ash soil layer and water-stable layer, and the linear correlation with $\boldsymbol{R^2}$=0.74, and $\boldsymbol{R^2}$=0.75 were found, respectively (D. Liu et al., 2016).

However, with more soil compacted, researchers realized that the correlation of the CMV and the material compactability was not always desirable, sometimes R^2=0.1 or even worse correlation was discovered. Kumar et al. (2016) discovered that for the same materials with various water content, the correlation between the CMV and its density differed dramatically. On the wet soil sample, an R^2=0.023 was found between the CMV and dry density. An R^2=0.27 correlation was established for the dry sample. Hu et al. (2020) verified this finding that the effect of the moisture content on the CMV is unneglectable. An R^2=0.1 to R^2=0.36 was identified for the same soil with different moisture contents. Meehan et al. (2017) found that the R^2=0.12-0.42 between the CMV and soil density measured by the nuclear density gauge at the different individual points. In summary, the correlation between the CMV and materials compactability is affected by the material compaction stage, moisture content of the soil, the supporting condition, the types of soil, etc.

The compaction of asphalt pavement is more complicated than soil because of its viscoelastic properties and the changing temperature during compaction. The coupling effect between the vibration drum and hot asphalt mixture is also unneglectable (Chang et al., 2014). To investigate the feasibility of the ICMV for compactability monitoring, the Transportation Pooled Fund collected compaction data from 13 states from 2008 to 2010 (Nieves, 2014). It was found that the use of IC can be a success in the asphalt mixture compaction monitoring, and the IC mapping did help identify soft and weak spots in the base layer as well as stiff areas before hot mix asphalt (HMA) placement. However, the results also indicated that the correlations between ICMV and HMA density (determined from both nuclear and non-nuclear gauges) were inconsistent and unstable. ICMV generally increased with increasing density but with highly scattered data. Similarly, correlations between ICMV and HMA core density were inconsistent, while correlations between ICMV and lightweight deflectometer (LWD) base layer modulus were generally fair. ICMV did increase layer modulus but with a low sensitivity and significantly scattered data. Federal Highway Administration (FHWA) then conducted the project “Intelligent Compaction: Quality

Assurance for In-Place Density Acceptance" (Chang et al., 2014). The purpose was to evaluate the application of IC technology for the HMA quality assurance, aiming to use ICMVs to substitute the field density testing. This study compared the projects in nine states from 2012 to 2014. The non-destructive density, core density, compaction response values, and ICMVs at each pass were collected for correlation. The results showed that the pass-by-pass ICMV correlated well with nuclear density gauge (NDG) measurements during breakdown compaction with $\boldsymbol{R^2}$ = 0.49 to 0.97. The major material densification was found to be achieved during breakdown compaction at high temperatures. IC thereby was assumed to be an enhanced tool for the quality control (QC) of HMA, especially in the breakdown stage. However, the final ICMV did not correlate well with core densities, only with an $\boldsymbol{R^2}$ = 0.01 to 0.24. The final ICMV data was not recommended to replace cores for acceptance. Several possible reasons caused this, including differences in measurement depths, temperature changes during compaction, and variations in density measurements at the finish compaction. Besides the federal endeavors, many scholars have applied the IC to asphalt compaction both in the laboratory and field compaction. IC technology was widely believed to be an effective method to improve the uniformity of asphalt pavement by performing full coverage monitoring and real-time ICMV calculation (Nieves, 2014) (Chang et al., 2014). The application of the geostatistical analysis further increases the uniformity evaluation of IC technology in asphalt pavement. Compared with the conventional quality control method, the geostatistical analysis of the ICMV can evaluate spatial uniformity and identify weak locations during compaction (Hu et al., 2018; Xu and Chang, 2013). Hu et.al (2019) investigated the effect of the supporting condition on the ICMV. It was found that different underlying supports can affect the sensitivity of CMV concerning the asphalt modulus. A higher correlation was identified at the cement-stabilized aggregate base layer than an untreated aggregate base layer, confirming that the ICMV is the indicator of the entire pavement structure instead of the asphalt layer.

As remote sensing technology increasingly permeates pavement engineering, how to process vast datasets for decision-making becomes an imperative task. The data-informed analysis, exemplified by the rapid evolution of artificial intelligence (AI) techniques, such as machine learning (ML) and artificial neural network (ANN), has been highlighted in various industries (Moayedi et al., 2019, Schmidhuber, 2014). AI techniques are proficient in learning from data, recognizing patterns, and autonomously making decisions. This proficiency not only minimizes human intervention but also significantly contributes to time savings and optimal utilization of computing resources (Gomber et al., 2018). During the year of 2015 to 2023, ANNs have become one of the most widely applied algorithms for pavement performance prediction. Ziari et al. (2015) compared ANN models with the conventional assessing approaches for international roughness index (IRI) prediction. The projects utilized the pavement structure, condition, traffic, and climate data from the LTPP database, and found that the ANN models can make more reliable IRI predictions for both short-term and long-term periods. Souza et al. (2018) proposed a low-cost pavement condition assessment system based on data collected by smartphone accelerometer sensors and ML methods. The dynamic classifier model can assess the pavement quality on a four-tier scale (Good, Average, Fair, Poor) with a 90% prediction accuracy. Nabipour et al. (2019) used support vector machine (SVM) classifier and genetic expression programming methods to predict the remaining service life of the pavement and confirm that artificial intelligence can be used as an optimization tool in pavement management systems. Georgiou et al. (2018) developed models based on ANN and SVM algorithms using time series IRI values to predict pavement roughness in a year. Both ANN and SVM were effective in accurately predicting the future IRI values, and the ANN models slightly outperformed the SVM models. The ANN models were then modified to predict IRI for ten flexible pavements from different climatic zones. The ANN can achieve the IRI prediction with an average root mean square error (RMSE) of 0.015 (Hossain et al., 2019). The effective ANN model was also applied to the rigid pavement and obtained a reasonable IRI

prediction. This project indicated that the AI methods of IRI prediction were versatile, and independent of the pavement type (Hossain et al., 2020). Marcelino et al. (2021) developed general pavement performance prediction models using ANN to predict the IRI development in the future. A reasonable predictive performance was achieved with the average mean squared error of 0.064 for the 5-year prediction model and 0.104 for the 10-year prediction model.

Another important application of AI techniques in asphalt pavement is material performance prediction. Commuri and Zaman (2006) collected the key features of the vibration signals as the inputs and eventually realized automated pavement compaction level classification. Kaya et al. (2018) Seitllari et al. (2019), and El-Badawy et al. (2018) developed multilayer perceptron neural networks (MLPNN) to predict the dynamic modulus for HMA and WMA mixtures by considering aggregate gradation, asphalt properties, and volumetric properties. Moussa and Owais (2020) proposed a convolutional neural network (CNN) model for HMA dynamic modulus prediction. Reasonable predictions of the dynamic modulus were achieved, but there is a potential risk for overfitting when the experimental data is limited. Eleyedath et al. (2020) present a novel hybrid machine-learning approach to predict the dynamic modulus of asphalt concrete. The finalized model with the existing regression-based equations indicated that the proposed hybrid model offers an efficient and accurate prediction of the dynamic modulus. Behnood et al. (2021) integrated biogeography-based programming (BBP) into dynamic modulus predictive models. The results showed that the prediction result even outperformed the Witczak model and Hirsch model. Zhang et al. (2021) integrated the machine learning model into the IC technology aiming to improve the correlation between the ICMV and density measurement from the NDG. By considering the pass count in the model, the density prediction accuracy of the ICMV improved, 95% of the model predicted residuals lie within the range of ± 0.6.

Intelligent Compaction (IC) technology emerges as a promising strategy for ensuring continuous control over soil and asphalt pavement compaction. The IC system excels in capturing

extensive and comprehensive information during compaction processes, leading to substantial enhancements in compaction uniformity. However, the inherent IC technology poses a challenge, as the attached accelerator gathers a combination of responses from the entire pavement structure. This data collection mechanism complicates the task of correlating the collected responses with the density of the asphalt layer, in the context of multilayered pavement structures. Numerous factors further complicate the correlation between Integrated Compaction Measurement Values (ICMV) and asphalt pavement density. These factors include temperature variations, the coupling effects between the roller drum and viscoelastic materials, and varying supporting conditions. The evolution of data-informed techniques presents a unique and potent tool for efficiently processing the substantial datasets acquired by IC sensors. Integrating these advanced techniques into IC technology holds great promise for refining the prediction accuracy of asphalt pavement compaction degree. Consequently, a pressing need exists for the development of a new technique or analytical method to enhance the correlation between IC technology and the compactability of asphalt mixtures. Achieving this objective stands as a crucial milestone and represents a significant stride toward the automation of pavement construction processes.

Summary of Literature Review

The conventional method in asphalt pavement construction relies heavily on experience due to a lack of a systematic understanding of the compaction mechanism. This approach often results in issues such as over-compaction, under-compaction, and uniformity problems, impacting the pavement's duration and long-term performance. In response to these challenges, Intelligent Compaction (IC) technology has been developed, incorporating GPS, various sensors, a thermometer, and a reporting system on the vibratory compactor. The implementation of IC technology allows for the comprehensive collection of pavement conditions and responses,

enabling adjustments to compaction strategies. This technological advancement proves effective in significantly enhancing compaction uniformity. However, it falls short as an accurate tool for monitoring in-situ pavement density. This limitation arises from the inconsistent correlation between the Intelligent Compaction Measurement Value (ICMV) and pavement density, highlighting the need for continued refinement and complementary approaches in density monitoring during asphalt pavement compaction.

Numerous researchers have uncovered that, rather than relying on external pavement responses, the kinematic or mechanical behaviors of asphalt particles serve as suitable indicators for assessing the compaction degree of asphalt pavement. In the context of a multilayered pavement structure, internal responses of asphalt particles exhibit effective correlations with the density of the asphalt layer. In contrast, the external responses are prone to be influenced by the base layer, temperature effects, and other factors. Current wireless sensing technology facilitates the collection of internal responses during compaction. The kinematic behaviors of particles are closely tied to mixture density and are associated with the formation of the pavement skeleton during compaction. This suggests that mesoscale information holds promise in elucidating the compaction mechanism of asphalt mixtures.

Furthermore, Discrete Element Method (DEM) simulation emerges as an efficient means to monitor the kinematic and mechanical behaviors of granular materials during compaction. This approach is cost-effective, allowing the evaluation of particle mesoscale behavior under various compaction scenarios with desirable effectiveness and simulation accuracy. Combining DEM simulation with experiments utilizing remote sensors enables a comprehensive investigation into the compaction mechanism of asphalt mixtures. Additionally, the progress in artificial intelligence techniques opens avenues for effectively processing vast amounts of data collected by remote sensors and making informed predictions regarding both pavement performance and construction

quality. The integration of sensing technology and AI techniques into asphalt pavement compaction presents a promising approach for compaction monitoring and degree prediction.

In conclusion, a comprehensive comprehension of the compaction mechanism plays a pivotal role in advancing the asphalt pavement construction process. This foundational knowledge is essential for the refinement of compaction techniques, ensuring increased efficiency and effectiveness. Moreover, understanding the compaction mechanism proves valuable in assessing the workability of asphalt mixtures. This is critical for enhancing mix designs and preserving the workability and properties of the asphalt mixture throughout the construction phase. Recognizing this correlation opens the door to a more streamlined construction process through real-time monitoring of particle behavior, ultimately paving the way for the potential automation of pavement construction.

Chapter 3

Methodology and Scope

This research aims to investigate the compaction mechanism of the particulate asphalt mixtures and develop an intelligent system to predict the compaction conditions of the asphalt pavement. Considering the limitations of the current compaction methods, the external compaction responses are easily disturbed by irrelevant factors but materials' compactability, resulting in the inconsistent indication of the density of the asphalt pavement. Therefore, the internal responses from the asphalt layer will be investigated in this research and used for compaction prediction.

A particle-sized Microelectromechanical systems (MEMS) device, SmartKli® (previously called "SmartRock"), would be utilized to collect the internal particle behaviors. Such a sensor could be embedded only in the asphalt layer to collect the particle kinematic behaviors during compaction so that the influences from other pavement layers and environments can be eliminated. The correlation between the particle kinematic behaviors and the compaction condition of the asphalt pavement can thus be investigated. The laboratory compaction tests, field compaction projects, and numeric modeling will be evaluated to comprehensively understand the compaction mechanism of the asphalt mixture. Specifically, Superpave gyratory compaction will be firstly conducted on multiple asphalt mixtures varying in gradation, binder types, asphalt content, etc. The wireless sensor will be placed inside the asphalt mixture to collect the particle kinematic and mechanical behaviors during compaction. This step is to find out the effective and robust parameter to evaluate the density of the asphalt mixture throughout the compaction process. The field compaction projects will then be performed to further verify the applicability of the parameter in-field practices. The relationship between the laboratory and field compaction will be investigated based on the selected parameter. However, given the fixed size of the wireless sensor, it is hard to understand the particle behaviors at different levels of particle geometries. Numerical modeling

will finally be carried out to complete the compaction mechanism theory. Different sizes of the asphalt particles will be monitored during the entire process of the compaction. Eventually, a comprehensive mesoscale understanding of the compaction mechanism of the asphalt mixture will be proposed.

The objective of the compaction prediction will be realized by remote sensing technology and Artificial Intelligence (AI). Due to the intricate interaction between the vibratory drum and the viscoelastic materials, along with the substantial data gathered by the sensor, the AI methodology exhibits an enhanced capability to process large volumes of data and discern internal correlations. Therefore, an AI-based model would be established to predict the compaction condition of the asphalt pavement. Based upon the proposed compaction mechanism, an AI model will be established and verified by the laboratory compaction data collected from various types of asphalt mixture. Once the model is calibrated, the model will be applied to the field compaction. The input parameters and model algorithm will be modified accordingly to achieve the desirable prediction quality in the field compaction. Eventually, such a model would be calibrated and verified by experiment data from laboratory and field compaction. Different monitoring and prediction models will be created for the needs of compaction requirements, including the compaction classification model and density prediction model. The construction agencies can select the appropriate model on a needed basis. With the understanding of the compaction mechanism of the asphalt mixture, and the assistance of the prediction model for compaction monitoring, more accurate compaction predictions of the asphalt pavement can be achieved, and more resilient and sustainable pavement will be built. The concept and scope of the proposed work are illustrated in Figure 3-1.

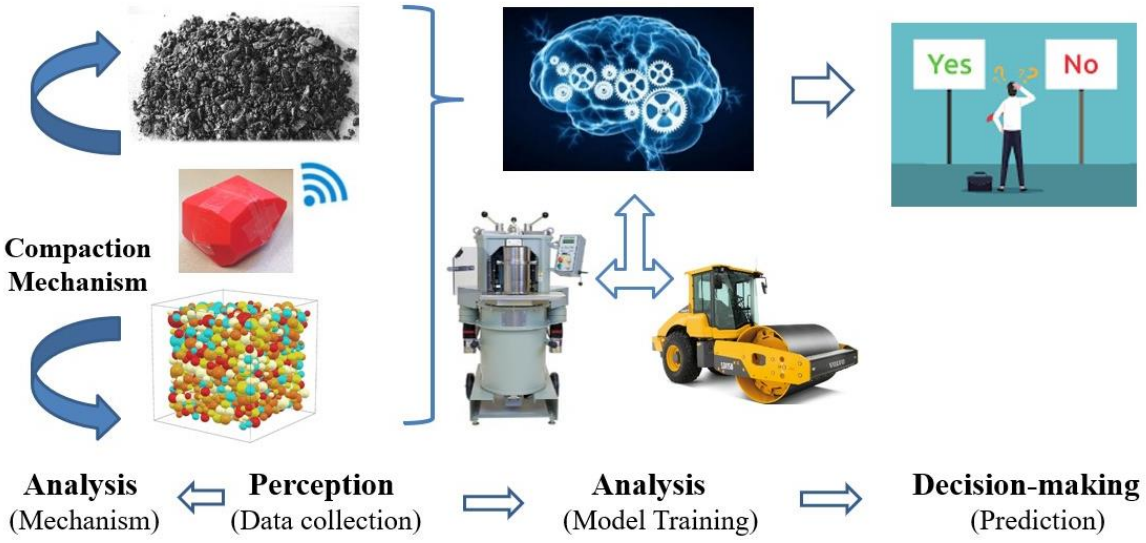

Figure 3-1 The concept of the automated compaction assessment

Chapter 4

Material, Device, and Experiment

Materials

Twenty types of asphalt mixture were tested throughout the research to investigate the compaction mechanism and create predictive models. Based on the objectives of each section, different combinations of the asphalt mixtures will be selected for compaction testing, workability evaluation, or density prediction. These mixtures differ in material type (HMA, WMA), gradation (dense-graded, SMA, open-graded), compaction temperatures (110℃-143℃), additives (Evotherm), incorporating recycled materials (RAP, Plastic), and producing methods (lab and plant mixing), etc. The mixtures' information is summarized in Table 4-1.

Table 4-1 Design for the asphalt mixtures

No.	Technology	NMAS	RAP	OVAC	Asphalt	Temp	Mixing
1	HMA	12.5	15%	5.8%	PG64-22	135℃	Plant
2	HMA	9.5	15%	5.9%	PG64E-22	135℃	Lab
3	HMA	12.5	0%	5.9%	PG64-22	110℃	Lab
4	HMA	12.5	0%	5.9%	PG64-22	143℃	Lab
5	0.35% Evotherm	12.5	0%	5.9%	PG64-22	127℃	Lab
6	0.7% Evotherm	12.5	0%	5.9%	PG64-22	110℃	Lab
7	0.7% Evotherm	12.5	0%	5.9%	PG64-22	143℃	Lab
8	Smart Foam	9.5	15%	5.9%	PG64E-22	135℃	Plant
9	HMA	12.5	25%	5.9%	PG64-22	135℃	Plant
10	Smart Foam	9.5	15%	5.9%	PG64E-22	135℃	Plant
11	Foam	9.5	15%	5.8%	PG64S-22	135℃	Plant
12	HMA	9.5	15%	5.2%	PG 64-22	135℃	Lab
13	Plastic (dry)	9.5	15%	4.73%	PG 64-22	135℃	Lab
14	Plastic (wet)	9.5	15%	4.73%	PG 64-22	135℃	Lab

15	HMA	9.5	15%	6.0%	PG 64-22	135℃	Lab
16	Plastic (dry)	9.5	15%	5.46%	PG 64-22	135℃	Lab
17	Plastic (wet)	9.5	15%	5.46%	PG 64-22	135℃	Lab
18	Plastic (dry)	9.5	15%	6.0%	PG 64-22	135℃	Lab
19	HMA (SMA)	12.5	0%	6.9%	PG 64-22	135℃	Lab
20	HMA (OGFC)	12.5	0%	6.0%	PG 64-22	135℃	Lab

Note: NMAS means nominal maximum aggregate size; OVAC is the optimal virgin asphalt content; Temp represents the compaction temperature.

MEMS Device

Particle Wireless Sensor

Due to the successful application of the Micro-electromechanical systems (MEMS) devices in the mesoscale research of geotechnical engineering, this research will adopt it to investigate the compaction mechanism of the particulate asphalt mixture. To collect the kinematic behaviors of the asphalt particles during compaction, the particle size, and wireless transmission are essential for the MEMS device selected. SmartKli® is a novel wireless particle-size sensor, as shown in Figure 4-1. The SmartKli® with angularity was initially used in railroad engineering to study the effect of ballast lateral stability (S. Liu et al., 2017; S. Liu et al., 2016). 3D print technology can design the SmartKli® with a similar morphology property as the ballast in the railway structure. As its size becomes smaller, SmartKli® has been applied in pavement engineering and material compaction (Wang et al., 2018b; C. Zhang et al., 2021).

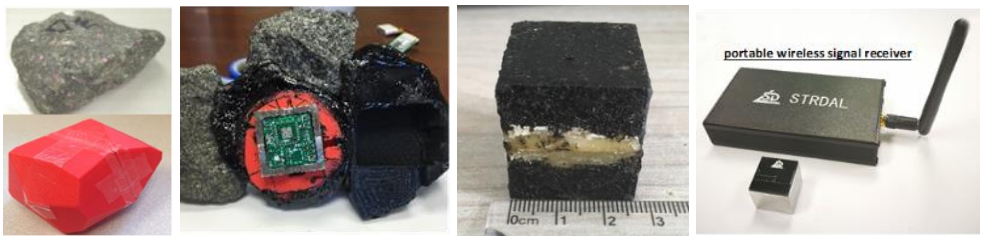

Figure 4-1 SmartKli® with real ballast morphology property (left), SmartKli® inside units (middle left), particle-size SmartKli® (middle right), and SmartKli® receiver (right)

The current version of the SmartKli® is a particle-size cube with a 27mm length. The morphology properties of the aggregates were eliminated to reduce their size. The external shell of the device was a resistant thermoplastic polymer material, Acrylonitrile butadiene styrene (ABS) with Nylon, which can survive in high-strength, high-temperature environments up to 150 ℃. This material shows good compatibility and cohesion with the asphalt binder, making it a desirable tool for investigating the compaction behaviors of the asphalt mixture. The internal units consist of a tri-axial accelerometer, a tri-axial magnetometer, and a tri-axial gyroscope, which can record particle translation, orientation, and rotation in 9 degrees of freedom. The location identification algorithm based on Bluetooth Low Energy (BLE) technology allows the raw data to be wirelessly transferred to a computer or a base station. Furthermore, the SmartKli® sensor is equipped with two operational modes to adapt to varying conditions: "working mode" and "sleeping mode," (or low energy consumption mode). The "working mode" is essential when the sensor is connected to a computer, enabling the completion of data collection and transmission processes. Conversely, the "sleeping mode" is designed for periods when intensive energy consumption is unnecessary. This mode can significantly prolong the sensor's service life, making it particularly beneficial in scenarios like field performance monitoring where continuous operation is not required. The utility of the “sleeping mode” is evident where energy efficiency and operational longevity are crucial.

The sampling frequency of the sensor is also adjustable from 0 to 200 Hz on a needed basis. The other information on SmarKli® can be found in Table 4-2.

Overall, SmartKli® has prominent advantages in convenience, innovation, and durability. Its size and wireless data transmission technology reduce disturbances to material movement during data collection. It has been used and verified in multiple projects, including ballast condition monitoring in railway systems, traffic speed determination, workability evaluation, and compaction prediction in pavement engineering (Liu et al., 2017; Liu et al., 2016; Wang et al., 2018; Zhang et al., 2021). Therefore, the SmartKli® sensor was selected in this research for the investigation of the compaction mechanism.

Table 4-2 SmartKli® parameters

Items	**Parameters**
Size	27×27×27mm
Weight	43g
Stress range	1-100 lb
Orientation range	360 °C
Accelerometer	±16g (max)
Gyroscope	±2000 °/s (max)
Magnetometer	±4800 uT
Sampling rate	200 Hz (max)
Temperature range	150 ℃ (max)

Sensing Data Analysis

Two coordinate systems exist in the SmartKli® system during data collection and analysis: local coordinate and global coordinate. Local coordinate system is the default coordinate attached to the sensor and it will change as the device's orientation. This coordinate is convenient for the data collection but introduces difficulties for consistent data analysis and comparison. As a result,

the global coordinate system was introduced. Unlike the local coordinate system, the global system is fixed in space and unaffected by the position and orientation of the object. In this research, all the compaction data was initially collected in the local system and then transformed into the global coordinate system for analysis. The process of coordinate transformation can be completed using the transformation matrix based on equations (4-1) and (4-2).

$$R = \begin{bmatrix} 1-2(q3^2+q4^2) & 2(q2q3-q1q4) & 2(q2q4+q1q3) \\ 2(q2q3+q1q4) & 1-2(q2^2+q4^2) & 2(q3q4-q1q2) \\ 2(q2q4-q1q3) & 2(q3q4+q1q2) & 1-2(q2^2+q3^2) \end{bmatrix} \quad (4\text{-}1)$$

$$z = R'z' \quad (4\text{-}2)$$

Where, *q1, q2, q3, and q4* are the quaternions from the initial transformation data. *z* and *z'* are global and local coordination data, respectively.

The SmartKli® sensor can directly collect the particle mechanical properties like acceleration and contact stress. Comparably, the monitoring of the particle rotation is achieved by collecting the quaternion. Quaternion is an expression to describe the orientation of an object in 3D space using an ordered set of four numbers. For example, when an object's orientation is expressed as $a + bi + cj + dk$, where *a, b, c, d* are real numbers and *i, j, k* are symbols of three spatial axes with unit vectors, the set of the four ordered numbers, *a*, *b*, *c*, and *d* is a quaternion. The quaternion was initially collected by the SmartKli® during compaction and then transformed to the Euler angle. Compared to the quaternion, Euler angles provide a straightforward and intuitive way to represent rotations by sequentially rotating around axes (Eberly, 2020). It is simpler and more accessible in applications where a clear understanding of each rotational component is important. Euler angle is an order set of three numbers introduced by Leonhard Euler to describe the orientation of a rigid body with respect to a fixed coordinate system (Eberly, 2020). The criteria of intrinsic rotation were

adopted where the rotations are about the axes of the rotating coordinate system XYZ, solidary with the moving body. The orientation of the rigid body changes for the extrinsic frame after each elemental rotation. The conversion between the quaternion *(q0, q1, q2, q3)* to the Euler angle *(α, β, γ)* is summarized in equation (4-3). Euler angle *(α, β, γ)* means rotating *α, β, γ* degrees around fixed axes x, y, z in order.

$$\begin{bmatrix}\alpha\\ \beta\\ \gamma\end{bmatrix} = \begin{bmatrix}atan2(2(q_0q_1 + q_2q_3), 1 - 2({q_1}^2 + {q_2}^2))\\ arcsin\,(2(q_0q_2 - q_1q_3))\\ atan2(2(q_0q_3 + q_1q_2), 1 - 2({q_2}^2 + {q_3}^2))\end{bmatrix} \quad (4\text{-}3)$$

Compaction Experiments

Laboratory Compaction Experiments

Superpave Gyratory Compactor (SGC) is a widely used compaction method in the laboratory. It can apply the shearing loading and kneading effect on the materials owing to its internal tilting angle. Multiple projects indicated that the SGC provides a more reprehensive specimen with the in-service pavement under the construction loadings (Button and Little, 1994; Roberts et al., 2002). In this research, the AFG2 Pine gyratory compactor is utilized with its 1.15° calibrated internal angle, 30rpm gyration speed, and constant 600Kpa compaction pressure. During compaction, the compactor can collect the compaction loadings, torque, and specimen height.

To collect the most representative kinematic behaviors of the asphalt particles, the SmartKli® sensor was embedded inside of asphalt mixture. The characteristic of the particle size and wireless transmission mode makes it possible to collect the mesoscale compaction behavior with limited disturbance. As for the sensor's location, Wang et al. (2018) compared the sensor location at the top center, middle center, and middle side of the specimen, and investigated its effect

on the compaction behaviors under the gyratory compaction. The results show that the sensing data at the center of the specimen was most stable regarding its rotation value and relative rotation. Her findings were consistent with X-ray CT results by Masad et al. (2009), who found that the larger and scattered air voids presented at the boundary of the specimen (top and bottom). Therefore, the SmartKli® was embedded in the center of the specimen. In a real experiment before compaction, half of the mixtures were first put in the mold, the SmartKli® was placed on top of the materials and the remaining materials were added afterward. During compaction, the SmartKli® will record the quaternion, acceleration, contact stress, and temperature. After compaction, the density of each specimen will also be measured for verification and analysis. Since the water would cause potential imprecision or damage to the internal sensor units, the specimen with the SmartKli® cannot soak in the water to measure the density. Therefore, two types of specimens for each asphalt mixture were compacted:

- **Reference specimen**: a specimen without the SmartKli® was compacted to measure the bulk specific gravity (G_{mb}) of the specimen in accordance with the AASHTO T166.
- **Test specimen:** the specimen with the SmartKli® sensor was compacted to investigate the particle compaction characteristics. Each test specimen will have the mass of a SmartKli® sensor (50g) subtracted from its total mass. This adjustment ensures that the conditions of the test specimen are consistent with those of the reference specimen.

To clarify, the same mixture conditioning was applied to the reference specimens. The compaction experiment of the test specimen consists of the following steps:

(1) Check the connection of the SmartKli® with the computer before compacting. Collect the initial data on a horizontal platform for the coordinate transformation.

(2) Short-term age the loose mixtures for 2 hours at the required compaction temperature.

(3) Start the compact process and use SmartKli® to collect the particle behaviors during the whole

compaction process. Meanwhile, the SGC compactor will collect the loadings, torque, and height of the compacted specimens.

(4) Extract the SmartKli® from the specimen after compaction and allow the sensor to cool down for the next series of tests.

Field Compaction Project

Field rolling compaction was carried out in this research to comprehensively investigate the compaction mechanism of the particulate asphalt particle under different modes of loadings. Various roller compactors were utilized in the field, including static roller, vibratory roller, and oscillatory roller. Two field projects were conducted in this research, where roller compactors, compaction designs, asphalt materials, pavement structures, and environmental conditions are different. Detailed information on the asphalt mixtures for the projects is presented in Table 4-3. In the field compaction, the SmartKli® sensor was embedded in the asphalt layer to collect the particle rotation during compaction. To control the depth of the sensors in the pavement, the SmartKli® is manually buried at the bottom of the asphalt layer after the mixtures are placed, as shown in Figure 4-2. The SmartKli® would collect the compaction data during the whole process of the compaction using the same sampling frequency in the laboratory compaction.

Table 4-3 Information on the asphalt mixtures for field projects

	Altoona	Indiana
Mixture type	WMA9.5	HMA12.5
Virgin binder	PG64E-22	PG 64-22
Virgin binder content	5.1%	4.7%
RAP content	15%	25%
Total binder content	5.9%	5.9%

Theoretical max specific gravity	2.469	2.496
Gyration at N_{design}	100	50

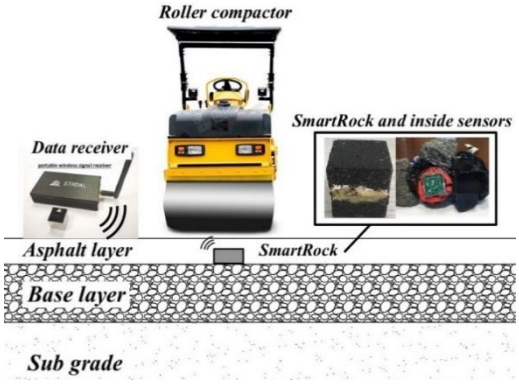

Figure 4-2 Compaction data collection by the SmartKli® system

Altoona Project

This first project was conducted in July 2021 in Altoona, Pennsylvania. The Altoona project is a maintenance and rehabilitation project on a current asphalt pavement. The original pavement was milled 6.35cm (2.5 inches) from the surface and overlaid with a 2.54cm (1 inch) leveling course and a 3.81cm (1.5 inches) wearing course. Detailed information on the asphalt mixture is in Table 4-3. 11 compaction cycles were applied to compact the pavement, including static roller (SAKAI SW 654 shown in Figure 4-3) and oscillatory roller (HD+ 120i VO Tandem Roller). The parameters of the static roller and the oscillatory roller are in Table 4-4. The sampling frequency was 17 and 100 Hz for collecting quaternion and acceleration, respectively. A camera records the whole compaction process for the following verification and analysis. After compaction, three core samples near the SmartKli® were drilled out to measure the density in the laboratory. SmartKli® installation and data collection are shown in Figures 4-3 and Figure 4-4.

Table 4-4 Information on the vibratory rollers

Parameters	Altoona project	Indiana project
Frequency (*f*)	42 Hz	45 Hz
Speed (*v*)	1.3 m/s	0.7 m/s
Material density (ρ)	2370 kg/m^3	2372 kg/m^3
Width (*b*)	1.98 m	1.8 m
Amplitude (*A*)	0.88 mm	0.84 mm
Weight (*m*)	12.2 t	18 t
Centrifugal force (*Fe*)	159 KN	214.9 KN

Figure 4-3 Static roller compactor (left) and oscillatory roller (right) in the Altoona project

Figure 4-4 SmartKli® installation and data collection in the Altoona project

Indiana Project

The second project was a newly constructed asphalt pavement in Angola, Indiana. This project was carried out in September 2021. The asphalt mixture used in this project is HMA-12.5 and detailed information is shown in Table 4-3. The target depth of the asphalt layer is 5.08cm (2 inches). The vibratory roller (Dynapac CC7200 as shown in Figure 4-5) was applied for compaction, and its detailed information is in Table 4-4. The same sampling frequencies of 17Hz and 100Hz are selected to collect the particle rotation and acceleration, respectively. A camera also records the whole compaction process for the following verification and analysis. After the compaction, two core samples near the SmartKli® were drilled out to measure the density in the laboratory. The SmartKli® installation and data collection are shown in Figure 4-6.

Figure 4-5 Vibratory roller in Indiana project

Figure 4-6 SmartKli® installation and data collection in Indiana project

Chapter 5

Compaction Mechanism

The compaction mechanism of the particulate asphalt mixture will be investigated from two perspectives: compaction experiment and numerical simulation. Firstly, different modes of compaction will be carried out, including the Superpave gyratory compaction and various roller compaction. The wireless particle-size sensor, SmartKli®, will be utilized to collect the particle kinematic behaviors during compaction. We aim to identify a parameter that can connect the particle behaviors and the material density, as well as correlate laboratory compaction with field practice. Additionally, the Discrete Element Method (DEM) simulation using the Particle Flow Code (PFC) will be implemented. This step is to further understand the compaction mechanism of the asphalt mixture, especially for the compaction scenarios that are hard to conduct in experiments, such as the effect of the particle size, particle angularity, and gradation on the compaction behaviors. Eventually, a comprehensive understanding of the compaction mechanism of the particulate asphalt mixtures will be given. This mechanism will serve as the foundation for the following compactability evaluation and compaction prediction.

Compaction Mechanism Based on Experiments

Particle Kinematic Behavior During Compaction

During Superpave gyratory compaction, the particle kinematic behaviors will be collected by the SmartKli® sensor. SmartKli®'s size is less than 1/5 of the diameter of the SGC mold, and it uses wireless techniques for data transmission. It is reasonable to assume that the kinematic responses are appropriate representatives of the coarse aggregate. Although it is still larger than the

coarse aggregate in the mixture, the good cohesion allows it to collectively move with the nearby asphalt particles. Several studies have verified its reasonableness in the research of ballast condition monitoring in railway systems, traffic speed determination, workability evaluation, and compaction prediction in pavement engineering (Liu et al., 2017; Liu et al., 2016; Wang et al., 2018; Zhang et al., 2021).

Early studies on the asphalt mixture compaction indicated that particle rotation plays a critical role in evaluating the compaction condition. Figure 5-1 depicts the three-directional Euler angle collected by SmartKli® during the compaction of the asphalt mixture. As seen, the sensor rotates cyclically every 2s, which is consistent with the gyratory period of the SGC compactor. In other words, the dominant motion behavior of SmartKli® follows the SGC trend. It can also be noticed that the amplitude of the Euler angle differs as the compaction proceeds. Based on this phenomenon, the Relative Rotation (RR) was defined as the difference between the peak and valley value of the Euler angle in a single cycle (Wang et al., 2018).

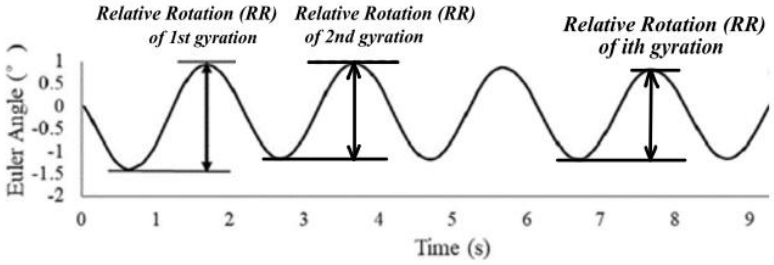

Figure 5-1 Illustration of the relative rotation

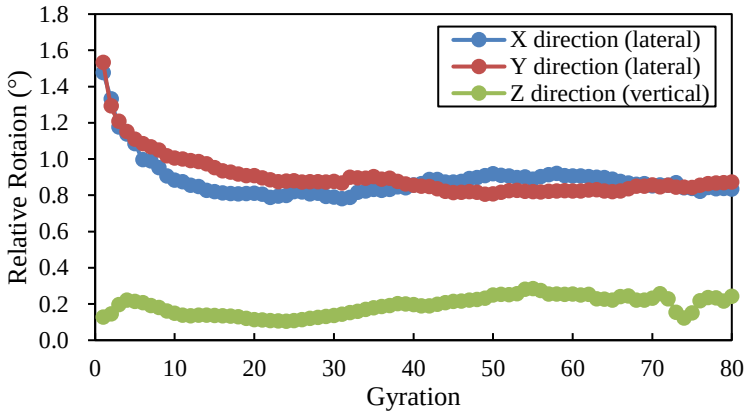

Figure 5-2 Relative rotation curves of SmartKli® in three directions

Figure 5-2 shows the relative rotation in three directions. It is seen that the relative rotation in the vertical direction (z-direction) fluctuates at a very small range and shows no certain correlation with the compaction condition. Comparably, the relative rotation at two lateral directions (X and Y direction) differ dramatically with compaction stages. Based on the relative rotation at lateral directions, three compaction stages were observed.

(I) Breakdown Stage: It is the beginning of the compaction, and asphalt mixture particles were loose and had limited contact. The shear and compression forces of SGC started to cause particles to rotate and translate. Particles had large relative rotation and a sharp reduction due to much compaction and height reduction. The fastest material densification occurs in this stage.

(II) Main Compaction Stage: More restrictions from the adjacent particles were applied to the sensor as the materials became denser. The skeleton formed at this stage, leading to reduced particle rotations and a lower rate of relative rotation. However, continuous compaction results in further reduction in the specimen height. This stage is characterized by the imbalanced interaction between compaction loadings and shear stress. Most material densification occurs in this stage but at a relatively low speed.

(III) Finishing Stage: The particle rotation is relatively stable at the last stage, and the particle rotation is relatively stable and the interaction between compaction and particle resistance reaches balance. Minimal densification but surface leveling occurs in this stage.

Correlation Between Particle Rotation and Material Density

To investigate the relationship between the particle kinematic behaviors and compaction condition of the asphalt mixture, the curve of the particle rotation and the change of the specimen height were displayed in the same figure. Since the loading and the mold geometry are symmetric at two lateral directions, and the particle relative rotation presented a similar trend in the magnitude as shown in Figure 5-2, the average of lateral relative rotation was used for the following evaluation, as displayed as the orange curve in Figure 5-3. The curve of the height change of the asphalt specimen is shown in blue.

It is worth noticing that the two curves follow a similar trend during the whole compaction stage. In the beginning, the specimen was rapidly compacted along with the sharp decline of the relative rotation because of the loose mixture properties and the gyratory compaction loadings. The coarse aggregates start to contact and form a skeleton. The friction and shears hinder the compaction, decreasing the rate of height and particle rotation. Eventually, the specimen height and particle rotation are stabilized at a relatively constant value. As seen, the curve of particle relative rotation and the specimen height are similar and even overlapping. Since the mass of the specimen stays unchanged during compaction, the change in height is hence an appropriate indicator for the density of the asphalt mixture. Therefore, the particle relative rotation is closely related to the mixture's density during compaction and could be used for the compaction evaluation.

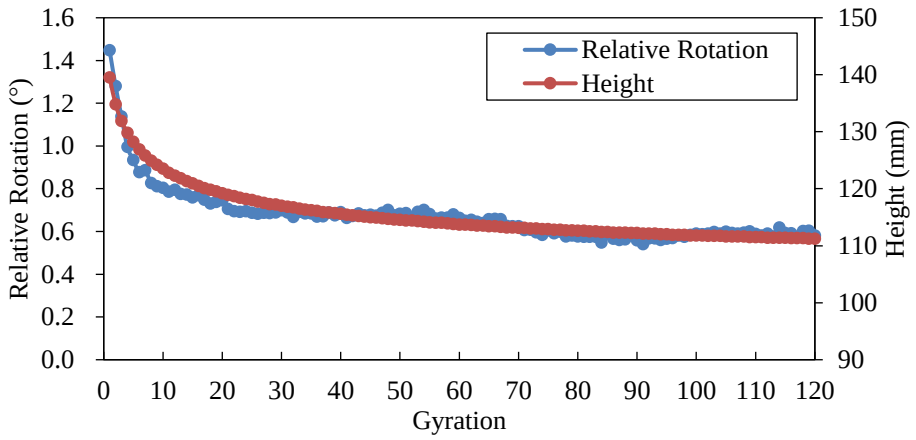

Figure 5-3 Curves of relative rotation and specimen height during compaction

To quantitatively assess the correlation between particle rotation and specimen height during the gyratory compaction, a Pearson correlation coefficient is calculated using equation (5-1). The Pearson correlation coefficient between these two curves was 0.949, demonstrating a very high correlation between the particle relative rotation and height (or density) change of the asphalt mixture. It should be noted that the correlation coefficient value could vary in terms of the properties of the asphalt mixture and the compaction conditions.

$$r = \frac{\sum(x_i - \bar{x})(y_i - \bar{y})}{\sqrt{\sum(x_i - \bar{x})^2 \sum(y_i - \bar{y})^2}} \qquad (5\text{-}1)$$

Where, $\boldsymbol{r}$ is the Pearson correlation coefficient; $\boldsymbol{x_i}$ is the particle rotation under gyratory compaction; $\bar{\boldsymbol{x}}$ is the mean of the $\boldsymbol{x}$ sample; $\boldsymbol{y_i}$ is the particle rotation under roller compaction; $\bar{\boldsymbol{y}}$ is the mean of the y sample.

Correlation Between Laboratory and Field Compaction

The particle kinematic behavior of the asphalt mixture under the roller compaction was then investigated. The data was from the Altoona project, and its detailed information was introduced in Chapter 4. The mixture was compacted by a combination of static and vibratory roller compactors. The SmartKli® sensor was placed inside the mixture, the particle relative rotation was analyzed and presented in Figure 5-4. The same materials were compacted under the gyratory compactor, and the curve of relative rotation in three directions was presented in the same figure.

The particle relative rotations demonstrate higher values in the horizontal direction than the vertical direction regardless of the compaction method. It is reasonable because the vertical loadings were exerted by both the gyratory and roller compaction. A comparison was thereby made between the particle rotation at the lateral direction. The magnitude and fluctuation of the two methods are different given the discrepancies in the compaction loadings and mechanism. However, the general trend of the particle rotation through the compaction process followed a similar trend, and three-stage compaction patterns can also be identified: (1) Breakdown stage: 1st to 7th cycle in the gyratory compaction and 1st and 2nd cycle in the roller compaction. (2) Main compaction stage: 8th to 50th cycle in the gyration compaction and 3rd to 8th cycle in the roller compaction. (3) Finishing stage: post-50th cycle in the gyration compaction and post-8th cycle in the roller compaction.

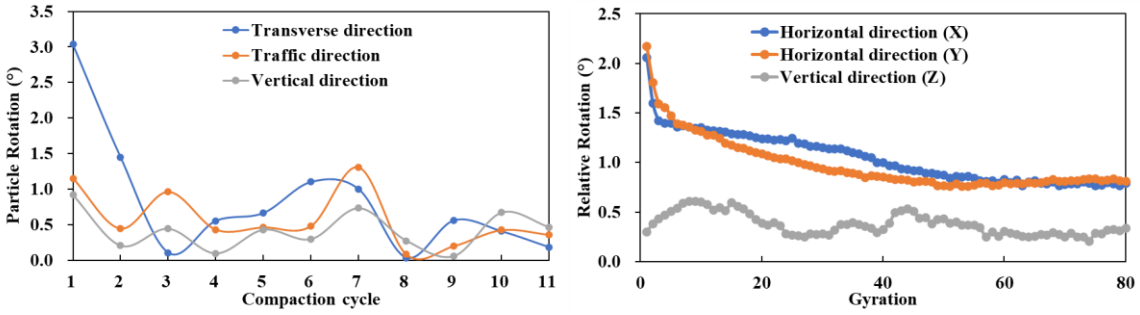

Figure 5-4 Particle rotation under roller compaction (left), and gyratory compaction (right)

The relationship between particle rotation under the gyratory and roller compactions was quantitively assessed using the Pearson correlation coefficient. Given the variance in the number of compaction cycles between the two methods, a comparative analysis of particle rotation was conducted at comparable levels to mitigate the disparities. The density-equivalent and energy-equivalent methods are performed.

To clarify, in the energy-equivalent method, the particle rotation is compared at a similar level of compaction energy. The compaction energy can be calculated based on the compaction loadings and mechanism for each method. Similarly, for the density-equivalent method, the particle rotation was compared at the same level of mixture density. After this step, the 80-cycle gyratory compaction can be processed to 11-cycle compaction, so that a correlation parameter can be obtained between the two compaction methods using equation (5-1). The processed particle rotation of both methods is presented in Table 5-1. The Pearson correlation coefficient was 0.818 (density-equivalent) and 0.806 (energy-equivalent), signifying a reasonable correlation between gyratory and roller compaction.

Table 5-1 Particle rotation under the same compaction energy

Cycle	Particle rotation under roller (°)	Density-equivalent particle rotation under SGC (°)	Energy-equivalent particle rotation under SGC (°)
1	2.094	1.779	1.705
2	0.950	1.431	1.371
3	0.536	1.396	1.267
4	0.495	1.345	1.189
5	0.566	1.297	1.140
6	0.794	1.236	1.072
7	1.153	1.197	1.024
8	0.063	1.154	0.945

9	0.383	1.134	0.875
10	0.418	1.085	0.838
11	0.273	1.045	0.816

Compaction Mechanism Based on Simulation

The wireless sensor provides a unique technique to investigate the particle behaviors during the compaction of the asphalt mixture. By utilizing the sensor in different types of asphalt mixtures under various conditions, the changing of particle rotations, the relationship between the particle rotation and the specimen density, and the correlation between the laboratory and field compaction were identified. However, given the condition of the SmartKli® sensor, it is impossible to evaluate the effect of particle size on the compaction behaviors. Therefore, numerical modeling was carried out to further investigate the compaction mechanism of the asphalt mixture. The discrete Element Method (DEM) was used in this study to evaluate the behaviors of granular materials. Specifically, the different sizes of the particles at three gradations (dense-graded, SMA, and open-graded) will be evaluated. Eventually, the sensing data and the simulation data will present a comprehensive understanding of the compaction mechanism of the asphalt mixture.

Discrete Element Method Modeling

The Particle Flow Code (PFC) 3D commercial DEM program from Itasca was utilized to investigate the particle kinematic behaviors during compaction. Only the asphalt mixture under the Superpave Gyratory Compaction (SGC) was simulated as the complexity to simulate the field asphalt compaction. In the discrete element modeling, the PFC 3D adopted several assumptions to simply the simulation process:

(1) All particles are assumed to be rigid bodies, and the deformation of the particle system is the summation of deformations in contact points of all particles.

(2) The contacts between particles happen at a tiny, small area (i.e., contact at point). However, the contact behavior of particles allows overlapping between rigid particles. This overlap is small compared to the particle size and its motion.

(3) The time step is small enough to enable each particle to only have a force effect on its contacted particles and will not affect other particles. The values of speed and acceleration are constant in such a small-time step, and the disturbances cannot propagate to any particles further than their immediate neighbors.

In the DEM modeling, if all the aggregates were simulated based on their real size and angularity, the great number of elements would affect the effectiveness and efficiency of the compaction simulation. Therefore, relevant simplifications were needed for the element generation. Chen et al. (2013) have investigated the effect of the minimum particle size on the simulation results of the DEM model, the result shown in Figure 5-5 pointed out that when the minimum particle size is smaller than 4.75mm, the variation of the air voids between the test results and DEM simulation is greatly reduced. In PFC 3D, the morphological characteristics of the aggregates can be generated using the clump. However, dozens and even hundreds of ball elements are needed to make a single clump (i.e., aggregate particle), which, on the other hand, significantly decreases the simulation efficiency. Comparably, the ball elements are widely adopted in many DEM simulations, and many scholars have discovered that using the ball elements can obtain reasonable kinematic and mechanical behaviors when the other conditions are well-established, such as the contact model, simulation calibration, etc. Therefore, all the aggregates larger than 2.36mm are generated based on their real size in the ball element, and the aggregates smaller than 2.36mm and asphalt binder were combined as asphalt mastic and represented by 2mm diameter ball elements. In this way, the

total number of ball elements can be controlled at a reasonable range to maintain the balance between computation efficiency and simulation accuracy (Nunn, 1978).

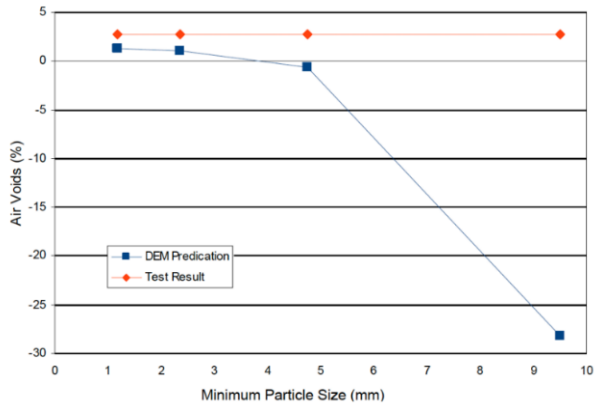

Figure 5-5 Effect of minimum particle size on the simulation results (Jing Chen et al., 2013)

Three gradations of asphalt mixtures were simulated in the DEM model to investigate the particle kinematic behaviors during compaction. These three gradations are a dense-graded mix (DGM), stone-matrix asphalt (SMA), and open-graded friction course (OGFC). The gradation of three mixtures is summarized in Table 5-2 and Figure 5-6.

Table 5-2 Gradation of three types of asphalt mixtures

Sieve No.	Sieve size (mm)	%Passing (DGM)	%Passing (SMA)	%Passing (OGFC)
3/4"	19	100	100	100
1/2"	12.5	91	95	96
3/8"	9.5	74	85	66
#4	4.75	43	31	21
#8	2.36	29	19	8
#16	1.18	19	15	6
#30	0.06	12	12	5
#50	0.03	8	11	4

#100	0.015	6	9	3
#200	0.0075	4	8	2
Asphalt Content		5.8%	6.9%	6.0%

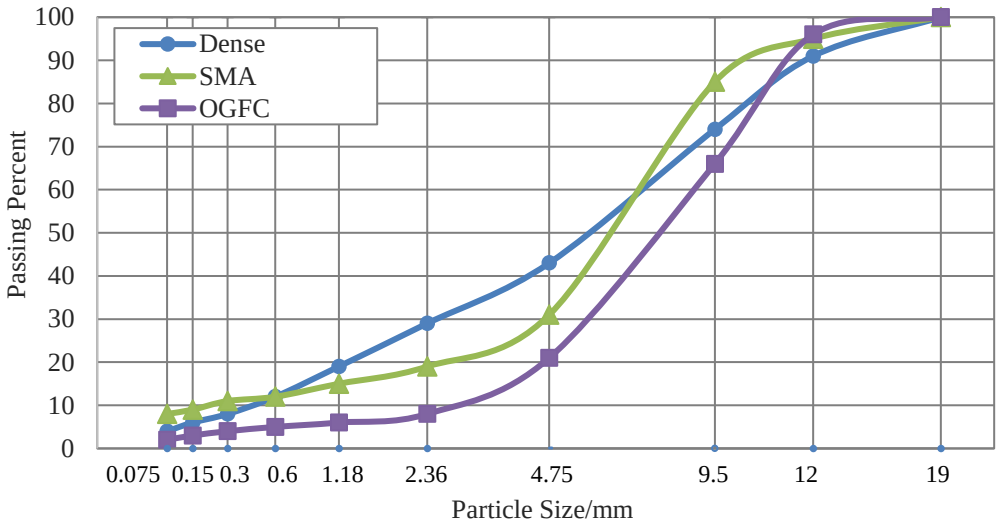

Figure 5-6 Gradation of three types of asphalt mixtures

During SGC compaction, the gyration angle of 1.15 degrees was set in the simulation. The particle volume of each particle size was calculated according to their gradation. Burger's model, as shown in Figure 5-7, was used to simulate the viscoelastic behaviors between particles. To investigate the effect of particle size on their behavior, four sizes of particles were generated for monitoring their rotation during compaction, including 12.5mm, 9.5mm, 4.75mm, and 2.36mm. The monitoring particles used a cube shape to better correlate the sensing data collected by the cubic SmartKli®. The DEM model will be calibrated based on the particle kinematic behaviors of the sensing data. These calibrated parameters include the contact model parameter, compaction loading, friction, damping ratio, etc.

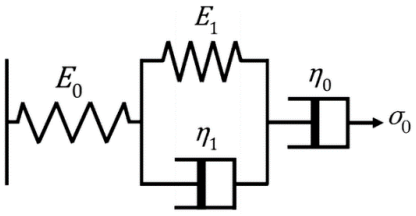

Figure 5-7 Burger's model for viscoelasticity simulation

Two assumptions were further made to realize the efficient gyratory compaction: (1) The scale of samples was reduced to 100mm diameter. The aggregate gradation was strictly controlled to ensure that the maximum aggregate size was smaller than one-third of the sample's diameter. (2) The gyration was accelerated by a scale factor so that the container could rotate with adequate efficiency. Gong et al. (2018) compared the simulation efficiency of the compaction mold of 100mm with that of 150mm. It showed that similar simulation results were achieved for both molds but only took ¼ of the simulation time for the smaller one. Moreover, the largest aggregates are smaller than 1/3 of the mold diameter, and the monitored particles are in the center of the mold. Therefore, using a 100mm-diameter mold is a reasonable simplification for the asphalt compaction at a 150mm-diameter mold. Eventually, the DEM simulation process as demonstrated in Figure 5-8 is summarized as follows:

(1) Generate compaction cylinder mold.

(2) Generate the cubic elements at the center area of the mold and fix its motion and rotation.

(3) Randomly generate particles in the mold according to the gradation of the asphalt mixture.

(4) Apply the inherent properties to the elements, including gravity, and density. Let the system relax until the unbalanced force reaches 0.01% of the contact force.

(5) Free the cubic particles and enable the unbalanced force to relax to 0.01% of the contact force.

(6) Generate the top plate and move the plate to the top of the particle system.

(7) Apply specific compaction loadings and spin the container around the center point of the top

plate simultaneously to simulate the process of the gyratory compaction.

(8) Record the Euler angles of the cubic particles during compaction.

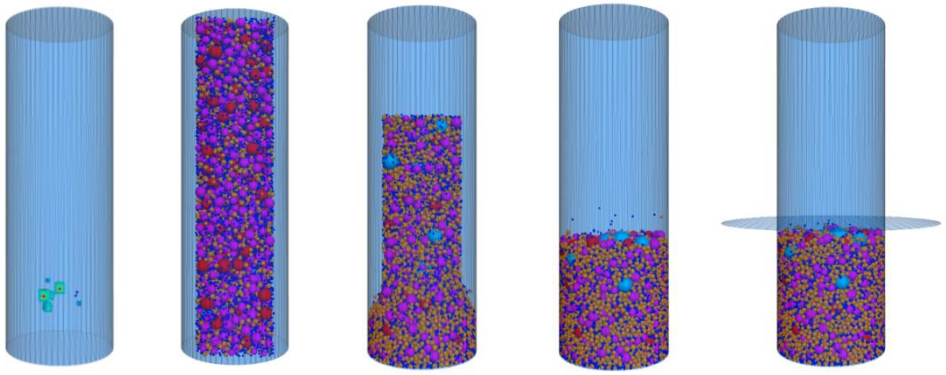

Figure 5-8 DEM simulation of the gyratory compaction

Model Correlation Using Sensing Data

In the DEM modeling, several parameters need to be determined and calibrated to ensure that the particle rotation is relatively equivalent to the ones collected by the wireless sensor. To make the simulation more reasonable, the monitoring particles in the DEM model were generated in the center of the asphalt particle elements as the real compaction did. Since the mold in the DEM was simulated 2/3 of the real size, an 18mm cube was used to simulate the 27mm sensor. The correlation will be made based on the magnitude and trend of the particle rotation. These critical parameters in the modeling include the value of Burger's model parameters, compaction loadings, particle friction, and damping. For clarification, the calibration process was conducted based on the sense-graded asphalt mixture.

Particle Contact Model

Burger's model was used to simulate the viscoelastic behaviors between asphalt particles during compaction. As shown in Figure 5-7, Burger's model is a series connection of one Maxwell model (a spring and a dashpot connected in series) and one Kelvin model (a spring and a dashpot connected in parallel). Two spring stiffness K_k, and K_m, two dashpot viscosity C_k, and C_m, and both normal and shear components were considered for each spring and dashpot parameter. A total of eight parameters need to be determined, including K_{kn}, K_{ks}, K_{mn}, K_{ms}, C_{kn}, C_{ks}, C_{mn}, and C_{ms}. The values of Burger's model parameters were calculated based on the dynamic modulus of the asphalt mixture at the simulated temperature. The relationship between the dynamic modulus and the phase angle of the asphalt mixture and the parameters in Burger's model is summarized in Equations 5-2 and 5-3 based on viscoelastic theory. The microscale parameter of Burger's model can be determined based on Equation series 5-4 (Yu and Shen, 2013) (Christensen and Anderson, 1992). Chen et al. (Chen, 2011) determined the parameters of Burger's model at the temperature of 150°C using the theory elaborated above. His DEM simulation results are consistent with the compaction tests, indicating the reasonableness of the determined parameters. Therefore, the initial values for the parameters of the Burger's model are:

$\boldsymbol{K_{kn}}$=6.40e3 Pa, $\boldsymbol{K_{mn}}$=9.98e4 Pa, $\boldsymbol{C_{kn}}$=1.86e5 Pa•**s**, and $\boldsymbol{C_{mn}}$=5.16e6 Pa•**s**.

$\boldsymbol{K_{ks}}$=2.10e4 Pa, $\boldsymbol{K_{ms}}$=3.33e4 Pa, $\boldsymbol{C_{ks}}$=6.20e4 Pa•**s**, and $\boldsymbol{C_{ms}}$=1.72e6 Pa•**s**.

$$|E^*| = \frac{1}{\sqrt{(D')^2+(D'')^2}} = \frac{1}{\sqrt{(\frac{1}{K_m}+\frac{K_k}{{K_k}^2+\omega^2{C_k}^2})^2+(\frac{1}{\omega C_m}+\frac{\omega C_k}{{K_k}^2+\omega^2{C_k}^2})^2}} \tag{5-2}$$

$$\delta = tan^{-1}\left(\frac{D''}{D'}\right) = tan^{-1}\left(\frac{K_m}{\omega C_m}\,\frac{{K_k}^2+\omega^2{C_k}^2+\omega^2 C_k C_m}{{K_k}^2+\omega^2{C_k}^2+K_k K_m}\right) \tag{5-3}$$

$$K_{ms} = \frac{K_m L}{1+\nu} \quad K_{mn} = K_m L \quad C_{ms} = \frac{C_m L}{1+\nu} \quad C_{mn} = C_m L$$

$$K_{ks} = \frac{K_k L}{1+\nu} \quad K_{kn} = K_k L \quad C_{ks} = \frac{C_k L}{1+\nu} \quad C_{kn} = C_k L \tag{5-4}$$

Where, E^* is the dynamic modulus; δ is the phase angle; D' is the real part of the complex compliance, and D'' is the imaginary part of the complex compliance; w is the radian frequency. Where ***L=R(A)+R(B)***, which is the summation of the radius of two contact balls. ν the Poisson's ratio, which is set to 0.5 for asphalt mastic (Christensen and Anderson, 1992). For clarification of these microscale notations, capital ***K*** means the spring stiffness and capital ***C*** means the dashpot viscosity. The first subscript ***k*** means the source of the spring, i.e., the Kelvin model, and ***m*** represents the source of the Maxwell model. The second subscript ***n*** means the normal component, and ***s*** indicates the shearing component.

Compaction Loadings

During DEM modeling, several simplifications were conducted to maintain the computing efficiency and simulation accuracy of the particle rotation during compaction. Under this condition, the compaction loading needs to be adjusted based on the SGC compaction loading of 600KPa. Five pressures were simulated to investigate their effects on the particle relative rotation, the simulation results are presented in Figure 5-9. As seen at a 100KPa compaction pressure, the fluctuations and the magnitude of the relative rotation are in a small range. A possible reason for this is that the skeleton was hard to form under the low compaction loadings so the loadings cannot be appropriately transformed between aggregates. Comparably, the relative rotation reduced very quickly at 600kPa, and there were very limited fluctuations at the stabilized stage, which is not

consistent with the real situation. The particle rotation at 200kPa, 300kPa, and 400kPa presented a similar trend of particle rotation as the sensing data, and the magnitude of the particle rotation was in a reasonable range. However, the maximum value of the relative rotation at the beginning of the compaction still indicates a discrepancy. That might be related to the smaller size of the monitoring cube compared with SmartKli®. Eventually, a 300kPa compaction pressure was utilized in the DEM model to simulate the particle's relative rotation during compaction.

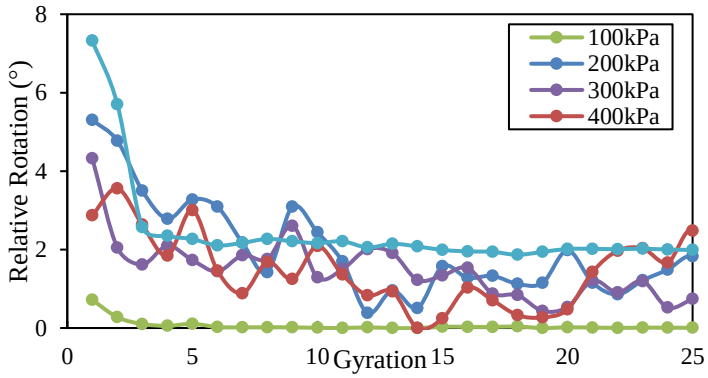

Figure 5-9 Effect of the compaction pressure on the particle rotation during DEM simulation

Friction coefficient and damping ratio

The friction coefficient is the ratio of the frictional force resisting the motion of two contact surfaces to the normal force pressing the two surfaces together (Hanaor et al., 2016). The friction coefficient is a critical parameter affecting the particle's kinematic behaviors during compaction. During the high-temperature compaction of the asphalt mixture, the viscous binder was coated around the aggregates and reduced their friction. Based on the friction angle of the mineral aggregates, many scholars used 0.5 as the friction coefficient (Abbas et al., 2005), and some adopted 0.3 for the DEM simulation (Zhou et al., 2020; Gong et al., 2018). In this section, the effect of the friction coefficient on the particle's relative rotation during compaction was investigated.

Three friction coefficients were selected, and the simulation results were presented in Figure 5-10. As seen, the smaller value of the friction resulted in a larger fluctuation of the relative rotation during compaction, which is agreeable with the common engineering knowledge that higher friction hinders the particle kinematic behaviors. By comparing the magnitude and trend of the relative rotation in the simulation with sensing data, the friction coefficient of 0.5 was determined for the following DEM simulation.

The damping ratio is to describe how oscillations in a system decay after a disturbance in physical systems (Escudier and Atkins, 2019). A range of 0-1 was used in the DEM models to allow the loss of the energy of the system by dissipating. Four values of the damping ratio were simulated in the DEM model to investigate its effect on particle rotation. As shown in Figure 5-10, the particle rotation under the damping ratio of 0.1 demonstrates a great distinction with the rest of the scenarios. The small value of the damping ratio indicates a limited dissipation of the energy during compaction, thereby a larger fluctuation of the particle rotation. With the increase of the damping ratio, the particle rotation stabilized, and the curve of the particle rotation became more consistent with the sensing data. Eventually, a damping ratio of 0.5 was selected in the DEM simulation of the asphalt mixture.

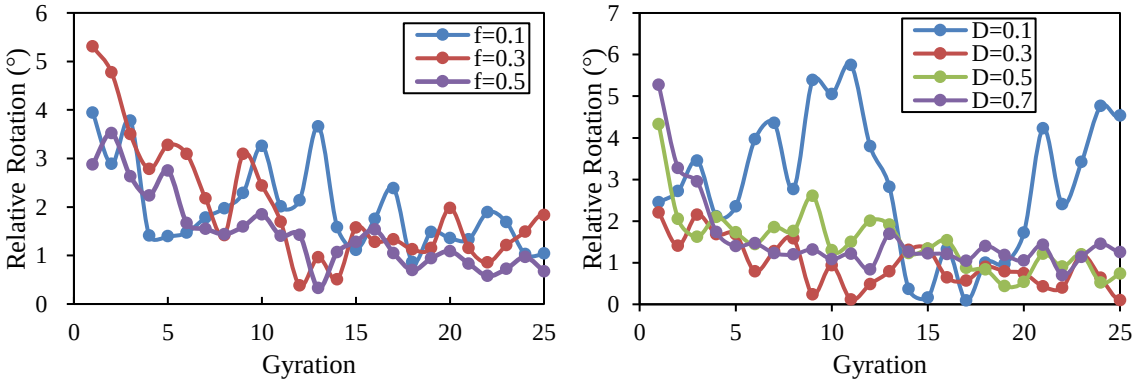

Figure 5-10 Effect of the friction coefficient (left) and dump ratio (right) on the particle rotation

Particle Behaviors at Different Scenarios

Model Repeatability

After sensitive analyses, the values of the contact model, compaction pressure, efficiency of friction, and damping were determined based on the sensing particle rotation during the gyratory compaction. The coarse aggregates (larger than 2.36mm) were molded as spherical elements according to their real size. The fine aggregates (smaller than 2.36mm) and mastic were using a 2mm sphere for simulation. The numbers of each size of the particles were determined following the gradation curve. For the different types of asphalt mixtures, the same volume was simulated in the DEM model for comparison. All parameters are summarized in Table 5-3.

Table 5-3 Summary of the DEM parameters

		DGM	SMA	OGFC
Numbers of particles	12.5 mm	30	13	10
	9.5 mm	83	86	222
	4.75 mm	784	1505	1103
	2.36 mm	6957	2705	2534
	2 mm	9380	11159	9703
Compaction Pressure (kPa)		300		
Friction		0.5		
Damp		0.5		

Note: The numbers of 2.36mm particles are the particle diameter range from 2.36 mm-4.75 mm, so are the 4.75mm, 9.5mm, and 12.5mm. The number of 2mm particles is the 2mm-diameter ball.

The simulation results are not the same as the sensing data collected during the gyratory compaction, but the magnitude of the particle rotation and the trend of its curve are in a reasonable

range. The simulation repeatability of the asphalt compaction using the DEM models was then evaluated. Only 30 gyration cycles were simulated for time saving. Three independent simulations were conducted based on the dense-graded mixture and the determined parameters shown in Table 5-3. A cube was generated in the center of the ball system to simulate the SmartKli®. The same relative rotation was calculated based on the simulation data, as presented in Figure 5-11. As seen, the repeatability of the relative rotation from three simulations is reasonable with limited variations. The curve trend is consistent with the relative rotation collected by the sensor: the particle rotates at a high value at the beginning and then decreases to a stabilized value. Therefore, the determined contact model and parameters are reasonable and will be used for the following evaluation.

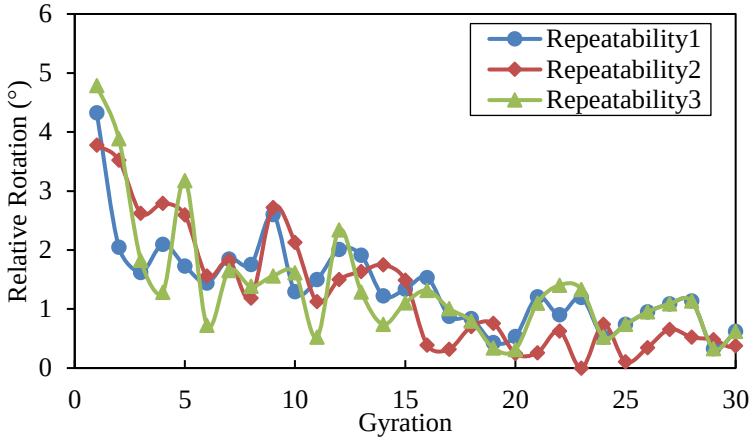

Figure 5-11 Repeatability of the particle relative rotation in DEM simulation

Particle Rotation of Difference Particle Sizes

To investigate the particle rotation of different sizes of the aggregates, eight cubes were generated in the center of the mold before compaction. To clarify, these eight cubes contain four different particle sizes: 12.5mm, 9.5mm, 4.75mm, and 2.36mm, and two particles for each size. The particle rotations of the eight cubes were recorded during 80 cycles of gyratory compaction.

The compaction of the dense-graded mix was first simulated. The particle rotation for four sizes of aggregates was summarized in Figure 5-12.

For the curve throughout the entire compaction, the coarse aggregate of 12.5mm, 9.5mm, and 4.75mm displayed a high resemblance, which is also identical to the height curve of the asphalt specimen during compaction. The highest particle rotation occurred at the beginning of the compaction and rapidly decreased to a relatively stable level but with fluctuations. Considering the magnitude of the particle rotation, the larger rotation and higher fluctuations were observed on the smaller asphalt particles, which is agreeable with common engineering knowledge. However, the rotation curve of the 2.36mm aggregate displayed a different trend. The largest rotation occurred at the middle stage of the compaction instead of at the beginning. This might be related to the formation of the skeleton and force chain. The coarse aggregates were compacted at the beginning to form the skeleton so that the force could be appropriately transferred between aggregates. Before that, the rotation of the fine aggregates was limited. Until roughly 40 gyrations, the fine aggregates started their dramatic rotation under the imbalanced forces and maintained a high value even at the late stage. It can be assumed that the fine aggregates were actively affected by the compaction loadings regardless of the compaction stages they were at. The fine aggregates would continue rotating to dissipate the applied energy if the compaction didn’t stop. Therefore, the behaviors of the fine aggregates are not recommended to evaluate the compactability or workability of the asphalt mixture. However, the definition of the fine aggregates of different gradations needs to be clarified in the following research.

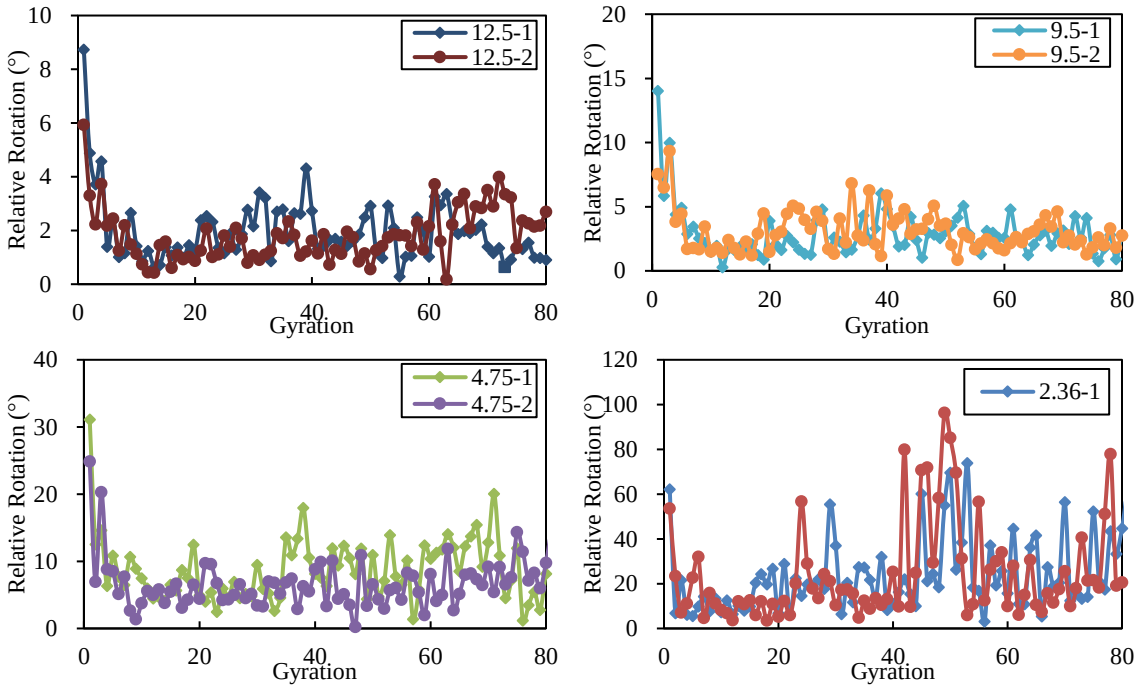

Figure 5-12 Relative rotation of the particle's size of 12.5mm (top left), 9.5mm (top right), 4.75mm (bottom left), and 2.36mm (bottom right) in a dense-graded mix

Particle Behaviors at Various Observation and Characterization Levels

The vertical translation of multiple particles was monitored during the DEM compaction. As seen in Figure 5-13, the vertical translation of four sizes of particles is similar in trend but discrepancies in magnitude, which presents the same trend of the specimen height change during compaction. The bulk height of the asphalt specimen monotonically decreased for the applied vertical compaction loadings. Comparably, the particles' vertical translation generally decreased but with a slight increase at the late stage, especially for the coarse aggregates. This might be related to the rearrangement of the smaller aggregates under compaction, the compression from these particles squeezed the coarse aggregates to move upward. The resemblance indicated a consistency between the mesoscale (particle level) properties and bulk scale (specimen level) properties during compaction of asphalt mixture.

The particle rotation and its vertical translation were plotted in Figure 5-14. For aggregates larger than 2.36mm, the particle rotation and its vertical translation demonstrate an analog trend. This interesting phenomenon verified a concurring change between the particle rotation and their vertical translation during compaction. When the coarse particle-stabilized, the vertical translation thereby displayed stability with limited variations. This correlation further verified the previous conclusion that the particle rotation of the coarse aggregate is appropriate for evaluating the workability of the asphalt mixture. For the fine aggregate (i.e., 2.36mm), the particle rotation and vertical translation did not converge in the same trend, especially at the late compaction stage. N summary, the coarse aggregates are more appropriate than the fine aggregate for the workability or compactability evaluation of the asphalt mixture.

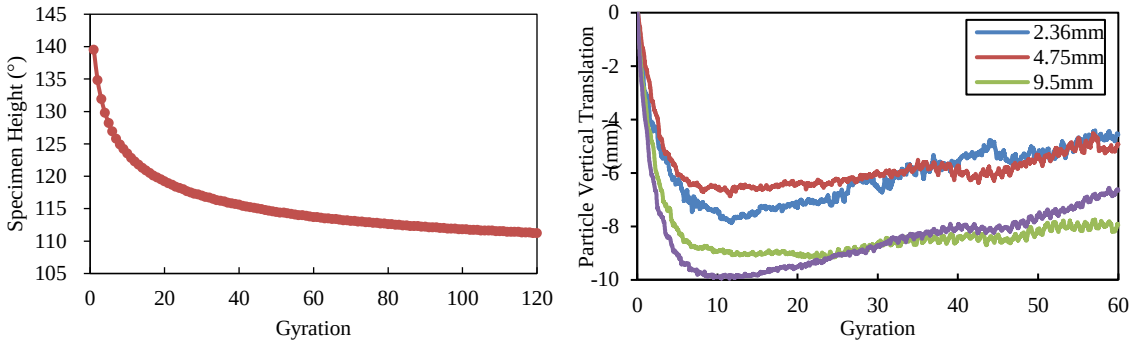

Figure 5-13 Comparison between the height change of the asphalt specimen (left) and various sizes of particles (right) during compaction

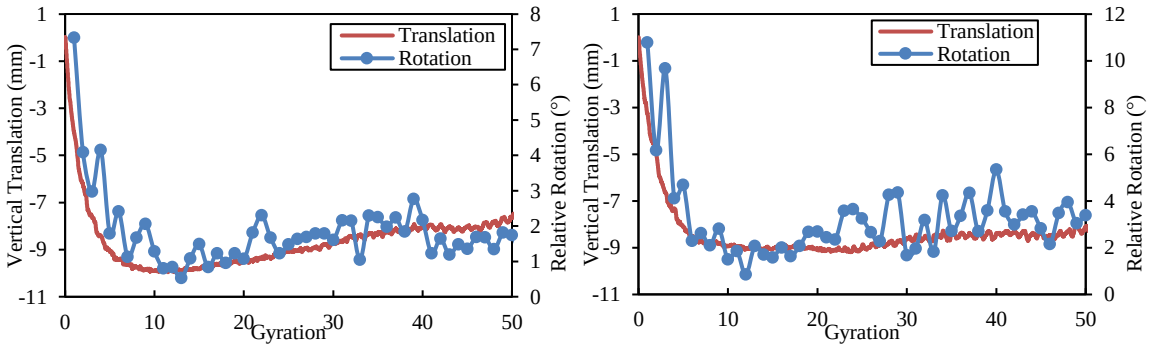

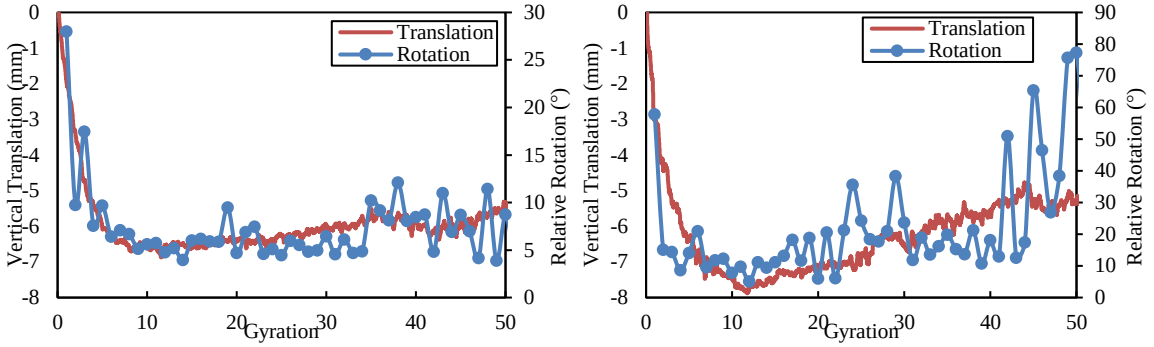

Figure 5-14 Correlation between the particle rotation and its vertical translation for sizes of 12.5mm (top left), 9.5mm (top right), 4.75mm (bottom left), and 2.36mm (bottom right)

Particle Behaviors at Distinct Gradation Levels

Three gradations of asphalt mixtures, including dense-graded mix, Stone mastic asphalt (SMA), and open-graded friction course (OGFC), were simulated in the DEM model to investigate the effect of the mixture gradation on the particle kinematic behaviors during compaction. Similarly, a total of eight particles of four sizes were recorded. The results of the particle relative rotation were summarized in Figure 5-15 to Figure 5-16.

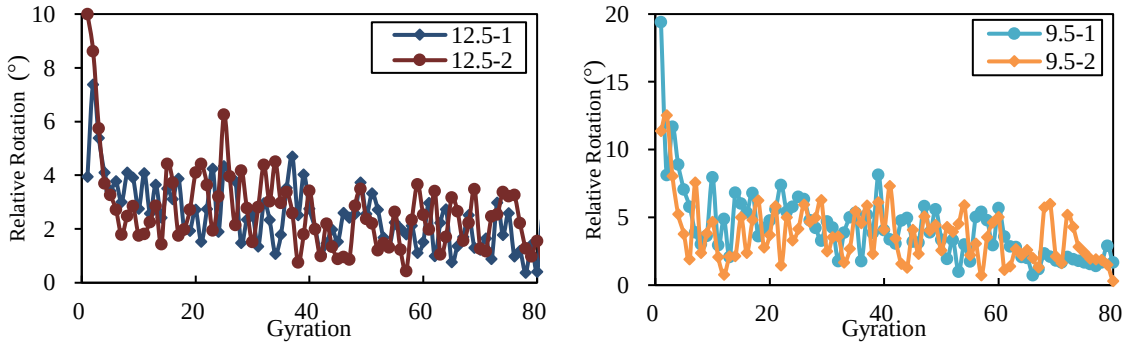

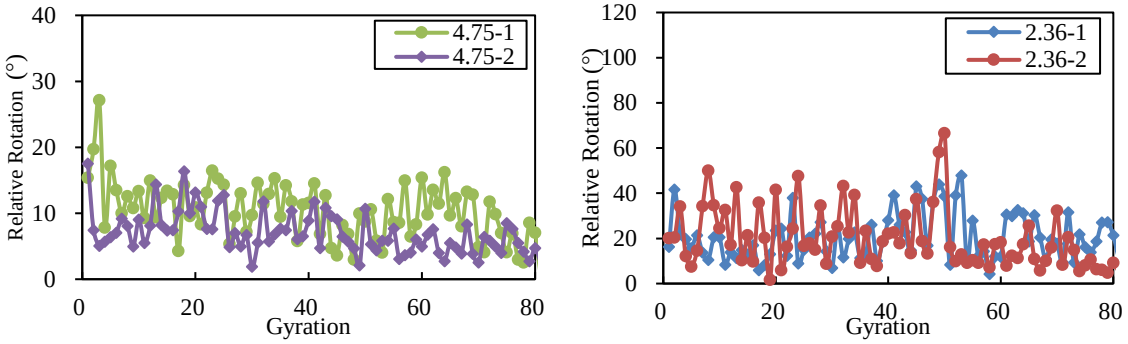

Figure 5-15 Relative rotation of the particle's size of 12.5mm (top left), 9.5mm (top right), 4.75mm (bottom left), and 2.36mm (bottom right) in a SMA

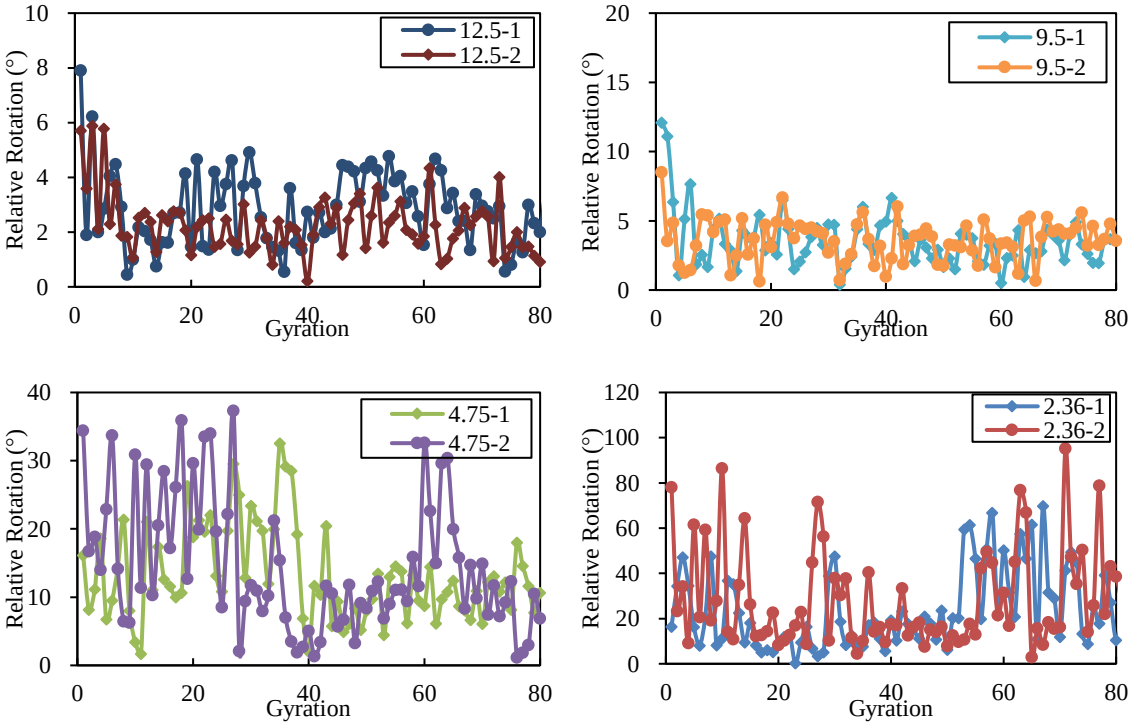

Figure 5-16 Relative rotation of the particle's size of 12.5mm (top left), 9.5mm (top right), 4.75mm (bottom left), and 2.36mm (bottom right) in an OGFC

For the coarse aggregates, the largest particle rotation occurred at the beginning of the compaction and then quickly decreased. This trend is consistent with the height changes of the asphalt specimen during compaction, making the particle rotation of the coarse aggregates an

appropriate indicator to evaluate the workability of the asphalt mixture. On the other hand, the largest particle rotation occurred at the middle stage or even later for the fine aggregates, and the variations of the particle rotation remained high even at the end of the compaction. Therefore, the kinematic behavior of the fine aggregate cannot correlate with the mixture's workability. More importantly, the classification of the coarse and fine aggregates differed from the mix gradation. For the dense-graded mix (DGM) and SMA, particles with sizes of 12.5mm, 9.5mm, and 4.75mm displayed the rotation pattern of the coarse aggregate, and 2.36mm presented the pattern of fine aggregates. However, for the OGFC, 12.5mm, and 9.5mm acted like the coarse aggregates, while 4.75mm and 2.36mm particles acted like the fine ones. This is aggregable with Bailey's method which the definition of the coarse and fine aggregates is associated with the packing and interlocking properties of the aggregates (Vavrik et al., 2002).

The particle rotation of different sizes of the coarse aggregates demonstrated resemblances in trend but variations in magnitude. For the category of coarse aggregates, larger particles rotated less dramatically than the fine ones under the same loadings but with the same trend. This conclusion validated the methodology of using a 27mm SmartKli® to evaluate the workability of the asphalt mixture. Even though it is a bit larger than most aggregates, the kinematic behavior can still be an appropriate parameter for the workability evaluation only at a smaller magnitude. Furthermore, gradation also affected the particle rotation even for the same size of the coarse aggregates. In cases on the 12.5mm aggregates, the particles stabilized earlier for the dense graded mixture than the open graded counterpart. The 12.5mm particles were roughly stabilized under 2° at 15^{th} gyration for the dense-graded mix. The same size of the particles decreased under 2° after around 40^{th} gyration for the SMA, while the particles in OGFC rotated higher than 2° even after 70th. compared with the SMA and OGFC. Therefore, the gradation greatly affected the compaction behaviors at the same compaction conditions. The dense-graded mixture is more prone to be densified and compacted compared to the open-graded mix under the same compaction energies.

Statement of Compaction Mechanism

The compaction mechanism of the asphalt mixture was investigated in this chapter by utilizing sensing technology and numerical modeling. The laboratory gyratory compaction, field roller compaction, and the discrete element method (DEM) were jointly adopted to investigate the particle kinematic behaviors in various scenarios, including particle size, gradation, compaction mechanism, etc. Several conclusions can be drawn accordingly:

- The compaction of the asphalt mixture contains three different stages based on its particle rotation: (1) Breakdown Stage occurs with large relative rotations, a sharp rate of reduction, and the fastest material densification. (2) The Main Compaction Stage is characterized by the formation of the skeleton and imbalanced particles' interaction. Most material densification occurs in this stage but at a relatively low speed. (3) The Finishing Stage is the stabilization stage and maintains relatively balanced interactions between particles. Minimal densification and surface leveling occur in this stage.
- The particle rotation under the laboratory gyratory compaction and field roller compaction presents a high correlation even though their compaction mechanism differs dramatically. The particle rotation thereby can connect the laboratory and field compaction and offers a possible solution to predict the field compaction condition using the more accessible laboratory compaction data.
- The particle relative rotation of the coarse aggregate is highly correlated with its vertical translation and the height change of the asphalt specimen during compaction. This correlation makes it an appropriate parameter to evaluate the workability or compactability of the asphalt mixture. However, fine aggregates' behavior did not present a connection with the translation of the particle or the specimen height during compaction.
- The size of the aggregate affects its rotation under loadings. Smaller particles are more prone

to rotate than coarse ones. However, the general trend of the coarse aggregates remains consistent during the entire compaction. The conclusion verified the methodology of using the SmartKli® to evaluate the workability of the asphalt mixture.

- The classification of the coarse and fine aggregates is dependent on the gradation of the asphalt mixture, which is related to Bailey's theory on the packing and interlocking behavior of the aggregates during compaction.

Based on the results from the compaction experiments and numerical modeling, the compaction mechanism of the asphalt mixture can be summarized:

The compaction process of the asphalt mixture is the coarse particulate materials gain restrictions and interlocking from neighboring aggregates to its self-stability. The particulate asphalt mixtures experience dramatic rotation and a rapid rate of decrease at the beginning, to a relative level of stability at the end. Under this context, a close correlation was identified between the particle rotation and the mixture's density during compaction, making the particle rotation an effective parameter to quantify the density during compaction. Particle rotation is also a measurable parameter both in the lab and field, making it a practical tool for compaction monitoring. Different sizes and gradations have unique rotation characteristics during compaction.

Chapter 6

Workability and Compactability Evaluation

Based on the compaction mechanism of the asphalt mixture, and the correlation between the particle rotation and mixture density, the compactability of various asphalt mixtures will be evaluated in this chapter. A more common terminology, workability, will be adopted to describe the relative ease of compaction of an asphalt mixture under compaction loadings. Three workability evaluation methods will be proposed, including particle kinematic parameters, particle rotation curves, and statistical analysis methodology.

Workability Evaluation Using Particle Kinematic Parameters

Workability Evaluation Parameter

Two new parameters were proposed based on the particle rotation during compaction to quantify and characterize the workability of the asphalt mixture. These two parameters are Relative Rotation Capacity (RRC) and Average Residual Rotation (ARR). Relative rotation capacity (RRC) is defined as the area between the relative rotation curve and the zero-horizontal line (x-axis), as shown in Figure 6-1 and its calculation is shown in Equation (6-1). The particle rotation from the beginning to the initial number of gyration (N_i) was eliminated to guarantee its repeatability, and only the particle rotation from the initial number of gyration (N_i) to the design number of gyration (N_d) was taken into account. Generally, a larger value of the RRC means more active particle rotation under the compaction loadings, hence better mixture workability.

$$RRC = \sum_{i=N_i}^{N_d} \frac{(RR_{i+1}+RR_i)\times l}{2} \qquad (6\text{-}1)$$

Where, RR_i is the relative rotation of the compacted asphalt mixture at i^{th} gyration; N_i means the initial number of gyrations of the compacted asphalt mixture; N_d is the design number of gyration of the compacted asphalt mixture; l is 1 compaction gyration.

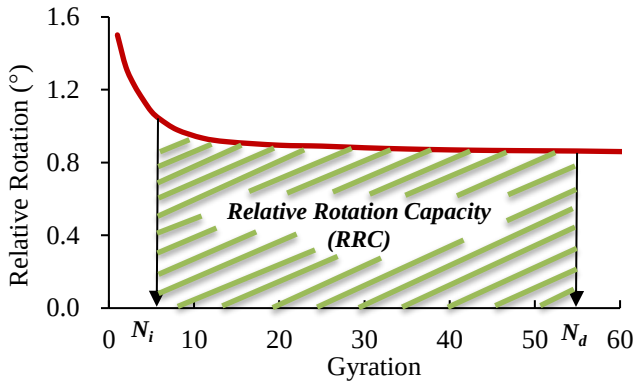

Figure 6-1 Illustration of relative rotation capacity (RRC)

To provide a direct and clear comparison between two asphalt mixtures, residual rotation was defined to evaluate the difference in the relative rotation between two asphalt mixtures (i.e., test mix and control mix) at a corresponding gyration. Figure 6-2 displays the curves of particle rotation of two asphalt mixtures on the left-hand side, and the corresponding residual rotation curve is shown on the right. The residual rotation is the difference in relative rotation between the test mix and control mix, a positive value indicates a more active particle relative rotation for the test mix than the compared control mix. For clarification, the test mix is the minuend (i.e., Mix B), and the control mix is the subtrahend (i.e., Mix A).

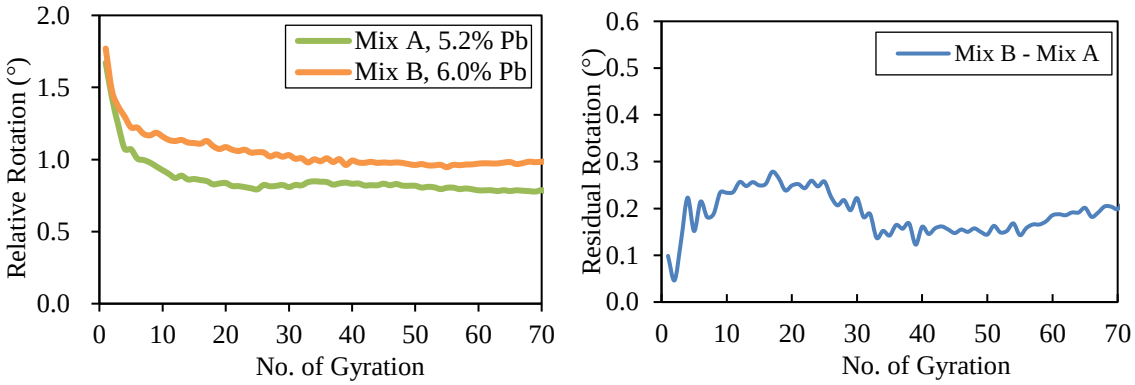

Figure 6-2 Curve of relative rotation (left) and residual rotation (right)

The average residual rotation (ARR) is the average value of the residual rotation from the initial number of gyrations (N_i) to the design number of gyrations (N_d), as shown in Figure 6-3. The parameter ARR can be calculated using Equation (6-2), and it is useful when comparing the workability of a new mixture relative to a control mixture. Particularly, the positive value of the ARR means the active particle rotation of the test mix compared to the control mix, hence better workability. In addition, the ARR can also be used to investigate the effects of various compaction conditions (e.g., compaction temperature) or mixture designs (e.g., additives or binder modifiers) on the workability of the asphalt mixture. In ARR calculation, the average relative rotation of each mix type is recommended to determine this parameter.

$$ARR = \sum_{i=N_i}^{N_d} \frac{(RR_{t,i} - RR_{c,i})}{N_d - N_i} \times A \qquad (6\text{-}2)$$

Where, $RR_{c,\,i}$ is the relative rotation of the control mix at i^{th} gyration; $RR_{t,\,i}$ is the relative rotation of the test mix at i^{th} gyration; A is an amplification factor for adjusting the sensitivity of the parameter, use 10 as the default.

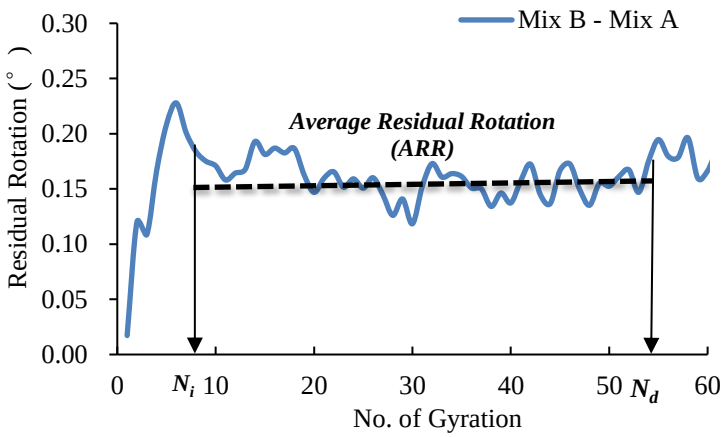

Figure 6-3 Illustration of average relative rotation (ARR)

Conventional Workability Parameters

To validate the evaluation of the ARR and RRC on the mixture's workability, a correlation was then conducted between the existing workability parameters and the new parameters. A total of six existing parameters were involved in this comparison, including three volumetric parameters and three mechanical parameters. The volumetric parameters are the gyration at 92%G_{mm}, air voids at $N_{d,}$ and locking point. Specifically, the %G_{mm} at any gyration of a specimen during gyratory compaction can be determined by equation (6-3). The concept of locking point is based on a simple height-base pattern, which is the second instance of two consecutive gyrations resulting in the same sample height (Xinjun and Gibson, 2011).

Three mechanical parameters are the compaction densification index (CDI), compaction force index (CFI), and normalized shear index (NSI). Specifically, CDI is the area under the densification curve from 8th gyrations to the number of gyrations to achieve 92%G_{mm}. It evaluates the energy required to compact the mixture to the desired density (as shown in Figure 6-4). CFI indicates how much resistive effort is needed to compact the mixtures from N_i to 92%G_{mm}. The resistive effort W in the CFI can be calculated by equation (6-4) (Guler et al., 2000; Stakston et al.,

2002). NSI is the summation of the normalized internal shear frictional resistance from the second gyration to when the specimen reached 92%G_{mm}. In determining the internal shear frictional resistance during compaction, it is assumed the sample is fully constrained and the energy due to surface traction is negligible. The shear resistance $\boldsymbol{\tau}$ at any gyration cycle can be written by equation (6-5) based on the law of energy conservation in Figure 6-5. Generally, the larger value of the mechanical parameters means more resistance is needed to overcome while compacting the materials, hence the worse workability (Mahmoud and Bahia, 2004).

$$\%G_{mm,i} = \frac{h_{end}}{h_i} \times \frac{G_{mb}}{G_{mm}} \quad (6\text{-}3)$$

$$W = \frac{4ePQ}{V} \quad (6\text{-}4)$$

$$\tau = \frac{M+PVQ}{V} \quad (6\text{-}5)$$

Where, $\%G_{mm,i}$ means the %G_{mm} of the specimen at *i*th gyration. h_{and} means the height of the specimen when compaction ended. h_i is the specimen height at i^{th} gyration; G_{mb} is the bulk specific gravity of the specimen when compaction ends. G_{mm} is the maximum specific gravity of the asphalt mixture. *e* is the eccentricity of the resultant force. *P* is the magnitude of the resultant force. *Q* is the tilting angle. M is the compactor torque. V is the volume of the specimen.

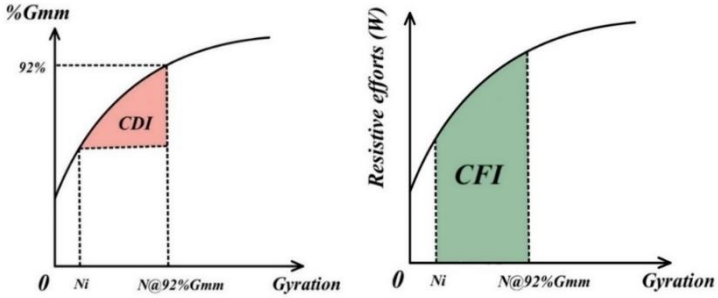

Figure 6-4 Illustration of CDI (left) and CFI (right)

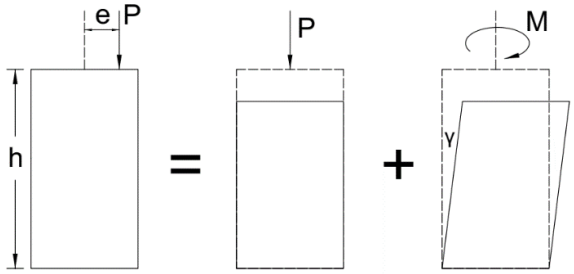

Figure 6-5 **Shearing during the SGC compaction**

Materials Used for Experiments

Five mixtures were used for comparison, as summarized as No.3~7 in Table 4-1. Detailed information on mix and experiment design was provided in Figure 6-6 and Table 6-1. The five mixtures are from a based mix, of which the differences are the dosage rate of the WMA additives (i.e., Evotherm M1) and mixing and compaction temperature. Evotherm M1 is a chemical additive that can improve the coating of aggregates by reducing the surface energy of the aggregate/binder interface and the inner friction (Li et al., 2016; Olivier et al., 2016). The temperature and dosage of the additives were determined based on the performance grade of the asphalt binder. To prepare for the WMA mixture in the laboratory, an appropriate dosage of the WMA additive is first added to the PG64-22 asphalt binder and hand-mixed at the desired temperature until fully mixed, following

the recommendations from WMA additive manufacturers. Such modified asphalt binder is then mixed at a target mixing temperature with aggregates to produce loose mixtures.

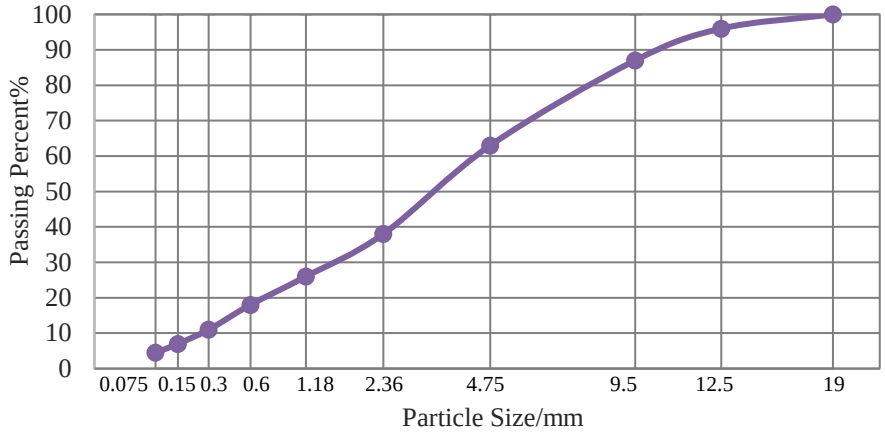

Figure 6-6 Gradation curve of the base asphalt mixture

Table 6-1 Information on the asphalt mixtures and the experiment conditions

Mix	Mix type	Additive	Asphalt	Mixing temp	Compaction temp
No. 1	HMA-12.5	0%	PG 64-22	118℃ (245℉)	110℃ (230℉)
No. 2	HMA-12.5	0%	PG 64-22	157℃ (315℉)	143℃ (290℉)
No. 3	WMA-12.5	0.35%	PG 64-22	135℃ (275℉)	127℃ (260℉)
No. 4	WMA-12.5	0.70%	PG 64-22	118℃ (245℉)	110℃ (230℉)
No. 5	WMA-12.5	0.70%	PG 64-22	157℃ (315℉)	143℃ (290℉)

Correlation with Existing Parameters

Three groups of parameters were calculated on the five asphalt mixtures. The same weight of asphalt mixtures was used under various compaction conditions. During compaction, three test specimens were compacted to collect the particle kinematic behaviors using SmartKli®, and a

reference specimen was produced to test the mixed volumetric properties. All parameters are presented in Table 6-2, Figures 6-7, and Figure 6-8. As seen, the parameters and their errors were calculated from three replicated specimens. The air void is determined by the reference specimen, and the RRC is calculated based on the average residual rotation, so no errors were presented.

A consistent workability was observed for the five mixes, and the workability form low to high is: No. 1 < No. 2 < No. 3 ≈ No. 4 < No. 5. It is reasonable according to the mixture design and production temperature. However, the sensitivity of each parameter differed considerably. The mechanical parameters are more sensitive than the volumetric parameters. The kinematic parameters, including relative rotation capacity (RRC) and average residual rotation (ARR), presented the highest sensitivity. It should also be noted that more asphalt mixtures are needed to investigate the efficacy of the new parameters.

Table 6-2 Workability evaluation parameters for all mixtures

Mix	Volumetric			Mechanical			Kinematic	
	N_i	*Va*	LP	CDI	CFI	NSI	RRC	ARR
No. 1	25±0	3.77%	52±1	1623.5±0.5	897.4±22.4	23.3±0.2	54.45±7.70	-0.83
No. 2	22±0	3.28%	53±1	1355.2±0.4	724.7±0.2	19.9±0.4	60.12±4.20	0
No. 3	20±0	2.83%	53±1	1177.2±0.1	677.8±16.6	18.4±0.0	62.43±1.71	0.34
No. 4	20±0	2.76%	51±2	1176.7±0.6	695.0±23.5	18.2±0.1	61.73±4.77	0.41
No. 5	18±0	2.56%	51±4	995.6±0.1	596.3±3.4	16.2±0.0	65.69±6.95	0.82

Note: $\boldsymbol{N_i}$ means the $\boldsymbol{N_i}$**@92%**$\boldsymbol{G_{mm}}$, ***Va*** is the ***Va*** **@**$\boldsymbol{N_{design}}$, and **LP** represents the locking point.

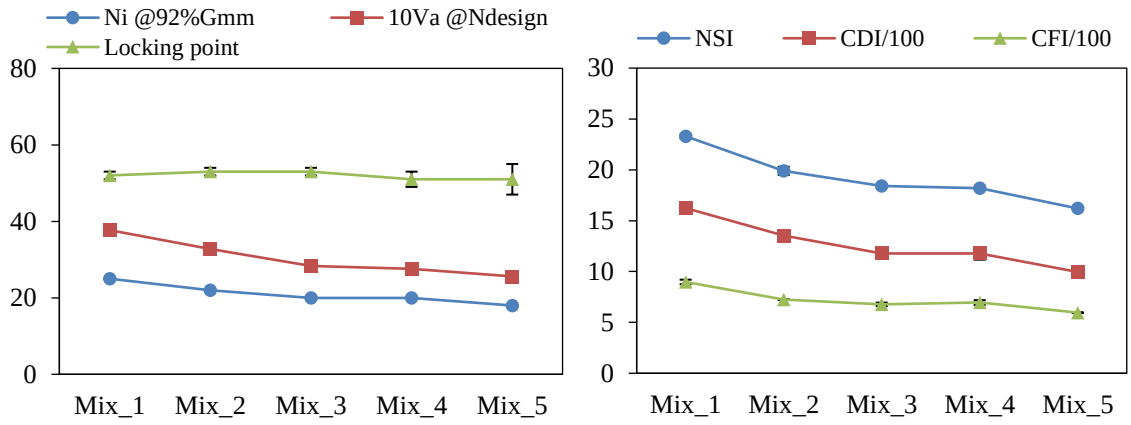

Figure 6-7 Workability evaluation by volumetric (left) and mechanical (right) parameters.

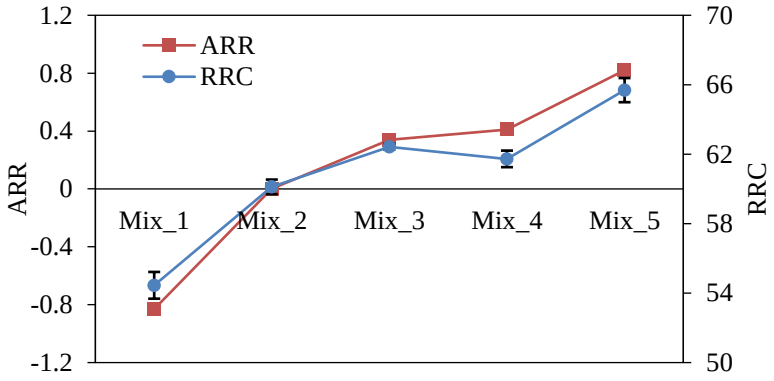

Figure 6-8 Workability evaluation by kinematic parameters

Workability Evaluation Using Particle Rotation Curves

The kinematic parameter can evaluate the mixture's workability based on the compaction efforts or particle behaviors during compaction. However, a single value of the parameter provided limited information for mix design or comparison. The compaction curve can illustrate the change in particle rotation during the whole compaction stage, which offers more insights into improving the mixture's design accordingly.

The curves of particle kinematics will be used to investigate the various effects on the mixture's workability, including asphalt content, compaction temperature, WMA additives, plastic processing methods, and their combined effects. As explained, the relative rotation is highly correlated with the mixture's density, making it an appropriate parameter for the workability evaluation. Generally, higher values of the relative rotation represent more active particle rotation during compaction, and thus better workability of an asphalt mixture. The residual rotation curve is another approach for workability evaluation. Compared with the relative rotation curve, it is clearer to evaluate the workability differences between two asphalt mixtures. The residual rotation is the difference in the relative rotations between the test mix (minuend) and the control mix (subtrahend).

Materials Used for Experiments

Twelve types of asphalt mixtures from two based mixtures were used in this section. Base mix No.1 (Mix No. 1~5 in Table 6-3) is a PG64-22 mix with a 6.0% optimal binder content and N_{design} of 75. Its nominal maximum aggregate size (NMAS) is 12.5mm. Base mix No. 2 (Mix No. 6~12) is with 5.9% PG64-22 optimal asphalt binder content and N_{design} of 75. The NMAS is 12.5mm. The aggregate gradations for the two base mixes are provided in Table 6-4.

Table 6-3 Detailed information on the asphalt mixtures

No.	Mix	Additives	NMAS	RAP	OVAC	Asphalt	Temp
1	HMA	N/A	12.5	0%	5.9%	PG64-22	110℃
2	HMA	N/A	12.5	0%	5.9%	PG64-22	143℃
3	WMA	0.35% Evotherm	12.5	0%	5.9%	PG64-22	127℃
4	WMA	0.7% Evotherm	12.5	0%	5.9%	PG64-22	110℃
5	WMA	0.7% Evotherm	12.5	0%	5.9%	PG64-22	143℃

6	HMA	N/A	9.5	15%	5.2%	PG 64-22	135℃
7	RPMA	9% LDPE (dry)	9.5	15%	4.73%	PG 64-22	135℃
8	RPMA	9% LDPE (wet)	9.5	15%	4.73%	PG 64-22	135℃
9	HMA	N/A	9.5	15%	6.0%	PG 64-22	135℃
10	RPMA	9% LDPE (dry)	9.5	15%	5.46%	PG 64-22	135℃
11	RPMA	9% LDPE (wet)	9.5	15%	5.46%	PG 64-22	135℃
12	RPMA	9% LDPE (dry)	9.5	15%	6.0%	PG 64-22	135℃

Note: RPMA is the recycled plastic-modified asphalt mixture. LDPE is the Low-Density Polyethylene. 9% LDPE in the column of "Additives" is the mass ratio of the LDPE to the asphalt content.

Table 6-4 Gradation of the two base mixes

Sieve No.	**Sieve size (mm)**	**%Passing of No.1**	**%Passing of No.2**
1/2"	19	100	100
1/2"	12.5	100	100
3/8"	9.5	87	96
#4	4.75	63	66
#8	2.36	38	40
#16	1.18	26	25
#30	0.06	18	18
#50	0.03	11	14
#100	0.015	7	9
#200	0.0075	4.5	6

The first batch of the asphalt mixtures (Mix No. 1~5) from the base mix No.1 are primarily different from the WMA additives (i.e., Evotherm M1). The Evotherm M1 and the producing methods for the WMA mixtures were already elaborated before, and no more explanations will be introduced here. The effect of WMA additives and temperature on the workability of the asphalt mixture can be evaluated. The second batch of the asphalt mixtures (Mix No. 6~12) from the base mix No.2 used different plastic processing methods. Low-Density Polyethylene (LDPE) was used

for its lower melting point and special geometry. They are very thin flakes of plastic film and are more suitable to interact with the binder, hence increasing the binder's lubricating effect (Caputo et al. 2020). LDPE was sourced from recycled agricultural films with shredded particles of irregular sizes and shapes. The nominal maximum dimension of any given particle is less than 1 cm, as shown in Figure 6-9.

Figure 6-9 Shredded LDPE particles used in this study

The impact of asphalt content on the mixture's workability can be analyzed by comparing the mixes with reduced asphalt content (No. 6-8) to those with optimal content (No. 9-11). Each asphalt content level was evaluated for three different mix types: virgin mix (without LDPE involvement), LDPE-modified mix using dry processing, and LDPE-modified mix using wet processing. This allows for assessing the influence of plastic processing methods. In the case of the dry method, two designs were considered: the conventional method, which typically replaces a portion of the virgin binder in the mix for economic reasons (Lugeiyamu et al., 2021; Movilla-Quesada et al., 2019), as demonstrated by Mix No. 7 and No. 10. An alternative dry method that omitted the replacement of the virgin binder was also prepared (Mix No. 12). Throughout the production of the asphalt mixtures, consistent experimental conditions were maintained. The LDPE

dosage was fixed at 9% by weight of the asphalt binder. All mixtures were laboratory-mixed and compacted using a Superpave gyratory compactor (SGC).

The procedures of the dry and wet processing methods are illustrated in Figure 6-10. The wet method involves mixing polymers with asphalt binders at high temperatures before introducing them to mineral aggregates. This process changed the binder properties and created the LDPE-modified binder. Specifically, the LDPE particles were added to the virgin binder at a temperature of 165 °C. The high-speed shearing mixer with a speed of 1300 rpm is used to mix the compound sporadically for at least 30 minutes to obtain a consistent mix of material. The modified binder was then blended with aggregates, RAP, and additives to produce the modified mixture. In the dry processing method, LDPE was treated as fines to blend with aggregates, RAP materials, and additives for 90 seconds. Virgin asphalt binder was added for another 90 seconds blending to form an asphalt mixture (Mushtaq et al., 2022). Before mixing, all aggregates and asphalt binder were heated at 160℃ for 2 hours, and the RAP materials were preheated at 110℃ for 1 hour. After mixing, the asphalt mixtures were short-term aging at 135℃ for 2 hours before compaction in accordance with AASHTO R30.

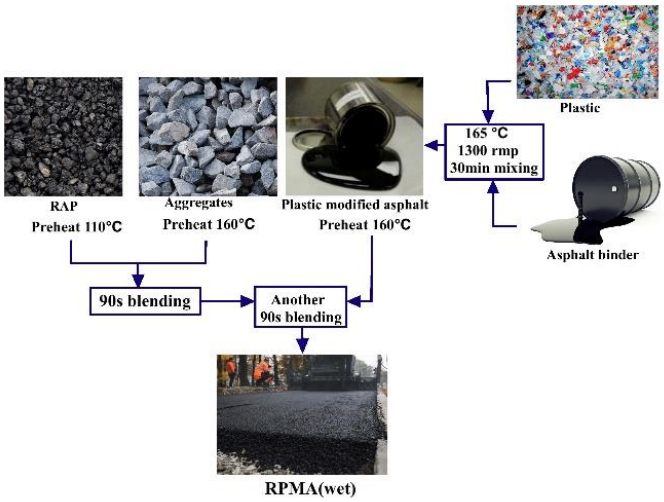

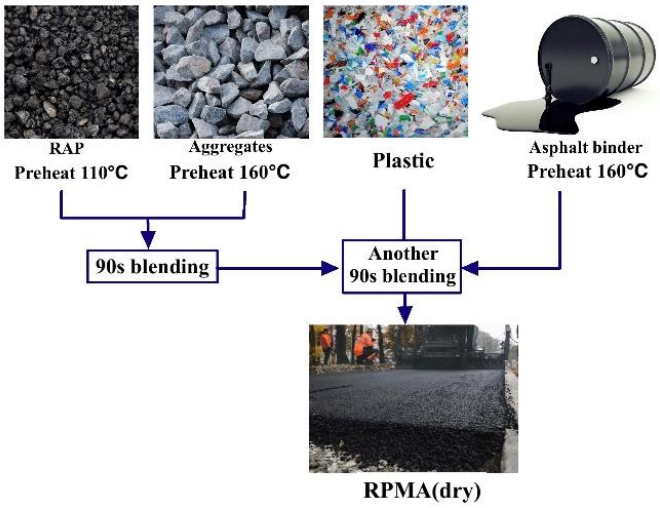

Figure 6-10 LDPE-modified mixes using wet (top) and dry (bottom) processing methods

Effects of Asphalt Content

The effect of asphalt content on the workability of the asphalt mixture can be evaluated by comparing Mix No. 6 and No. 9 in Table 6-3, which utilized the same gradation and compaction conditions, but with 5.2% and 6.0% asphalt content, respectively. Three replicate samples for each scenario were compacted, and the average value of relative rotations was used for the workability evaluation. As seen in Figure 6-11, the relative rotation for two asphalt mixtures is similar in trend but much different in magnitude. 6.0% asphalt content results in a more active particle rotation than 5.2% during the whole compaction stages, indicating better workability. This conclusion is consistent with the engineering experience that asphalt acts like a lubricant to assist the aggregate in rotating and translating under the compaction loadings.

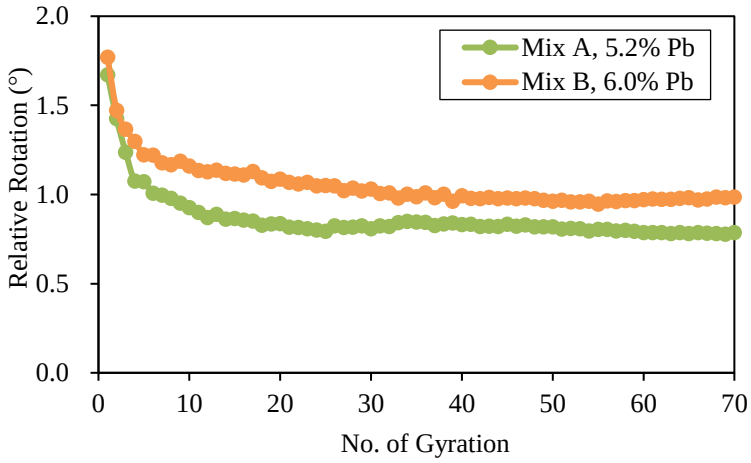

Figure 6-11 Relative rotation at different asphalt contents

Various mixtures were compacted to examine the influence of asphalt content on workability, including the virgin mix and RPMA (Recycled Plastic Modified Asphalt, i.e., LDPE-modified asphalt mixture). The curve of residual rotation can investigate the effect of the same gap of asphalt content on the mixture's workability in different scenarios. Figure 6-12 summarizes three types of mixes with a similar asphalt gap. The test mix, which contains a higher binder content, is compared with the control mix featuring a lower binder content. The blue curve represents the residual rotation between the virgin mixture containing 6.0% and 5.2% virgin binder (Mix No.6 and in No.9 Table 6-3), while the gray curve corresponds to the RPMA utilizing the dry processing method, with binder contents of 5.46% and 4.73% (Mix No.7 and No.10). The orange curve illustrates the RPMA mix using the wet method with the same binder contents as the previous scenario (Mix No. 8 and No.11). The variation in binder content for the RPMA mix is slightly below the targeted 0.8% difference, owing to the introduction of LDPE particles. As depicted in Figure 6-12, all three scenarios exhibit positive residual rotations throughout the compaction process, indicating that an increase in virgin binder content enhances particle rotation and subsequently improves workability. This finding confirms that asphalt binder as a lubricant can

facilitate particle rotation and compaction. The effect of similar asphalt gaps on the workability differed slightly for the three mixture types. The improvement for the RPMA using the wet processing method is higher than the other two mixtures. This could be related to the worse workability of RPMA at the low asphalt content, the increased asphalt content could introduce a higher improvement in workability.

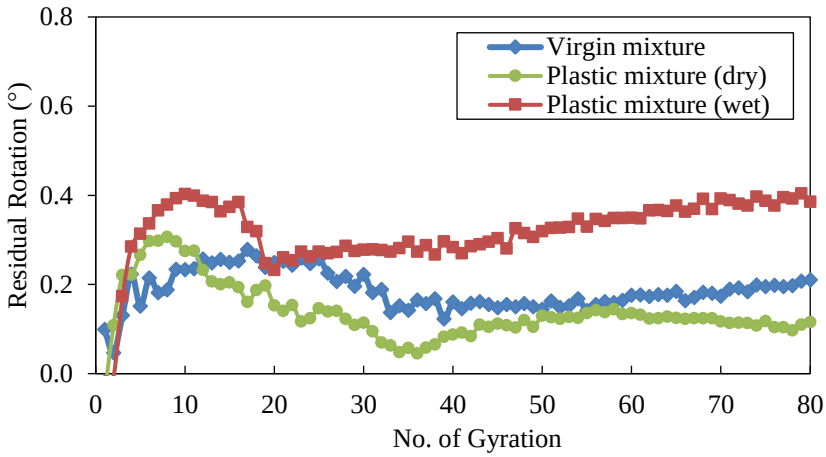

Figure 6-12 Effect of asphalt content on mixture's particle rotation

Effects of Temperature

Figure 6-13 shows the residual rotation curve between different compaction temperatures. Mix No. 1 and No. 2 are the same HMA compacted at 110℃, and 143℃, respectively. Mix No. 4 and No.5 are the same WMA produced at 110℃, and 143℃. The mix compacted at low temperature is the test mix and the mix at high temperature serves as the control. For the HMA scenario, most of the residual rotations are negative, meaning the particle rotations are less active for the test mix (i.e., the mix compacted at a low temperature). The findings confirm that the

reduced temperature resulted in worse workability. The same conclusion also stands for the WMA scenario.

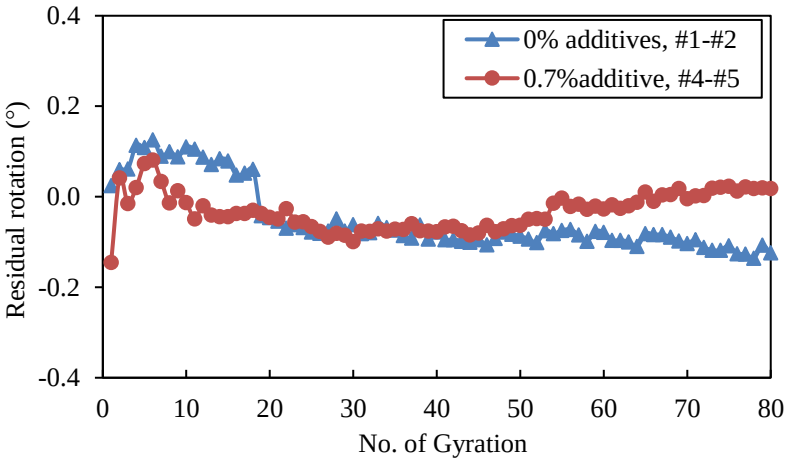

Figure 6-13 Residual rotation curve for temperature investigation

Effects of Plastic and Plastic Processing Methods

Figure 6-14 presents the effect of the plastic on the workability of asphalt mixtures. The orange curve is the residual rotation curve between the virgin mix and the RPMA using the dry method (Mix No.9 and No. 10 in Table 6-3). The blue curve is the residual rotation between the virgin mix and the RPMA using the wet method (Mix No. 9 and No. 11). The RPMA mix is considered the test mix, while the virgin mix serves as the control. It is important to note that the LDPE particles replace a portion of the virgin binder in the design of the RPMA using the dry method (i.e., Mix No. 10). Most orange points are negative, indicating that directly incorporating LDPE decreased the particle rotation during compaction. This could be attributed to the less lubrication resulting from a reduced binder and increased viscosity due to the LDPE involvement. Regarding the comparison between the virgin mix and the RPMA using the wet method (blue curve), the fluctuations in particle rotations fall within a minimal range, suggesting similar

workability between the two mixes. It can be concluded that LDPE particles can effectively modify the mixture using the wet processing method without a significant reduction in its workability.

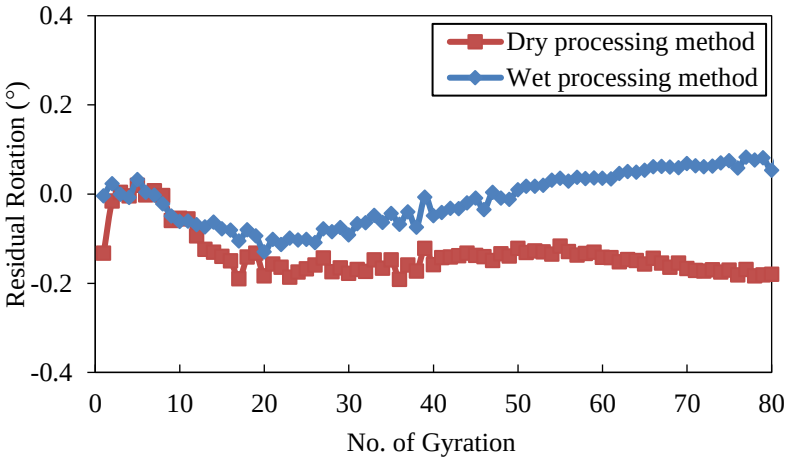

Figure 6-14 Effect of the LDPE processing method on the particle rotation

Another RPMA mix using the dry method (No. 12 in Table 6-3) was produced with an extra binder content to compare its workability with the virgin mix and RPMA produced with the wet method. This comparison can evaluate the effect of additional binders on the improvement of workability. The orange curve in Figure 6-15 compares the virgin mix with the RPMA (dry) using an extra binder (Mix No.9 and No.12). The blue curve focuses on the PMA prepared using the dry and wet processing methods (Mix No.11 and No. 12). The RPMA mix using the dry method serves as the test mix, while the virgin mix serves as the control in the orange curve and the modified mix using the wet method serves as the control in the blue curve. Two curves exhibit positive values, indicating that more virgin binder (without replacement by LDPE) can maintain the workability compared to the corresponding virgin mix and the RPMA using the wet method. Therefore, in terms of workability specifically, it is suggested that LDPE is added without replacing the virgin binder

in the dry processing method. However, it is important to consider other properties and economic benefits related to the mixture during the design of the LDPE-modified mix.

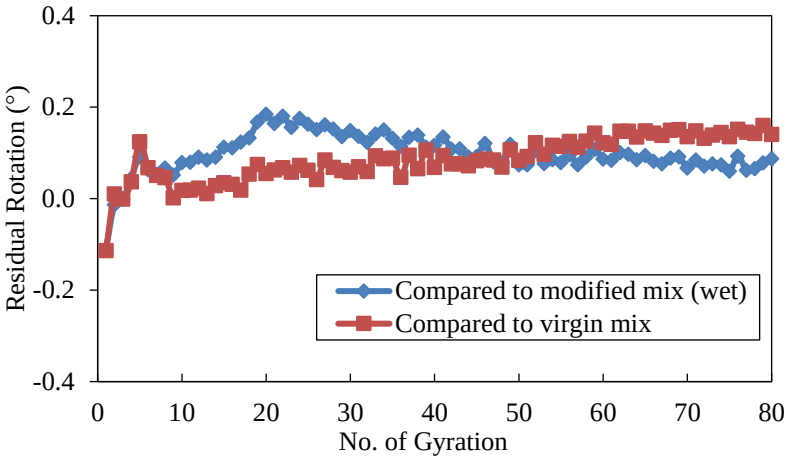

Figure 6-15 Effect of additional binder content on residual rotation

Effects of WMA Additive

The effect of the WMA additive (i.e., Evotherm M1) on the mixture's workability was also investigated. Figure 6-16 shows the residual rotation curve between the HMA and WMA. The blue curve compared the HMA and the WMA (0.7% additive) compacted at 110℃ (Mix No.1 and No.4). The orange curve shows the residual rotation between the HMA and WMA (0.7% additive) compacted at 143℃ (Mix No.2 and No.5). The WMA serves as the test mix, and the HMA serves as the control. As seen, the positive values for both scenarios indicated that the Evotherm could increase the particle rotation and improve the workability of the asphalt mixture. For the same 0.7% chemical additives, its effect on the particle rotation at a lower temperature is slightly more effective than at a high temperature. This study verified that the Evotherm can serve as a compaction aid to improve the mixture's workability, especially at reduced temperatures.

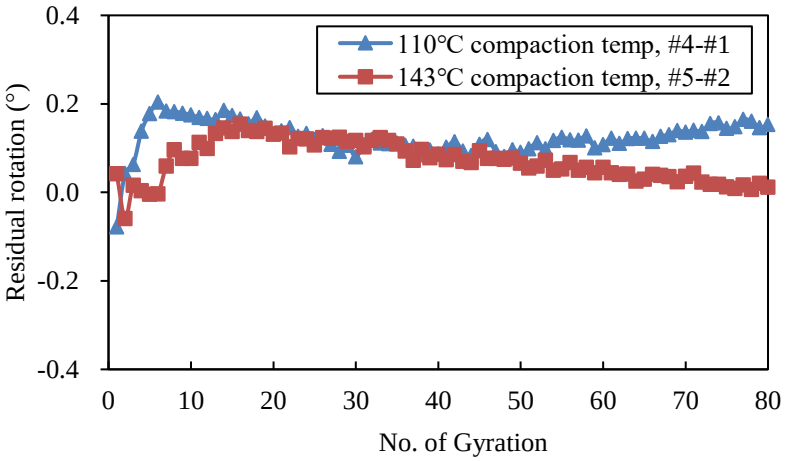

Figure 6-16 Residual rotation curve for additive investigation

A combined effect of the WMA additive and compaction temperature on the mixture's workability was investigated in Figure 6-17. Three scenarios were conducted, including (1) 0.35% more additives but 17°C lower compaction temperatures for the WMA (Mix No.4 and No.3); (2) 0.35% more additives but 17°C lower compaction temperatures for the HMA (Mix No.3 and No. 2); and (3) 0.7% more additives but 33°C lower compaction temperature for the HMA (Mix No.4 and No.2). To clarify, the mix produced at the lower temperature and higher dosage of WMA additives serves as the test mix. As shown in Figure 5-16, three curves of residual rotations are near or slightly above the zero-horizontal line (x-axis), suggesting each of the comparison pairs has similar workability in general. Therefore, it is concluded that the WMA mixture produced under the following strategy can achieve similar or slightly better workability than the original HMA: (a) Adding 0.35% additives but reducing 17°C compaction temperature, and (b) Adding 0.7% additives but reducing 33°C compaction temperature.

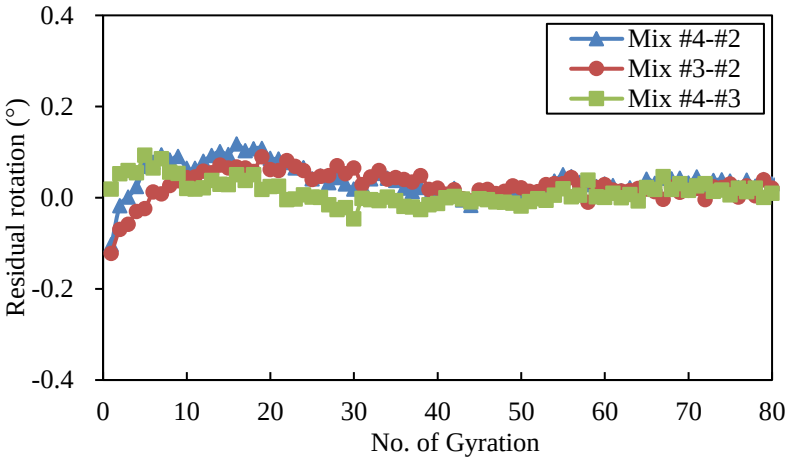

Figure 6-17 Residual rotation curve for the engineering application

Workability Evaluation Using Statistical Analysis

When comparing the workability between two asphalt mixtures, the magnitudes of residual rotation are insubstantial to determine whether the change is significant. Therefore, a statistical method was proposed to determine the significance of various factors on workability change. The Two-One-Sided T-Test (TOST) and the T-test are utilized in this method to determine whether a specific change in mix design or compaction condition could have a significant effect on the mixture's workability, as evidenced by the particle rotation. For the asphalt mixture, the curve of relative rotation presented a similar trend, the numbers of rotation data points from ***Ni*** to ***Nd*** are more than 60, it is thus reasonable to assume the residual rotation (difference between two relative rotations) follows the normal distribution. Specifically, the TOST is used to assess the equivalence of the test data, while the T-test is to evaluate differences between the test data.

Statistical Analysis Procedures

Statistical Methods

Two-one-sided T-test (TOST) is a statistical tool commonly used in the pharmaceutical industry. It can compare the performance of generic drugs with established drugs using several acceptable metrics (Schuirmann, 1987). This test can check whether the difference between groups is within an equivalent limit that is application-specific and below any potentially relevant effect. The null and alternative hypotheses of the two one-sided tests are shown below. The t-value of the TOST is presented in equation (6-6).

$$H_o: \ |\mu - \delta| \geq \Delta$$

$$H_1: \ |\mu - \delta| < \Delta$$

$$t_L = \frac{\mu - \delta - \Delta_L}{SD/\sqrt{N}} \ \ and \ \ t_U = \frac{\mu - \delta - \Delta_U}{SD/\sqrt{N}} \qquad (6\text{-}6)$$

Where μ is the observed mean of the residual rotation; δ is the value that the mean is tested against; Δ_L and Δ_U are the lower and upper equivalent limit, respectively; SD is the observed standard deviation of the differences between the paired residual rotations of two mixtures, and N is the number of paired residual rotations.

Before testing, the equivalent limit for each scenario will be determined based on the relative rotation of the replicated asphalt mixtures. For the asphalt mixture compaction, it is important to acknowledge that a certain level of variation exists even under identical test conditions by the same operator. This variation can be assumed as the equivalent limit for each scenario. To determine this limit, three replicate samples were compacted under the same condition by a single

operator, as presented in Figure 6-18. As seen, the maximum differences between two rotation curves will be identified (i.e., replicate 1 and replicate 3). The maximum residual rotation between these two replicate samples was computed using equations (6-7) and (6-8). This number will serve as the equivalent limit for the statistical analysis. A change in the mix design or compaction condition was deemed to have a limited effect on the mixture's workability if the residual rotation was significantly smaller than the equivalent limit tested by the TOST.

$$\boldsymbol{\delta = max\,[A_i]} \tag{6-7}$$

$$\boldsymbol{A = \frac{1}{(N_d - N_i)} \sum_{i=N_i}^{N_d} ReR_i} \tag{6-8}$$

Where, the notations represent the meaning in equation (1) and (2). Three A (A_{12}, A_{13}, A_{23}) should be computed; To clarify, A_{12} is the difference between the replicate sample No.1 and No.2.

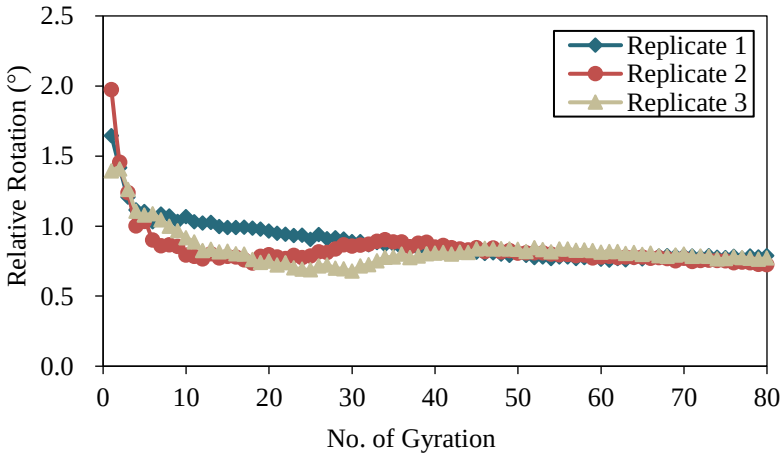

Figure 6-18 Relative rotation of three replicate samples for Mix 1

TOST test was used to test the equivalence between two asphalt mixtures regarding their particle rotations. If the equivalence conclusion was not made in the TOST test, a subsequent test will be conducted to test its differences using the T-test. The T-test is designed to compare the means of two populations from one sample with observations from the other sample (Xu et al., 2017). In this project, hypothesis testing was performed on the compaction data before and after changing the design or compaction conditions. The T-test can determine whether the improvement or reduction in the particle rotations because of this change is significant. The null and alternative hypotheses for the T-test are presented below, and the t value can be calculated using the equation (6-9). The symbols here have the same meaning in Equation (6-6).

$$H_o:\ \mu - \delta = 0$$

$$H_1:\ \mu - \delta \neq 0$$

$$t_L = \frac{\mu - \delta}{SD/\sqrt{N}} \qquad (6\text{-}9)$$

Power Analysis

The power analysis in the equivalence test is to test the probability of rejecting the null hypothesis when the alternative is true (Anderson et al. 2016). A power value of at least 0.9 is usually considered adequate in the equivalence test with a reasonable equivalent limit and sufficiently large data size. A power of 0.9 indicates a 90% chance of demonstrating equivalence when the difference between the population means is within the equivalent limits. To ascertain the adequacy of the power in each scenario, the equivalent limit and sample size are determined beforehand. The power analysis is conducted in this project to verify whether the calculated power

exceeds the 0.9 threshold. Equation (6-10) is utilized to compute the approximate power of the two one-sided t-tests (TOST) (Shieh, 2016).

$$\Psi_A = P\{t(\nu, \Delta_2) < -t_{\nu, \alpha}\} - P\{t(\nu, \Delta_1) < t_{\nu, \alpha}\} \quad (6\text{-}10)$$

Where, Ψ_A is the power in the equivalence test. $t(\nu, \Delta)$ is the noncentral t distribution with degrees of freedom ν, and the non-centrality parameter Δ. α is the significance level in the equivalence test.

Overall Steps of the Statistical Analysis

Summarizing all the steps presented above, the statistical analysis procedures based on the sensing data collected by SmartKli® were elaborated on below:

- Compact the asphalt mixture in the SGC compactor, and collect the particle kinematic data (i.e., relative rotation) using SmartKli® during compaction.
- Determine the equivalent limit for each type of asphalt mixture based on their replicability.
- Perform the power analysis to check if the determined equivalent limit and the sample size are adequate in the equivalence test.
- Conduct the equivalence test (TOST) to determine whether a specific effect on the mixture's workability is within a narrow equivalent limit.
- If there is insufficient evidence to conclude the equivalence, the T-test should be performed to determine whether the specific effect is significant on the mixture's workability.

Materials Used for Experiments

Seven types of asphalt mixtures were used in this section for statistical analysis. They are from the same base mix with a 6.0% PG64-22 asphalt binder and an N_{design} of 75. Its nominal maximum aggregate size (NMAS) is 12.5mm. The aggregate gradations for the base mixes are provided in Table 6-5 No.1. HMA and RPMA (Recycled Plastic Modified Asphalt) mixtures were produced at two levels of asphalt content: reduced asphalt content (5.2%) and optimum asphalt content (6.0%). The reduced asphalt content was prepared to investigate the effect of asphalt content on the mixture's workability. A 0.8% asphalt content difference was set for the workability evaluation. At reduced asphalt content, Mix No.1-3 were produced using the HMA, and RPMA with the dry and wet processing method. At optimum asphalt content, the same three types of mixtures, as shown in No. 4-7, were prepared. To clarify, the dry processing method (Mix No. 2, and No.4) is designed by the conventional method, which replaces the virgin binder with the LDPE for economic benefits (Xu et al., 2021). Another modified dry processing method (Mix No.7) was designed using more virgin binders (i.e., without replacing the virgin binder with the LDPE). The detailed information on seven mixtures is summarized in Table 6-5.

Table 6-5 Detailed information on the asphalt mixtures used in this section

No.	Mix	Additives	NMAS	RAP	OVAC	Temp
1	HMA	N/A	9.5	15%	5.2%	135℃
2	RPMA	9% LDPE (dry)	9.5	15%	4.73%	135℃
3	RPMA	9% LDPE (wet)	9.5	15%	4.73%	135℃
4	HMA	N/A	9.5	15%	6.0%	135℃
5	RPMA	9% LDPE (dry)	9.5	15%	5.46%	135℃
6	RPMA	9% LDPE (wet)	9.5	15%	5.46%	135℃
7	RPMA	9% LDPE (dry)	9.5	15%	6.0%	135℃

Note: RPMA is the recycled plastic-modified asphalt mixture. LDPE is the Density Polyethylene. 9% LDPE in the column of "Additives" is the mass ratio of the LDPE to the asphalt content.

Statistical Analysis Results

Using the seven types of asphalt mixtures, eleven comparisons were conducted to evaluate the effects of asphalt content and LDPE processing methods on the mixture's workability. The power analysis was performed before the equivalence test, the results for all eleven scenarios were nearly 1, indicating the reasonableness of the equivalent limit and sample size. For the convenience of the readers, the eleven compaction scenarios were summarized below:

I: Effect of asphalt content on the mixture's workability

(1) Comparison of the HMA mixtures with different asphalt content. The control mix (Mix No.1) has 6.0% asphalt content, and the test mix (Mix No.4) has 5.2% asphalt content.

(2) Comparison of the RPMA mixtures (dry method) with different asphalt content. The control mix (Mix No.2) has 5.46% asphalt content, and the test mix (Mix No.5) has 4.73% asphalt content.

(3) Comparison of the RPMA mixtures (wet method) with different asphalt content. The control mix (Mix No.3) has 5.46% asphalt content, and the test mix (Mix No.6) has 4.73% asphalt content.

II: Effect of introduction of LDPE and its processing method on the mixture's workability

(4) Comparison of the HMA and RPMA mixtures produced by the dry method. The control mix (Mix No.1) is HMA, and the test mix (Mix No.2) is RPMA mixture (dry). The mixes were designed for reduced asphalt content.

(5) Comparison of the HMA and RPMA mixtures produced by the dry method. The control mix (Mix No.4) is HMA, and the test mix (Mix No.5) is the RPMA mixture (dry). The mixes were designed at optimum asphalt content.

(6) Comparison of the HMA and RPMA mixtures produced by the wet method. The control mix (Mix No.1) is HMA, and the test mix (Mix No.3) is the RPMA mixture (wet). The mixes were

designed for reduced asphalt content.

(7) Comparison of the HMA and RPMA mixtures produced by the dry method. The control mix (Mix No.4) is HMA, and the test mix (Mix No.6) is the RPMA mixture produced (dry). The mixes were designed at optimum asphalt content.

(8) Comparison of the RPMA mixture produced by the dry method and RPMA mixture produced by the wet method. The control mix (Mix No.2) is the RPMA mixture (dry) and the test mix (Mix No.3) is the RPMA mixture (wet). The mixes were designed for reduced asphalt content.

(9) Comparison of the RPMA mixture produced by the dry method and RPMA mixture produced by the wet method. The control mix (Mix No.5) is the RPMA mixture (dry) and the test mix (Mix No.6) is the RPMA mixture (wet). The mixes were designed at optimum asphalt content.

III: Effect of modified plastic dry processing method on the mixture's workability

(10) Comparison of the HMA and RPMA mixture produced by the modified dry method. The control mix (Mix No.4) is MHMA, and the test mix (Mix No.7) is the RPMA mixture produced by the modified dry method. To clarify, the modified dry processing method uses extra virgin binders compared with the conventional dry method.

(11) Comparison of the RPMA mixture produced by the wet method and RPMA mixture produced by the modified dry method. The control mix (Mix No.6) is the RPMA mixture produced by the wet method and the test mix (Mix No.7) is the RPMA mixture produced by the modified dry method.

Table 6-6 summarizes the average residual rotation (ARR) and the statistical results obtained from the equivalence test (TOST) and standard test (T-tests). The ARR represents the difference in workability between the test and the control mix, with a positive value indicating better workability for the test mix. The statistical analysis was performed using the same residual

rotation data, and the resulting P-values and conclusions are also presented. The same procedure was followed for all eleven scenarios.

Table 6-6 Statistic analysis of the workability of various asphalt mixtures

Effect	Compare	ARR	Limit (TOST)	P value (TOST)	TOST conclusion	P value (T-test)	T-test conclusion
Asphalt content	1 vs 4	1.900	0.126	1.00	Not equivalent	0.00	Different
	2 vs 5	1.335	0.134	0.16	Not equivalent	0.00	Different
	3 vs 6	3.256	0.234	1.00	Not equivalent	0.00	Different
LDPE (dry)	1 vs 2	-0.874	0.077	1.00	Not equivalent	0.00	Different
	4 vs 5	-1.439	0.134	1.00	Not equivalent	0.00	Different
LDPE (wet)	1 vs 3	-0.210	0.161	1.00	Not equivalent	0.00	Different
	4 vs 6	-1.566	0.136	0.00	Equivalent	0.52	No different
Processing method	2 vs 3	1.229	0.234	0.00	Equivalent	0.00	Different
	5 vs 6	0.692	0.136	0.00	Equivalent	0.00	Different
Additional asphalt	4 vs 7	0.878	0.234	0.00	Equivalent	0.00	Different
	6 vs 7	-1.088	0.234	0.00	Equivalent	0.00	Different

Note: When calculating ARR, the first mixture in column "Comparison" serves as a control mix, and the second mixture serves as a test mix.

Based on the ARR and P-values of the TOST and T-test, several findings can be derived at a 5% significant level:

(1) The asphalt content significantly affects the workability of the mixture. Increasing the asphalt content by approximately 0.8% leads to a significant improvement in workability.

(2) When LDPE replaces a portion of the virgin binder in the dry processing method, the RPMA mixture produced by the dry processing method exhibits decreased workability compared to the virgin mixes (the corresponding HMA).

(3) The workability of the RPMA produced by the wet processing method is dependent on the asphalt content. At reduced asphalt content, the RPMA mixture demonstrates reduced workability compared to the corresponding HMA. However, equivalent workability is

observed between the two mixes at optimum asphalt content.

(4) For the same mix design, the workability of the RPMA mixtures does not significantly differ from each other when using the wet or dry processing methods.

(5) Compared to the corresponding HMA, the RPMA mixture using the modified dry method does not lead to a decrease in workability. To clarify, the modified dry method uses an extra binder content compared with the conventional dry processing method.

Summary

The workability or compactability evaluation of the asphalt mixture was conducted in this chapter based on the proposed compaction mechanism. Various asphalt mixtures, including HMA (Hot Mix Asphalt), WMA (Warm Mix Asphalt), and RPMA (Recycled Plastic Modified Asphalt) with distinct mix designs and compaction conditions were compacted. The following findings and recommendations regarding the application of the WMA additives, and recycled plastic (LDPE) processing method in the asphalt mixture can be concluded.

- Three methods were proposed to evaluate the workability of asphalt mixtures, including (a) Particle kinematic parameters; (b) Particle rotation curves, and (c) Statistical analysis method. The particle kinematic parameter offers the most straightforward approach to compare the mixture's workability, but a single value of the kinematic parameter can provide limited information. The particle rotation curves can thus be used to clearly illustrate the particle rotation at different compaction stages. To compare the small differences in particle rotation between two asphalt mixtures, the statistical method was developed, involving the equivalency test (i.e., Two One-Sided T-tests, TOST) and difference test (i.e., one sample T-test) to analyze the residual rotation between two asphalt mixtures. This approach could determine whether a particular factor, such as alterations in the mix design or compaction conditions, has a

significant impact on the asphalt mixture's workability.

- The chemical additive, higher temperature, and more asphalt binder can increase the particle rotation and thus improve the mixture’s workability. The findings are consistent with the common engineering sense and, in turn, validate the developed evaluation methods of using particle kinematic behavior to evaluate the workability of asphalt mixtures.
- Based on the particle rotation during compaction, an equivalent workability can be achieved for asphalt mixtures considering the following WMA application methods: (a) adding 0.35% additive (Evotherm M1) but reducing 17ºC compaction temperature; (b) adding 0.7% Evotherm M1 but reducing 33ºC compaction temperature.
- For the RPMA scenario, when the LDPE particles replaced the virgin binder in the design of the dry processing method, a notable workability decrease was observed. The wet processing method proved to be more effective in processing the LDPE, as the workability of the RPMA using the wet method remained equivalent to the corresponding HMA.
- When incorporating LDPE into asphalt mixtures using the dry processing method, maintaining an adequate amount of binder content is crucial to preserve workability. Therefore, a modification method was proposed for adding plastics without replacing any virgin binder. If so, the statistical results indicated that the workability of the RPMA remained equivalent to that of the corresponding HMA. However, it is important to consider other properties and economic benefits when designing the RPMA using the dry processing method.

Chapter 7

Compaction Modeling and Prediction

Compaction prediction is another application based on the compaction mechanism. An intelligent model will be developed in this chapter to predict the density of the asphalt pavement by integrating remote sensing technology and artificial intelligence. The model aims to improve the compaction quality of the asphalt pavement compared with the conventional methods with the density verification at selected spots. This model can also assist in the prediction accuracy of the compaction degree for intelligent compaction (IC) technology. This system will process the real-time data collection by the wireless sensor and perform density prediction using neural networks. The process of the model establishment, verification, and application in the laboratory and field compaction projects will be elaborated in this chapter.

Preliminary Compaction Modeling

Model Development

A preliminary compaction model will first be established to check the applicability of machine learning (ML) techniques in the field of pavement compaction. The input variables and output will be determined. A preliminary model will then be established to predict the compaction conditions of the asphalt pavement. This step is essential to ensure the development and verification of the following complex prediction model for asphalt pavement compaction.

Input Variables Candidates

Several potential parameters were selected as the candidates for the input variable for the compaction prediction model, including:

- Particle kinematic behavior during compaction (i.e., particle relative rotation). This parameter was proved to be highly correlated with the density of asphalt mixtures during compaction.
- Mechanical parameters, such as the shearing resistances between asphalt particles. The interaction between compaction loadings and aggregate shears dominated the compaction process of the asphalt mixture.
- Compaction energy is applied to the paved materials, which is one of the most important parameters to affect the material densification.
- Material properties, such as aggregate gradation, asphalt binder content and type, etc. These parameters will affect the particle shearing during compaction, thus impacting the compaction conditions.
- Environmental parameters, such as temperature. Asphalt mixture is a viscoelastic material, and its properties are greatly impacted by the compaction temperature.

Kinematic Parameter

Compaction is a process of particulate material rearranging and consolidating in response to external forces. Preliminary research has found that the kinematic behaviors (e.g., particle rotation) of the particulate asphalt mixture would act differently at different compaction stages. How the particulate materials respond under applied compaction energy should have a direct impact on the densification of the asphalt pavement. It is hypothesized that a well-compacted pavement should have stable and limited particle rotation, while a large unstable rotation suggests pavement is still under compaction. The kinematic parameter, relative rotation, was defined as the difference

between the peak and the valley value of the Euler angle in a single compaction cycle. It is proposed to describe the particle rotation during compaction. The relative rotation shows clear distinctions at various compaction stages. From the considerable rotation at the beginning to the stable status at the end, the particle rotation is an indication of the skeleton formation and the interaction between the compaction loadings and particle shearing resistance. Furthermore, the curve of relative rotation and the specimen height were highly correlated during compaction with a 0.949 Pearson correlation coefficient. Therefore, the particle rotation during compaction was selected as an input variable for the compaction prediction of the asphalt pavement.

Mechanical Parameter

The compaction of the asphalt mixture is affected by the contact and interlocking behaviors between aggregates (Manzi et al., 2017). The mechanical properties between particles were related to the particle rotation and interlocking during compaction, as well as the workability of the asphalt mixture. Several commonly used mechanical parameters will be considered for developing the compaction prediction model (Bahia and Faheem, 2004), including the compaction densification index (CDI), compaction force index (CFI), and normalized shear index (NSI). The definitions of these three parameters were already elaborated in Chapter VI. A brief introduction of the parameters will be made as follows. CDI is the area under the densification curve from 8th gyrations to the number of gyrations to achieve 92%$\boldsymbol{G_{mm}}$. It evaluates the energy required to compact the mixture to the desired density. However, CDI is calculated from the $\boldsymbol{\%G_{mm}}$, which was used to determine the compaction condition. Therefore, CDI is not a suitable input variable for the model. CFI indicates how much resistive effort it overcame to compact the mixtures from the initial cycle to 92% $\boldsymbol{G_{mm}}$. NSI represented the work applied by the compactor to resist the frictional shear during compaction. CFI and NSI are selected as the input variables for the prediction model.

Compaction Energy

Compaction energy is the most straightforward and crucial factor that impacts the densification of the asphalt mixture during compaction. Three compactors have been widely used in laboratory and field compaction practices, including the Superpave gyratory compactor (SGC), static roller compactor, and vibratory roller compactor. The determination of the compaction energy applied by these three compactors is explained below.

The SGC can impart vertical loadings and constant shear forces throughout the asphalt mixture sample. The introduction of the gyration angle generates both shearing and kneading effects on the asphalt mixtures. Therefore, the total gyratory compaction energy per unit mass is the sum of the energy due to the vertical loading force (E1) and the moment by the eccentricity of the applied force (E2), as determined in equation (7-1) (DelRio-Prat et al., 2011).

Vibratory rollers can apply two types of compaction effort: the static weight by the weight of the drums and the frame and the dynamic impact force by a rotating eccentric weight located concentrically to the drum. The weight of the roller, compaction speed, and vibration condition (i.e., the frequency and amplitude of the vibration) would impact the compaction energy of the vibratory roller to the asphalt pavement. The compaction energy of the vibratory roller compactor per unit mass per compaction cycle can be determined based on equation (7-2) (D. Liu et al., 2016).

Static roller uses its weight to compact the materials or level the surface at the beginning or finishing compaction. The weight of the static roller is the key factor in its compaction energy, which is determined based on equation (7-3) (Zhao et al., 2021). The compaction energy of the static roller is also affected by the rolling resistance coefficient, which is determined based on the interaction material and the compaction process.

$$E = E_1 + E_2 = \frac{P \cdot S \cdot \Delta h}{m} + \frac{4\pi\theta}{m} \sum M_i \qquad (7\text{-}1)$$

$$E_v = \frac{f}{v\rho hb} \cdot 2A \cdot (Wg + \frac{\pi F_e}{4}) \quad (7\text{-}2)$$

$$E_s = c \cdot \frac{Wg}{\rho hb} \quad (7\text{-}3)$$

Where, $\boldsymbol{P}$ is the applied vertical force of the gyratory compactor, $\boldsymbol{S}$ is the cross-section area of the specimen, $\boldsymbol{\theta}$ is the tilting angle, $\boldsymbol{M}$ is the moment by the eccentricity of the applied force, and $\boldsymbol{m}$ is the mass of the material. $\boldsymbol{A}$ is the amplitude of the roller vibration, $\boldsymbol{f}$ is the vibratory frequency, $\boldsymbol{Fe}$ is the centrifugal force of the roller, $\boldsymbol{v}$ is the speed of the roller, $\boldsymbol{h}$ is the depth of the material, and $\boldsymbol{b}$ is the width of the roller drum, $\boldsymbol{\rho}$ is the density of the asphalt mixture, and $\boldsymbol{W}$ is the weight of the roller. $\boldsymbol{c}$ is the rolling resistance coefficient.

Output Determination

For many compaction of asphalt pavement, agencies usually select a density threshold to classify whether the compaction is completed (U.S. DOT, 2020). Therefore, a preliminary two-category model was first developed. The two categories are "Compaction Needed" and "Compaction Done" that was determined based on the density of the compacted asphalt material. The determination of the threshold is based on the construction Specification of the Pennsylvania Department of Transportation (PennDOT) with the Percent Within Limit (PWL) (Transportation, 2020). The threshold in real practice is adjustable to the agency's requirements. Two predictive levels are considered in the prediction, (1) classification with a fixed threshold value based on the %$\boldsymbol{G_{mm}}$ and (2) classification with a buffer zone. Details of these two predictive levels are explained below.

(1) Classification with a fixed threshold value

- Compaction Needed: The mixture with the %$\boldsymbol{G_{mm}}$ is smaller than 92%.
- Compaction Done: The mixture with the % $\boldsymbol{G_{mm}}$ is greater than 92%.

(2) Classification with a buffer zone:

- Compaction category: The $\%G_{mm}$ of the asphalt mixture that is beyond the $\pm 0.5\%G_{mm}$ of the threshold must be classified to the corresponding category.
- Buffer Zone: The $\%G_{mm}$ of the asphalt mixture that is within the $\pm 0.5\%G_{mm}$ of the threshold is acceptable to be classified in either neighbor category.

In the development of the preliminary model, the compaction data was collected from the Superpave gyratory compaction. During the gyratory compaction, the height and the G_{mb} (bulk specific gravity) of the specimen can be measured; thus the $\%G_{mm}$ (maximum specific gravity) at each gyration can be calculated using equation (7-4) to serve the output of the model.

$$\%G_{mm,i} = \frac{h_{end}}{h_i} \times \frac{G_{mb}}{G_{mm}} \quad (7\text{-}4)$$

Where, $\%G_{mm,\,i}$ mean the $\%G_{mm}$ of the specimen at i^{th} gyration. h_{end} means the height of the specimen when compaction ended, h_i is the specimen height at i^{th} gyration.

Preliminary Model Algorithms

The compaction dataset used in the preliminary compaction model was collected from the gyratory compaction. Using equations (7-4), the compaction condition of each compaction cycle can be calculated as a reference for the model training and testing. Three supervised machine learning models were selected for the model development, including a support vector machine (SVM) classifier, logistic regression (LR), and K-nearest neighbor (KNN). The mechanism of the three compaction models is presented in Figure 7-1.

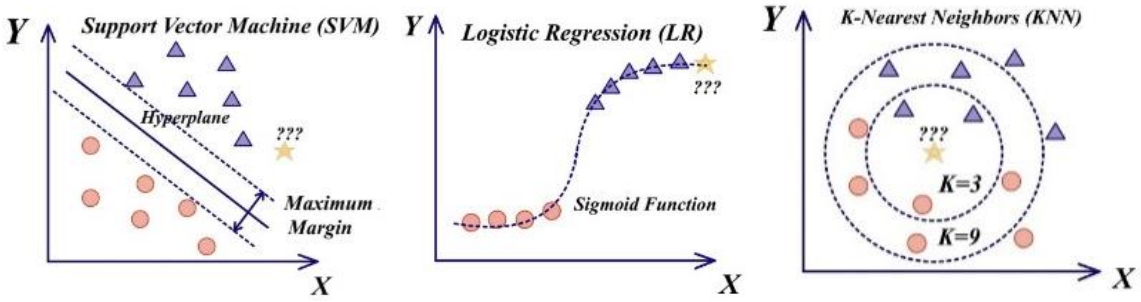

Figure 7-1 Illustration of the SVM (left), LR (middle), and KNN (right) algorithms

Support Vector Machine

Support Vector Machine (SVM) is a supervised ML model for two-group classification problems. Its purpose is to find a plane that has the maximum margin (i.e., the maximum distance between data points of both classes) from the infinity of possible planes. If the original data can be separated linearly, the SVM would create a decision boundary (hyperplane) that can distinctly classify the N-dimensional data points (Dong et al., 2022). If not, the SVM would create a new variable using the kernel function to move the original data to a higher dimension and do the nonlinear separation. The kernel function used in the SVM could be linear, polynomial, radial, etc. The data points that are closest to the hyperplane are the support vectors, which significantly influence the position and orientation of the hyperplane. The SVM classifier is notable for its effectiveness in the high-dimensional data case, which is why it was selected for the compaction prediction.

Logistic Regression

Logistic Regression (LR) is a relationship between predictor variables and a categorical response variable. It is an extension of the linear regression model for classification problems. LR gives the probability between 0 and 1 based on the sigmoid function (Cervantes et al., 2020). To

predict which class a data belongs to, a possibility threshold would be set. One of the most significant advantages of logistic regression is that it is not only a classification model but also gives you probabilities for each prediction, which offers much more insights and information to the decision-makers.

K-Nearest Neighbor

The K-Nearest Neighbor (KNN) algorithm is a supervised machine learning algorithm used to solve classification problems. It stores all available cases and classifies new cases based on the selected features. Simply put, the known data would be arranged in a space defined by the specific feature. The algorithm will compare the classes of the K closest data to determine which category the new data belongs to. The KNN is simple yet efficient. Without any assumptions about the underlying data distribution, it classifies data points based on their proximity and similarity to other available data points. However, the calculation speed would decrease rapidly as the training data increases (Taunk et al., 2019).

Materials Used for Modeling

Eleven asphalt mixtures are used in this chapter for the compaction modeling. These asphalt mixtures varied in mixture types, mixing methods, and compaction temperatures. All mixtures' information and gradation curves are summarized in Table 7-1 and Figure 7-2.

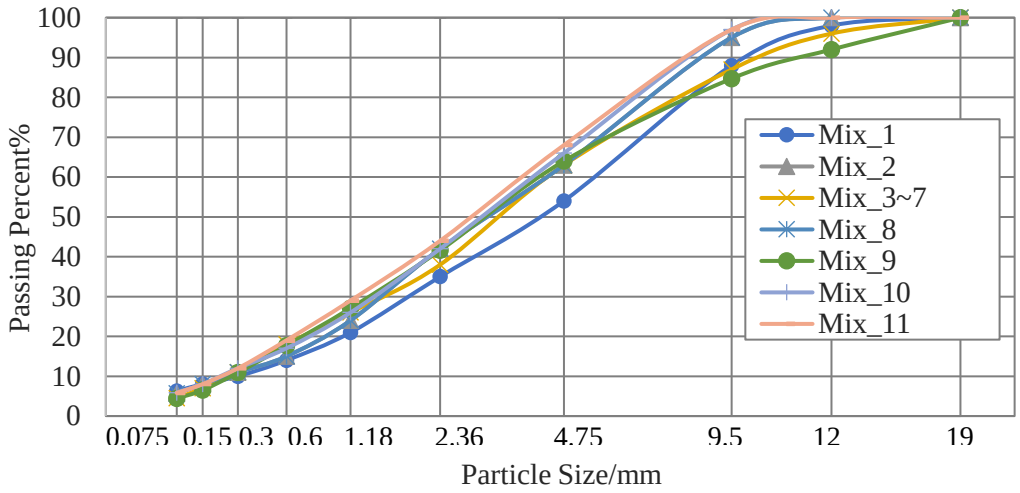

Figure 7-2 Gradation of the asphalt mixtures

Table 7-1 Design parameters for the asphalt mixtures

No.	Technology	NMAS	RAP	Pb	Asphalt	Temp	Mixing
1	HMA	12.5	15%	5.8%	PG64-22	135℃	Plant
2	HMA	9.5	15%	5.9%	PG64E-22	135℃	Lab
3	HMA	12.5	0%	5.9%	PG64-22	110℃	Lab
4	HMA	12.5	0%	5.9%	PG64-22	143℃	Lab
5	0.35% Evotherm	12.5	0%	5.9%	PG64-22	127℃	Lab
6	0.7% Evotherm	12.5	0%	5.9%	PG64-22	110℃	Lab
7	0.7% Evotherm	12.5	0%	5.9%	PG64-22	143℃	Lab
8	Smart Foam	9.5	15%	5.9%	PG64E-22	135℃	Plant
9	HMA	12.5	25%	5.9%	PG64-22	135℃	Plant
10	Smart Foam	9.5	15%	5.9%	PG64E-22	135℃	Plant
11	Foam	9.5	15%	5.8%	PG64S-22	135℃	Plant

Note: NMAS is the nominal maximum aggregate size; RAP is the content of the reclaimed asphalt pavement; Pb is the virgin asphalt content; Temp is the compaction temperature.

Preliminary Model Prediction

From the input variable candidates, a Support Vector Machine (SVM) model was first built to select the most proper input variables for the compaction prediction. To eliminate the effect of the material properties on the compaction condition, the same type of asphalt mixture was used in this process. 240 compaction data points from mixture No.1 in Table 7-1 were utilized for input variable determination. Five models with different candidate variables were established to predict whether compaction energy is needed to achieve 92%G_{mm}. The model details and prediction accuracy are shown in Table 7-2.

Table 7-2 Pre-model results for input selection

No.	Input Variables	Errors	Accuracy (%)
1	CFI + Temp	31/240	87.08
2	CFI + Rotation + Temp	16/240	93.33
3	Rotation + Temp	17/240	92.92
4	NSI + Rotation + Temp	2/240	99.17
5	Energy + Rotation	3/240	98.75

Note: CFI is the compaction force index; Temp is the temperature collected by SmartKli®; NSI is the normalized shear index.

As seen, Models No.4 and No.5 both present great prediction accuracy, indicating that the combination of the NSI (normalized shear index), particle rotation, temperature, and combination of compaction energy and particle rotation are suitable combinations of inputs for compaction prediction. Moel No.5 removed temperature because, at this moment, the temperature data collected by the SmartKli® sensor has a delay in reaching the true temperature of the asphalt mixture. By comparison, the NSI in Model No.4 can be determined in the lab since the gyratory compactor can monitor the loading conditions and volume changes. However, this information is hard to obtain in field compaction. The compaction energy used by Model No.5 can be calculated both in

the laboratory and field compaction. Therefore, Model No.5 is selected as the basic model. To enable the model to apply to various asphalt mixtures, material properties will also be considered. Eventually, the inputs of the machine learning model include:

(1) Particle kinematic behavior, which is the relative rotation.

(2) Accumulated compaction energy per unit mass.

(3) Mixture design information, which includes mixture type (WMA or HMA), WMA additive content, NMAS (Nominal maximum aggregate size), and high-temperature grade of virgin asphalt binder.

After determining the input variables, output compaction conditions, and the machine learning algorithms, three preliminary models were established to check the applicability of the data-informed method in the compaction prediction. 11 asphalt mixtures in Table 7-1, a total of 32 specimens (i.e., 3 replicates per mix except for one mix with only 2 replicates due to loss of one specimen) with 4154 compaction points, were used for prediction modeling. Because of the limited space of the thesis, only partial data were displayed in Table 7-3 and the presented data points cannot represent the distribution of the entire data points. To clarify, the first 7 columns served as the inputs. The column "target" served as the output for the model. Among these 4154 data points, 896 data points are categorized as target "0", and the rest of the 3258 data points are the target "1". The last column "$\%\boldsymbol{G_{mm}}$" calculated by equation (7-4) did not serve as input but was only for determining the compaction status (i.e., the column "target").

Table 7-3 Partial data of the ML prediction

Type	Additive	NMAS	Binder	Rotation(x)	Rotation(y)	Energy	Target	$\%G_{mm}$
1	0	9.5	76	1.193	1.491	155.4	0	84.74
1	0	9.5	76	1.169	1.499	170.7	0	85.26

1	0	9.5	76	1.126	1.461	185.8	0	85.73
1	0	9.5	76	1.121	1.500	201.0	0	86.19
1	0	9.5	76	1.146	1.170	363.0	0	89.48
1	0	9.5	76	1.163	1.168	377.5	0	89.70
1	0	9.5	76	1.155	1.100	392.0	0	89.91
1	0	9.5	76	1.154	1.112	406.3	0	90.06
1	0	9.5	76	1.140	0.907	620.9	1	92.24
1	0	9.5	76	1.150	0.895	635.4	1	92.40
1	0	9.5	76	1.157	0.893	663.9	1	92.55
1	0	9.5	76	1.145	0.871	678.5	1	92.71
1	0	9.5	76	1.143	0.890	692.8	1	92.79
1	0	9.5	76	1.151	0.827	807.1	1	93.49
1	0	9.5	76	1.139	0.812	821.4	1	93.57
1	0	9.5	76	1.138	0.788	849.8	1	93.73
1	0	9.5	76	1.125	0.791	878.2	1	93.89
1	0	9.5	76	1.127	0.803	892.4	1	93.97
1	0	9.5	76	1.108	0.767	906.6	1	94.05
1	0	9.5	76	0.682	0.981	1511.9	1	96.10
1	0	9.5	76	0.667	1.002	1526.1	1	96.18
1	0	9.5	76	0.656	0.993	1540.1	1	96.18
1	0	9.5	76	0.652	0.979	1554.3	1	96.26
1	0	9.5	76	0.656	0.980	1568.3	1	96.26
1	0	9.5	76	0.646	0.989	1582.2	1	96.26

Note: “Type” represents the type of asphalt mixture. 0 is the HMA, and 1 is the WMA.
“Binder” refers to the high-temperature performance grade (PG) of the virgin binder.
“Energy” is the accumulated compaction energy from the beginning to the specific gyration.
“Target” 0 and 1 represent the “Compaction Needed” and “Compaction Done”.

In machine learning modeling, distinct datasets are crucial to constructing a reasonable and robust prediction model that efficiently processes information and generalizes effectively with new,

unseen data. As a result, 10-folder cross-validation and three dataset scenarios have been created to facilitate the development and refinement of the model.

- All compaction data points serve as the training data to build the model and check the prediction accuracy.
- 70% of random compaction data points serve as the training data to establish the model, and the rest of the 30% data points serve as the test data to examine the prediction quality.
- 8 mixture compaction data points served as the training data to establish the model, and the rest of the 3 mixtures' data points were used to verify the mode quality.

Three metrics were used to assess the compaction prediction of the binary compaction model. By comparing the prediction results with the reference (real value), four cells were assigned in Table 7-4, and the sensitivity, specificity, and accuracy can thus be calculated using the equation (7-5) -(7-7). Generally, sensitivity, specificity, and accuracy can inspect whether the model can correctly predict the target "0", target "1", and the overall dataset.

Table 7-4 Compaction Prediction Configuration

Prediction (Model)	Reference (%Gmm)	
	Target 0	Target 1
Target 0	True Positive (TP)	False Positive (FP)
Target 1	False Negative (FN)	True Negative (TN)

$$Sensitivity = TP / (TP + FN) \quad (7\text{-}5)$$

$$Specificity = TN / (TN + FP) \quad (7\text{-}6)$$

$$Accuracy = (TP + TN) / (TP + FP + TN + FN) \quad (7\text{-}7)$$

During modeling, the linear kernel function was selected for the SVM model after trials and errors. K=5 was eventually determined for the KNN algorithm by the cross-validation method to achieve the most accurate prediction quality. The prediction results of three ML models under three different dataset scenarios are shown in Table 7-5.

Table 7-5 Compaction prediction for the preliminary compaction model

Scenario	Parameters	No buffer zone			Buffer zone setup		
		SVM	KNN	LR	SVM	KNN	LR
I	Errors	49/4154	41/4154	48/4154	4/4154	5/4154	5/4154
	Accuracy (%)	98.82	99.01	98.84	99.90	99.88	99.88
	Sensitivity (%)	97.43	97.54	97.32	99.78	99.67	99.78
	Specificity (%)	99.20	99.42	99.26	99.94	99.94	99.91
II	Errors	16/1247	16/1247	16/1247	1/1247	3/1247	2/1247
	Accuracy (%)	98.72	98.72	98.72	99.92	99.76	99.84
	Sensitivity (%)	97.77	97.65	98.51	99.63	99.61	99.63
	Specificity (%)	98.98	98.99	98.77	100	99.80	99.90
III	Errors	17/1442	38/1442	14/1442	0/1442	16/1442	0/1442
	Accuracy (%)	98.82	97.36	99.03	100	98.89	100
	Sensitivity (%)	99.72	95.73	99.43	100	97.72	100
	Specificity (%)	98.53	97.89	98.90	100	99.27	100

It is worth noticing that the prediction results using three ML models are higher than 95%. The number of errors was considerably reduced for scenarios II and III because the size of their test dataset is only about 1/3 of the size of Scenario I. However, the test dataset of scenarios II and III is different from their training dataset. The high prediction accuracy of these two scenarios verified the high robustness of the ML algorithm for the compaction prediction. In addition, the KNN model presented more errors than the other two models for scenario III whether or not the buffer zone was set. The test dataset for scenario III used different mixtures from the training

mixtures. A higher error rate of the KNN algorithm indicated its weakness in controlling the out-of-sample errors. On the other hand, the prediction quality of the SVM and LR classifiers is similar and stable for all three dataset scenarios. The prediction accuracy considerably improved when the buffer zone was set. This phenomenon shows that most errors occurred near the threshold, which is acceptable for the field compaction project. The prediction quality of the SVM and LR models were all higher than 97% and even reached 100% when the buffer zone was set. These results confirmed that the SVM and LR algorithms are appropriate and promising for predicting the compaction condition of the laboratory asphalt mixtures. However, the selection of either model needs to consider the inherent characters and demands of the prediction situation.

Although a promising prediction accuracy was achieved by the binary compaction model, it still has limitations to be applied in the field to guide the compaction practice. Based on the pavement compaction conditions, two advanced machine learning models will be developed aiming at different purposes and applications.

- **Compaction classification model**. This model can process the input variables and classify the pavement into multiple compaction categories based on the pavement density. This model possesses great computational efficiency and is particularly suitable when a specific density range is sufficient to meet the construction requirement.
- **Density prediction model**. The density prediction model provides more direct and valuable information on pavement density, making it particularly useful when pavement density is the primary construction requirement. The compaction strategies can be effectively adjusted to meet the desired quality standards.

Compaction Classification Model

Based on binary prediction experiences and the multicategory classification condition, Multinomial Logistic Regression (MLR) is selected as the machine learning algorithm for the compaction classification model (Yu and Shen, 2023). It is an extension of binary logistic regression that allows for more than two categories of the dependent variable. Binary Logistic Regression models a relationship between predictor variables and a categorical response variable. LR gives the probability between 0 and 1 based on the sigmoid function (Montgomery and E.A. Peck, 2021). To predict which class a data belongs to, a possibility threshold would be set. Likewise, MLR uses maximum likelihood estimation to evaluate the probability of categorical membership. In the multicategory prediction, a reference category is selected, and a series of binary logistic regressions is performed for the rest categories to determine which class the data belongs to.

Table 7-6 Output category and density for the compaction classification model

Category	Compaction Condition	Criteria
Class 1	Far under compaction	$< 88\% G_{mm}$
Class 2	Under compaction	88%-91% G_{mm}
Class 3	Good compaction	91%-93% G_{mm}
Class 4	High-density compaction	93%-96% G_{mm}
Class 5	Over compaction	$> 96\% G_{mm}$

The outputs of the compaction classification model are set 5 groups of compaction conditions according to the volumetric property of the asphalt pavement, including "Far under compaction", "Under compaction", "Good compaction", "High-density compaction", and "Over compaction". Similarly, the thresholds were determined based on the construction Specification of the Pennsylvania Department of Transportation (PennDOT) with the Percent Within Limit (PWL) (Transportation, 2020). The threshold in real practice is adjustable to the agency's requirements.

Two predictive levels are considered in this section, (1) classification with a fixed threshold value based on the %Gmm and (2) classification with a buffer zone. Details of these two predictive levels are explained in Table 7-6 and below.

(1) Classification with a fixed threshold value:

- Far under compaction (Class 1): The mixture with the %Gmm is less than 88%.
- Under compaction (Class 2): The mixture with the %Gmm is between 88% and 91%.
- Good compaction (Class 3): The mixture with the %Gmm is between 91% and 93%.
- High-density compaction (Class 4): The mixture with the %Gmm is between 93% and 96%.
- Over compaction (Class 5): The mixture with the %Gmm is greater than 96%.

(2) Classification with a buffer zone:

- Compaction category: The %Gmm of the asphalt mixture that is beyond the ±0.5%Gmm of the threshold must be classified to the corresponding category.
- Buffer Zone: The %Gmm of the asphalt mixture that is within the ±0.5%Gmm of the threshold is acceptable to be classified in either neighbor category.

Laboratory Compaction Classification

In classification modeling, the same 11 asphalt mixtures, a total of 32 specimens with 4154 compaction points, are used to build the multinominal logistic regression (MLR) model. As shown in Table 7-2, the First 7 columns display the input data, and the column "target" serves as the output. Based on the $\%G_{mm}$ of the specimen, 364 data points are categorized as "Far under compaction" (class 1), 342 data points are categorized as "Under compaction" (class 2), 439 data points are categorized as "Good compaction" (class 3), 1316 and 1693 data points are categorized to "High-density compaction" (class 4) and "Over compaction" (class 5), respectively. Three metrics,

including sensitivity, specificity, and accuracy, jointly evaluate the prediction quality for the imbalanced distribution of the five categories. The calculations of three metrics are presented in Table 7-7 and equations (7-8) -(7-10). The same three distinct dataset scenarios have been utilized to facilitate the development and refinement of the model.

Table 7-7 Prediction configuration of the MLR model

Prediction (Model)	Reference ($\%G_{mm}$)				
	Class 1	Class 2	Class 3	Class 4	Class 5
Class 1	True (A11)	False (A12)	False (A13)	False (A14)	False (A15)
Class 2	False (A21)	True (A22)	False (A23)	False (A24)	False (A25)
Class 3	False (A31)	False (A32)	True (A33)	False (A34)	False (A35)
Class 4	False (A41)	False (A42)	False (A43)	True (A44)	False (A45)
Class 5	False (A51)	False (A52)	False (A53)	False (A54)	True (A55)

$$Sensitivity\ of\ Class\ k = {A_{kk}}\Big/{\sum_{i=1}^{5} A_{ik}} \tag{7-8}$$

$$Specificity\ of\ Class\ k = {(\sum_{i=1}^{5} A_{ii} - A_{kk})}\Big/{(\sum_{i=1}^{5}\sum_{j=1}^{5} A_{ij} - \sum_{i=1}^{5} A_{ik})} \tag{7-9}$$

$$Accuracy = {\sum_{i=1}^{5} A_{ii}}\Big/{\sum_{i=1}^{5}\sum_{j=1}^{5} A_{ij}} \tag{7-10}$$

The prediction results of the MLR model under different scenarios are shown in Table 7-8. As displayed, almost all scenarios' predictions are higher than 90% when the fixed threshold is used. When the fixed threshold was adopted, the lowest prediction of the sensitivity occurred in different scenarios. For Scenario I, the lowest sensitivity occurred in the category "Class 2". For Scenario II and III, the lowest sensitivity appeared in the categories "Class 3" and "Class 4", respectively. This phenomenon indicated that the most challenging predictions were around the category of "Good Compaction" (i.e., Class 3). However, when the buffer zone was set, the number

of errors was greatly reduced, and prediction quality considerably improved, verifying that most errors occur near the threshold, especially around the category of “Good Compaction”. Tolerance in the field practice can improve the prediction quality of the asphalt pavement. More importantly, the tolerance (i.e., the range of the buffer zone) can be adjusted according to the needs of projects and construction agencies. For scenarios II and III, where the test dataset is different from the corresponding training dataset, satisfactory prediction quality was also achieved. That reveals the robustness of the MLR model for the compaction prediction and the appropriate selection for the input variables.

Table 7-8 Compaction prediction for the MLR model

Scenario/Parameters		Class 1	Class 2	Class 3	Class 4	Class 5
No buffer zone						
I	Accuracy (error)	92.87% (296/4154)				
	Sensitivity (%)	96.15	89.77	88.16	91.57	95.04
	Specificity (%)	99.60	99.16	98.55	95.84	96.87
II	Accuracy (error)	93.58% (80/1247)				
	Sensitivity (%)	97.98	88.54	91.20	93.47	94.30
	Specificity (%)	99.39	99.48	98.66	95.60	98.01
III	Accuracy (error)	91.75% (119/1442)				
	Sensitivity (%)	97.96	88.64	86.98	85.91	98.55
	Specificity (%)	99.07	98.63	98.98	98.50	93.53
Buffer zone setup						
I	Accuracy (error)	99.64% (15/4154)				
	Sensitivity (%)	99.18	98.54	99.77	99.77	99.82
	Specificity (%)	99.68	99.74	99.62	99.58	99.51
II	Accuracy (error)	99.76% (3/1247)				
	Sensitivity (%)	100	99.42	100	100	99.94
	Specificity (%)	99.92	99.97	99.92	99.89	99.92
III	Accuracy (error)	99.38% (9/1442)				
	Sensitivity (%)	100	98.83	99.77	99.70	100

	Specificity (%)	99.76	99.87	99.78	99.82	99.63

Field Compaction Classification

In the field compaction, limited numbers of compaction cycles were performed to compact the asphalt pavement, only several data thereby can be obtained in a field project, which makes it hard to use the data-informed method to predict the field compaction condition. However, a reasonable correlation was identified between the laboratory and field compaction based on the particle rotation in Chapter V. Because of this correlation, the field compaction condition can be validated or trained by the more accessible and convenient lab compaction data. Two field projects were conducted in this study to train and verify the intelligent model, including the Altoona project and the Indiana project. Detailed information on these two projects has been introduced in Chapter IV. These two projects were dramatically different in terms of the pavement structure, asphalt mix design, applied compactor, and compaction design. Specifically, the Altoona project used a static roller and vibratory roller for the pavement compaction, and a total of 11 compaction cycles were applied. On the other hand, the Indiana project only applied two cycles of vibratory roller on the asphalt pavement. Similarly, the SmartKli® sensor was embedded inside the asphalt pavement to collect the particle kinematic behavior during compaction. All collected information for the compaction prediction is shown in Table 7-9. For the asphalt pavement compaction project in Altoona, the static roller is used in the middle and end of the compaction. A rolling resistance coefficient of 0.09 and 0.05 was used for the calculation of the compaction energy in the middle and finishing phases, respectively (Zhao et al., 2021). The information on the vibratory rollers used for the two projects is presented in Chapter 4 Table 4-4.

Table 7-9 summarizes the results from the compaction classification model for these two field projects. As shown, the compaction condition of both projects was reasonably classified into

"Far under compaction," "Under compaction," and "Good compaction" categories, which is in agreement with the density progression trend during compaction. After compaction, several pavement cores were drilled out and their density was measured in the lab for model verification. For the Altoona project, the density of the pavement cores near the SmartKli® sensor is 93.1% and 93.6% G_{mm}, respectively, which are in the buffer zone between Class 3 and Class 4. For the Indiana project, the pavement is predicted "Good compaction" at the end cycle of compaction. The density near the SmartKli® is 92.8% and 92.5% G_{mm}, which is in the volumetric range of the "Good compaction" (Class 3) category. The consistency between the model prediction and core density indicated the effectiveness and robustness of the compaction classification model.

Table 7-9 Field compaction prediction based on the MLR model

Type	Additive	NMSA	Binder	Rotation(x)	Rotation(y)	Energy	Roller	Prediction
Altoona Project								
1	0	9.5	76	3.03	1.15	77.9	V	Class 1
1	0	9.5	76	1.45	0.44	155.9	V	Class 1
1	0	9.5	76	0.10	0.96	233.8	V	Class 1
1	0	9.5	76	0.55	0.43	298.4	S	Class 1
1	0	9.5	76	0.66	0.46	363.1	S	Class 2
1	0	9.5	76	1.10	0.48	427.7	S	Class 2
1	0	9.5	76	1.00	1.30	505.7	V	Class 2
1	0	9.5	76	0.03	0.08	583.6	V	Class 3
1	0	9.5	76	0.56	0.20	661.6	V	Class 3
1	0	9.5	76	0.41	0.42	697.5	S	Class 3
1	0	9.5	76	0.18	0.36	733.4	S	Class 3
Indiana Project								
0	0	12.5	64	8.17	2.05	229.7	V	Class 2
0	0	12.5	64	3.59	1.04	459.4	V	Class 3

Note: Roller "V" and "C" mean vibratory and static roller compaction; Class "1", "2" and "3" represent "Far under compaction", "Under compaction" and "Good compaction", respectively.

Density Prediction Model

Compared with the compaction classification model, sometimes the direct way to predict the pavement density is preferable for compaction agencies and engineers for the strategies adjustment. The density prediction model was established for these scenarios. For the machine learning algorithm, the Artificial Neural Network (ANN) is one of the fastest-growing artificial intelligence (AI) techniques (Moayedi et al., 2020). It is inspired by an animal's central nervous system and intended to simulate the behavior of biological systems composed of "neurons". For the advancements in data science and computing capacity, ANN has been applied to process complex problems in pavement construction and performance prediction (Hou et al., 2021) (Yang et al., 2021). A neural network usually contains the input layer, hidden layers, and output layer, as shown in Figure 7-3. The input and output layers are to feed raw information into the network and provide the prediction from the algorithm. The hidden layer connects the input and output and determines the activity of each hidden unit by calculation algorithms (Moayedi et al., 2020).

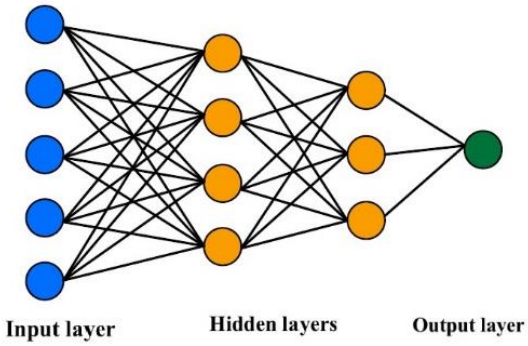

Figure 7-3 Configuration of the artificial neural network (ANN)

Laboratory Compaction Prediction

A density prediction model was developed based on the same database which contains 11 asphalt mixtures, 32 asphalt specimens, and 4154 compaction points. Like the MLR modeling, the same variables serve as the inputs, including particle relative rotation, compaction energy, and material property information, as shown in the first seven columns in Table 7-2, which means 7 neurons in the input layer. The column "% G_{mm} " serves as the output for the model. The predictive quality can be obtained by comparing the specimen density with the ANN prediction results.

For the laboratory compaction, the specimen density at each gyration cycle can be determined according to the height at each gyration and the final bulk specific gravity. The Mean Relative Error (MRE) and Root Mean Square Error (RMSE) were used for the prediction evaluation, and their calculations were shown in equations (7-11) and (7-12), respectively. Typically, larger MRE and MSE indicate more variation between the predictions and the true values, thus lower prediction accuracy.

$$MRE = \frac{1}{n}\sum_{i=1}^{n}\frac{|Y_i - X_i|}{X_i} \times 100\% \qquad (7\text{-}11)$$

$$RMSE = \sqrt{\frac{1}{n}\sum_{i=1}^{n}(Y_i - X_i)^2} \qquad (7\text{-}12)$$

Where, Y_i and X_i are the predictive density and measured (or calculated) density at the i^{th} data point, respectively. n is the number of data points.

In ANN modeling, two hidden layers are selected since it is an efficient configuration for most prediction problems and can also avoid overfitting (Malekian and Chitsaz, 2021). The neurons of hidden layers are usually between the numbers of input and output neurons (Malekian and Chitsaz, 2021). Therefore, 9 configurations of ANN models are built in Table 7-10 to test

prediction accuracy. To clarify, the number series 7-6-5-1 means the number of neurons in the input layer, first and second hidden layer, and output layer. Configurations 7-5-3-1, 7-5-2-1, and 7-4-2-1 are not displayed in the table since they cannot converge the results under certain calculation steps. Eventually, the configuration of 7-6-3-1 is selected for its smallest prediction errors.

Table 7-10 Prediction comparison for different ANN configurations

Configuration of ANN	RMSE	MRE (%)
7-6-5-1	0.3743	0.2987
7-6-4-1	0.3741	0.3054
7-6-3-1	0.3649	0.2954
7-6-2-1	0.3752	0.3013
7-5-4-1	0.3788	0.3072
7-4-3-1	0.3718	0.3037

After selecting the model's input, output, and configuration, the ANN model was created based on the laboratory compaction. The prediction results under three dataset scenarios are shown in Figure 7-4. It should be noted that all prediction errors are smaller than 1% MRE and 0.5 RMSE. Satisfactory prediction quality is also achieved for Scenarios II and III, in which the test dataset differs from the corresponding training dataset. These results affirm the appropriate selection of the input variables and the robustness of the ANN model for the compaction prediction.

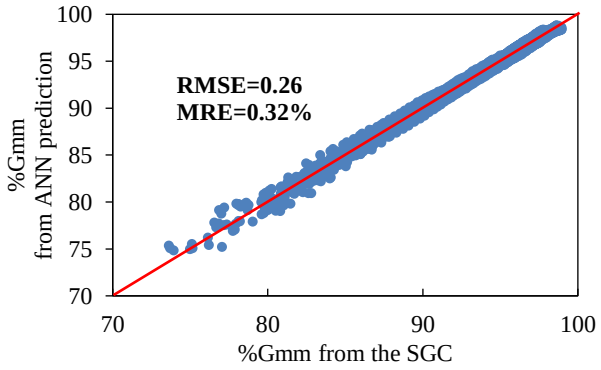

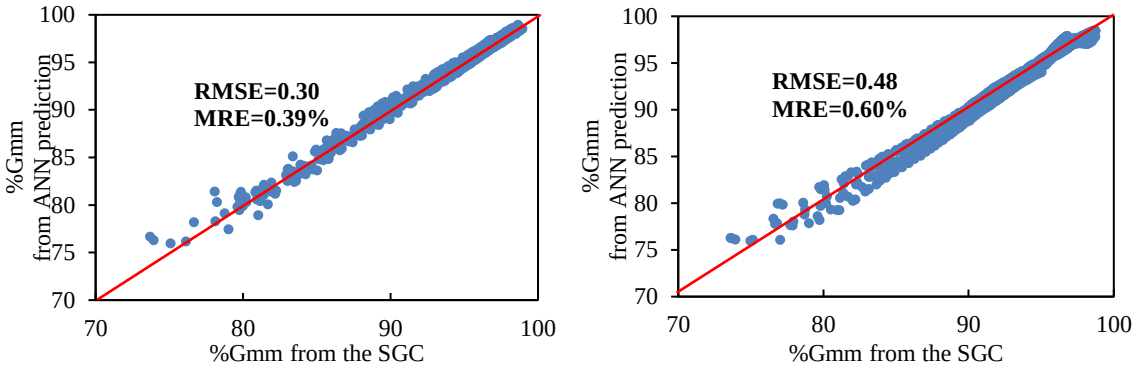

Figure 7-4 Comparison between the SGC specimen density and ANN prediction for Scenario I (top), Scenario II (left), and Scenario III (right)

Field Compaction Prediction

Given the reasonable correlation between the lab and field compaction according to the particle relative rotation, the density prediction model was then further applied to the field compaction prediction. The data collected in the same field projects, including the Altoona project and Indiana project, were involved. The input data were presented in Table 7-10, and the predictions were summarized in Table 7-11. As seen, the pavement density is predicted in good order from the beginning to the end of the compaction, even though the compaction cycles, roller compactors, and asphalt materials are different from these two projects. The measured density of the pavement cores was also displayed. For the Altoona project, the density of the core samples near the SmartKli® is 93.1% and 93.6% $\boldsymbol{G_{mm}}$. Compared with the model prediction of 93.1%G_{mm}, the mean relative error (MRE) was 0.27%. For the Indiana project, 92.5% and 92.8% $\boldsymbol{G_{mm}}$ of the core samples are close to the prediction of 93.1% $\boldsymbol{G_{mm}}$, of which the prediction error was 0.48% MRE. Two successful applications of the density prediction model confirmed the practicality and feasibility of using the ANN model to predict the density of asphalt pavement. The concept of using more accessible and

convenient laboratory compaction data to train the model and to predict the density in the field is also feasible.

Table 7-11 Field compaction prediction based on the ANN model

Project	Altoona Project										
Cycle	1	2	3	4	5	6	7	8	9	10	11
Roller	V	V	V	S	S	S	V	V	V	S	S
ANN	78.2	83.7	88.3	88.8	89.8	90.3	91.4	92.2	92.4	92.8	93.1

Project	Indiana		Note:
Cycle	1	2	Core density is the density of the core sample (%*Gmm*) for verification.
Roller	V	V	The core density for the Altoona Project is 93.1%, 93.6%G_{mm}.
ANN	91.7	93.1	The core density for the Indiana Project is 92.5% and 92.8 %G_{mm}.

Summary

Laid on the foundation of the compaction mechanism, this chapter developed two intelligent models to predict the compaction conditions or density of asphalt pavement using sensing technology and machine learning algorithms. Starting from a preliminary binary compaction model, the applicability of the data-informed method in pavement compaction prediction was verified. The input variables were determined by comparing the different combinations of candidate variables. Both laboratory and field compactions were conducted for the data collection and model verification. Several conclusions were obtained below:

- Particle relative rotation, compaction energy, and the material properties, including asphalt binder high-temperature performance grade (PG), nominal maximum aggregates size (NMAS), mixture type, and additives content, can serve as the input variables to predict reasonable compaction conditions of asphalt pavements.
- The Support Vector Machine (SVM) and Logistic Regression (LR) are appropriate algorithms to predict the binary compaction condition of the asphalt mixture. However, the selection for

either model needs to consider their inherent characters and demands of the prediction situation.

- A multinomial logistic regression (MLR) was established to classify the compaction conditions of the asphalt pavement into five categories: Far under compaction, Under compaction, good compaction, High-density compaction, and Over compaction. An artificial neural network (ANN) was built to predict the density of the asphalt pavement. Both models were reasonable and effective in predicting the compaction conditions of asphalt pavement.
- This study substantiated the reasonableness of building compaction prediction models based on laboratory data and applying the model to predict field compaction conditions. This methodology was justified by the high correlation in the particle kinematic behaviors between the laboratory and field compactions. This approach was practical and beneficial for compaction optimization as laboratory compactions are convenient and can be performed on various mixtures and compaction conditions.

Chapter 8

Conclusion and Future Work

Conclusions

The objectives of this study are to investigate the compaction mechanism of the particulate asphalt mixture and use this concept as a foundation to evaluate the workability of the asphalt mixture and predict the compaction condition of the asphalt pavement, thereby prompting the automation in pavement construction. To achieve this, various techniques and technologies were utilized, including the MEMS (micro-electromechanical system) device (i.e., wireless particle size sensor, SmartKli®), laboratory and field compaction experiments, numerical modeling, artificial intelligence, and statistical analysis. The primary conclusions are summarized as follows.

Compaction Mechanism of the Asphalt Mixture

The compaction mechanism of the asphalt mixture was summarized according to the compaction experiment with the remote sensor, and the numerical modeling. This mechanism stands on the mesoscale level, which emphasizes the behavior of the asphalt particles: The compaction of asphalt mixtures can be described in three distinct stages in terms of particle rotation: (a) Breakdown Stage involves substantial relative rotations, leading to a marked reduction and rapid densification of the material. (b) The Main Compaction Stage is characterized by the formation of a structural skeleton and the interaction of imbalanced particles. Most densification continues at a slower pace. (c) The Finishing Stage is where particle interactions stabilize, resulting in minimal densification and the leveling of the surface.

The variation in particle rotation is closely linked to their vertical translation and the height change of the asphalt specimen, rendering it an effective parameter for assessing the workability of the asphalt mixture. Laboratory gyratory and field roller compaction are interconnected through this particle rotation. This connection allows for the utilization of more accessible and convenient laboratory data to support and guide field compaction practices, paving the way for automation in pavement construction. Furthermore, particle size plays a pivotal role in kinematic behavior and its relationship with the compactability of the asphalt mixture. The particle rotation of the coarse aggregates presents a high correlation with the mixture's compactability, while the fine aggregate did not. Therefore, selecting the appropriate size of the particle is crucial for the workability evaluation and density prediction, which should consider the packing and interlocking properties of aggregates.

Workability or Compactability Evaluation

Based on the compaction mechanism, the workability evaluation of the asphalt mixture was conducted on various asphalt mixtures, including HMA (Hot Mix Asphalt), WMA (Warm Mix Asphalt), and RPMA (Recycled Plastic Modified Asphalt) with distinct mix designs and compaction conditions. The following findings and recommendations can be concluded.

(1) Three methods were proposed to evaluate the mixture's workability, including (a) Particle kinematic parameters, a straightforward approach but limited information can be provided. (b) Particle rotation curves. This method can clearly illustrate the variation of the particle rotation at different compaction stages. (c) Statistical analysis can determine whether a significant improvement or reduction in workability occurred because of the change in the mixed design and compaction condition.

(2) The particle kinematic parameter offers the most straightforward approach to quantify the

mixture’s workability, but a single value of the kinematic parameter can provide limited information. The particle rotation curves can thus be used to clearly illustrate the particle rotation at different compaction stages. Furthermore, the statistical method was developed to compare the workability differences in particle rotation. It involves the equivalency test (i.e., Two One-Sided T-tests, TOST) and difference test (i.e., one sample T-test) to analyze the residual rotation between two asphalt mixtures. This approach could determine whether a particular factor, such as alterations in the mix design or compaction conditions, has a significant impact on the asphalt mixture's workability.

(3) The application of the chemical additive, temperature, and asphalt binder verified the reasonableness of the three methods in the workability evaluation. Specifically in the WMA application, equivalent workability can be achieved following these two designs: (a) adding 0.35% additive (Evotherm M1) but reducing 17^{o}C compaction temperature; (b) adding 0.7% Evotherm M1 but reducing 33^{o}C compaction temperature.

(4) For the RPMA (Recycled plastic modified asphalt) scenario, the conventional dry processing method can reduce the workability of the RPMA. Comparably. The wet processing method is more effective in processing the LDPE, as the workability of the RPMA remains equivalent to the corresponding HMA. However, when the alternative dry design method was used, which added plastics without replacing any virgin binder, the workability of the RPMA remained equivalent to that of the corresponding HMA. Therefore, maintaining an adequate amount of binder content is crucial to preserve workability for the RPMA designed by the dry processing method. It is also important to consider other properties and economic benefits when designing the RPMA using the dry processing method.

Compaction Prediction Based on Compaction Mechanism

Intelligent compaction models are another application of the concept of the compaction mechanism. After the applicability check, input, and output determination according to the binary preliminary model, two compaction models were established on laboratory and field compaction practices. Several conclusions are obtained as summarized below.

(1) Particle relative rotation, compaction energy, and material properties, including asphalt binder performance grade, gradation information, mixture type, and additives content, can serve as the input variables for the compaction prediction.

(2) An effective binary compaction model was created using the Support Vector Machine (SVM) and Logistic Regression (LR), proving the feasibility of the data-informed method in intelligent compaction prediction. After that, a compaction classification model based on the multinomial logistic regression (MLR), and a density prediction model based on the artificial neural network (ANN) were established. Both models are reasonably effective in predicting the compaction conditions of asphalt pavement.

(3) This study connects the laboratory and field compaction because of the reasonable correlation of the particle kinematic behaviors between these two compaction methods, substantiating the reasonableness of applying the more accessible and convenient lab compaction data to predict field compaction conditions.

Future Works

This study delved into the compaction mechanism of asphalt mixtures through compaction experiments, sensing technology, and numerical modeling. In light of these findings, a novel workability evaluation method was introduced to address the absence of a standard test method for

assessing asphalt mixture workability. This method has potential implications for enhancing the design and construction processes of asphalt pavements. Furthermore, innovative compaction models were developed by integrating artificial intelligence and sensing technology into pavement construction. This model can realize real-time data collection and compaction condition prediction for asphalt pavements, allowing engineers to adjust strategies proactively, thereby enhancing the overall compaction quality of asphalt pavements. Nevertheless, the compaction of asphalt pavements remains a vast and intricate subject. Despite the considerable efforts invested in this study, numerous avenues for further research and development still exist. The following outlines key areas for future exploration and refinement:

The investigation revealed a strong correlation between the kinematic behaviors of coarse aggregates and the density of asphalt mixtures during compaction, as evidenced by sensing compaction data and Discrete Element Method (DEM) simulations. Conversely, no such correlation was observed for fine aggregates. An additional noteworthy finding was the inconsistent classification of aggregates as coarse or fine, particularly in mixtures with distinct gradations. For instance, aggregates of the same size (e.g., 4.75mm) exhibited coarse behavior in dense-graded mixtures but acted as fine particles in open-graded friction courses. It was hypothesized that interlocking and packing properties played a role in influencing the compaction behaviors of different aggregates. Consequently, further research is imperative to elucidate the relationship between particle size and compaction behaviors. A comprehensive understanding of aggregates' interlocking properties and compaction behaviors will contribute to a more nuanced mix design from a structural perspective and enhance the overall compaction effectiveness of asphalt pavements.

The compaction mode and behaviors of aggregates of different sizes are expected to be interconnected. For instance, varying vibration frequencies will impact the rotation or translation of aggregates differently based on their size and compaction characteristics. Therefore, it is

essential to delve into the relationship between compaction mode variables, including vibration frequency, compaction modes, and loading magnitude, and the kinematic behaviors exhibited by particles. Accomplishing this task will facilitate the design of optimal compaction practices, determining the suitable frequency, speed, and loading for diverse asphalt mixtures, pavement structures, and base layers. This investigation aims to enhance the precision and effectiveness of compaction processes in asphalt construction.

The compaction prediction model still requires refinement. Existing models have been formulated and validated using a limited range of asphalt mixtures and field compaction projects. To enhance model accuracy and applicability, various factors such as supporting conditions, asphalt thickness, climate, and others should be considered in the model. Advanced neural network models can be employed to accommodate a broader range of construction and materials scenarios. The goal is to establish and calibrate a comprehensive compaction model that is applicable across different climate zones. If universal applicability proves challenging, an alternative approach involves developing a robust compaction model tailored to specific climate zones, taking into account local inputs for increased accuracy and reliability.

One of the paramount objectives is to realize automation in asphalt pavement compaction. Embedding remote sensors within the asphalt layer effectively mitigates the influences of the multilayered pavement structure on collected responses. However, the fixed positioning of sensors falls short in providing comprehensive monitoring coverage of the entire asphalt pavement, leading to potential variations and biases across the pavement surface. A potential solution to this challenge involves integrating the AI-based prediction model with intelligent compaction (IC) technology. While IC technology significantly enhances the compaction uniformity of asphalt pavements, its prediction accuracy for compaction degree may be less precise. The model, processing the initial response, can offer a reliable density prediction for the asphalt layer. The synergistic combination

of these two technologies holds promise as an approach to achieving full-coverage compaction monitoring and accurate density prediction in asphalt pavement construction.

Reference

Abbas, A., Masad, E., Papagiannakis, T., and Shenoy, A. (2005). Modeling asphalt mastic stiffness using discrete element analysis and micromechanics-based models. *International Journal of Pavement Engineering, 6*(2), 137-146. https://doi.org/10.1080/10298430500159040

Adam D, and Brandl, H. (1997). *Sophisticated continuous compaction control of soils and granular materials* 14th International Conference on Soil Mechanics and Foundation Engineering Hamburg. https://www.issmge.org/uploads/publications/1/31/1997_01_0009.pdf

Adhikari, S., and You, Z. (2011). Investigating the Sensitivity of Aggregate Size within Sand Mastic by Modeling the Microstructure of an Asphalt Mixture. *Journal of Materials in Civil Engineering, 23*(5), 580-586. https://doi.org/10.1061/(ASCE)MT.1943-5533.0000212

Al-shamsi, K., and Mohammad, L. (2007). A Look at the Bailey Method and Locking Point Concept in Superpave Mixture Design. *Transportation Research Circular, E*(C124), 12-32. http://www.trb.org/Publications/Blurbs/159461.aspx

Anjan Kumar, S., Aldouri, R., Nazarian, S., and Si, J. (2016). Accelerated assessment of quality of compacted geomaterials with intelligent compaction technology. *Construction and Building Materials, 113*, 824-834. https://doi.org/https://doi.org/10.1016/j.conbuildmat.2016.03.117

Bahia, H. U., and Faheem, A. (2004). *Using gyratory compactor to measure mechanical stability of asphalt mixtures*. Wisconsin Highway Research Program., https://minds.wisconsin.edu/bitstream/handle/1793/6907/05%2002.pdf?sequence=1&isAllowed=y

Behnood, A., and Mohammadi Golafshani, E. Predicting the dynamic modulus of asphalt mixture using machine learning techniques: An application of multi biogeography-based programming. *Construction and Building Materials, 266*, 120983. https://doi.org/https://doi.org/10.1016/j.conbuildmat.2020.120983

Buttlar, W. G., and You, Z. (2001) Discrete Element Modeling of Asphalt Concrete: Microfabric

Approach. *Transportation Research Record, 1757*(1), 111-118. https://doi.org/10.3141/1757-13

Button J W, and Little D N, Jagadam V. (1994). Correlation of selected laboratory compaction methods with field compaction. *Transportation Research Record, Transportation Research Board,* (1454), 193-201. https://onlinepubs.trb.org/Onlinepubs/trr/1994/1454/1454-022.pdf

Cervantes, J., Garcia-Lamont, F., Rodríguez-Mazahua, L., and Lopez, A. (2020) A comprehensive survey on support vector machine classification: Applications, challenges and trends. *Neurocomputing, 408*, 189-215. https://doi.org/https://doi.org/10.1016/j.neucom.2019.10.118

Chang, G. K., Xu, Q., Rutledge, J. L., and Garber, S. I. (2014). A Study on Intelligent Compacting and In-Place Asphalt Density https://rosap.ntl.bts.gov/view/dot/38554

Chen, C., and McDowell, G. R. (2014, 2016/01/01). An investigation of the dynamic behaviour of track transition zones using discrete element modelling. *Proceedings of the Institution of Mechanical Engineers, Part F: Journal of Rail and Rapid Transit, 230*(1), 117-128. https://doi.org/10.1177/0954409714528892

Chen, J. (2011). *Discrete Element Method (DEM) Analyses for Hot-Mix Asphalt (HMA) Mixture Compaction* Ph.D. Dissertation, The University of Tennessee, Knoxville. https://trace.tennessee.edu/cgi/viewcontent.cgi?article=2102&context=utk_graddiss&httpsredir=1&referer=

Chen, J., Huang, B., and Shu, X. (2013). Air-Void Distribution Analysis of Asphalt Mixture Using Discrete Element Method. *Journal of Materials in Civil Engineering, 25*(10), 1375-1385. https://doi.org/10.1061/(ASCE)MT.1943-5533.0000661

Chen, J., Zeng, L., and Yin, J. (2013 Discrete Element Method (DEM) Analyses of Hot-Mix Asphalt (HMA) Mixtures Compaction and Internal Structure. *Advanced Materials Research, 639-640*, 1287-1294. https://doi.org/10.4028/www.scientific.net/AMR.639-640.1287

Chen, J., Zeng, L., and Yin, J. (2013). Discrete Element Method (DEM) Analyses of Hot-Mix Asphalt (HMA) Mixtures Compaction and Internal Structure. *Advanced Materials Research, 639-640*, 1287 - 1294. https://doi.org/10.4028/www.scientific.net/AMR.639-640.1287

Cheng, Z., Zhang, D., Xie, S., Polaczyk, P. A., and Wang, T. (2022). SmartRock-Based Research on Gyratory Locking Point for Stone Mastic Asphalt Mixture. *Buildings, 12*(2), 97.

https://www.mdpi.com/2075-5309/12/2/97

Christensen, D. W., and Anderson, D. A. (1992). Interpretation of dynamic mechanical test data for paving grade asphalt cements. *Conference of Asphalt Paving Technology* http://worldcat.org/issn/02702932

Collop, A. C., McDowell, G. R., and Lee, Y. (2004). Use of the Distinct Element Method to Model the Deformation Behavior of an Idealized Asphalt Mixture. *International Journal of Pavement Engineering, 5*(1), 1-7. https://doi.org/10.1080/10294830410001709164

Collop, A. C., McDowell, G. R., and Lee, Y. W. (2006 Modelling dilation in an idealised asphalt mixture using discrete element modelling. *Granular Matter, 8*(3), 175-184. https://doi.org/10.1007/s10035-006-0013-3

Commuri, S., and Zaman, M. (2006) A novel neural network-based asphalt compaction analyzer. *International Journal of Pavement Engineering, 9*. https://doi.org/10.1080/10298430701232018

Cundall, P. A. (1971). A computer model for simulating progressive, large-scale movements in blocky rock systems. *Proceedings of the Symposium of the International Society of Rock Mechanics, 2, 2-8.*

Dai, Q., and You, Z. (2007). Prediction of Creep Stiffness of Asphalt Mixture with Micromechanical Finite-Element and Discrete-Element Models. *Journal of Engineering Mechanics-asce - J ENG MECH-ASCE, 133*. https://doi.org/10.1061/(ASCE)0733-9399(2007)133:2(163)

DelRio-Prat, M., Vega-Zamanillo, A., Castro-Fresno, D., and Calzada-Pérez, M. Á. Energy consumption during compaction with a Gyratory Intensive Compactor Tester. Estimation models. *Construction and Building Materials, 25*(2), 979-986. https://doi.org/https://doi.org/10.1016/j.conbuildmat.2010.06.083

Ding, X., Ma, T., and Huang, X. (2019 Discrete-Element Contour-Filling Modeling Method for Micromechanical and Macromechanical Analysis of Aggregate Skeleton of Asphalt Mixture. *Journal of Transportation Engineering, Part B: Pavements, 145*(1), 04018056. https://doi.org/10.1061/JPEODX.0000083

Dong, Q., Chen, X., Dong, S., and Ni, F. (2022). Data Analysis in Pavement Engineering: An Overview. *IEEE Transactions on Intelligent Transportation Systems, 23*(11), 22020-22039. https://doi.org/10.1109/TITS.2021.3115792

Eberly, D. (2020). Euler Angle Formulas *Geometric Tools*. https://www.geometrictools.com/

El-Badawy, S., Abd El-Hakim, R., and Awed, A. (2018) Comparing Artificial Neural Networks

with Regression Models for Hot-Mix Asphalt Dynamic Modulus Prediction. *Journal of Materials in Civil Engineering, 30*. https://doi.org/10.1061/(ASCE)MT.1943-5533.0002282

Eleyedath, A., and Swamy, A. K. (2020). Prediction of dynamic modulus of asphalt concrete using hybrid machine learning technique. *International Journal of Pavement Engineering*, 1-16. https://doi.org/10.1080/10298436.2020.1841191

Escudier, M., and Atkins, T. (2019). *A Dictionary of Mechanical Engineering*. Oxford University Press. https://doi.org/10.1093/acref/9780199587438.001.0001

Fang, Z., Zhu, Y., Ma, T., Zhang, Y., Han, T., and Zhang, J. (2022) Dynamical response to vibration roller compaction and its application in intelligent compaction. *Automation in Construction, 142*, 104473. https://doi.org/https://doi.org/10.1016/j.autcon.2022.104473

Georgiou, P., Plati, C., and Loizos, A. (2018) Soft Computing Models to Predict Pavement Roughness: A Comparative Study. *Advances in Civil Engineering, 2018*, 5939806. https://doi.org/10.1155/2018/5939806

Gomber, P., Kauffman, R. J., Parker, C., and Weber, B. W. (2018) On the Fintech Revolution: Interpreting the Forces of Innovation, Disruption, and Transformation in Financial Services. *Journal of Management Information Systems, 35*(1), 220-265. https://doi.org/10.1080/07421222.2018.1440766

Gong, F., Zhou, X., You, Z., Liu, Y., and Chen, S. (2018) Using discrete element models to track movement of coarse aggregates during compaction of asphalt mixture. *Construction and Building Materials, 189*, 338-351. https://doi.org/https://doi.org/10.1016/j.conbuildmat.2018.08.133

Guler, M., Bahia, H., Bosscher, P., and Plesha, M. (2000) Device for Measuring Shear Resistance of Hot-Mix Asphalt in Gyratory Compactor. *Transportation Research Record, 1723*, 116-124. https://doi.org/10.3141/1723-15

Hanaor, D., Gan, Y., and Einav, I. (2016 Static friction at fractal interfaces. *Tribology International, 93*, 229-238. https://doi.org/10.1016/j.triboint.2015.09.016

Harold Von Quntus, Chuck S Hughes, and Scherocman, J. S. (1988). *NCHRP Asphalt-Aggregate Mixture Analysis System,* https://onlinepubs.trb.org/Onlinepubs/trr/1992/1353/1353-013.pdf

Hossain, M., Gopisetti, L. S. P., and Miah, M. S. (2020). Artificial neural network modelling to predict international roughness index of rigid pavements. *International Journal of Pavement Research and Technology, 13*(3), 229-239. https://doi.org/10.1007/s42947-020-

0178-x

Hossain, M. I., Gopisetti, L. S. P., and Miah, M. S. (2019 International Roughness Index Prediction of Flexible Pavements Using Neural Networks. *Journal of Transportation Engineering, Part B: Pavements, 145*(1), 04018058. https://doi.org/10.1061/JPEODX.0000088

Hou, Y., Li, Q., Zhang, C., Lu, G., Ye, Z., Chen, Y., Wang, L., and Cao, D. (2021) The State-of-the-Art Review on Applications of Intrusive Sensing, Image Processing Techniques, and Machine Learning Methods in Pavement Monitoring and Analysis. *Engineering, 7*(6), 845-856. https://doi.org/https://doi.org/10.1016/j.eng.2020.07.030

Hu, W., Jia, X., Huang, B., and Park, H. (2017) Evaluation of compactability of asphalt mixture utilizing asphalt vibratory compactor. *Construction and Building Materials, 139*, 419-429. https://doi.org/https://doi.org/10.1016/j.conbuildmat.2017.02.070

Hu, W., Jia, X., Zhu, X., Gong, H., Xue, G., and Huang, B. (2019) Investigating key factors of intelligent compaction for asphalt paving: A comparative case study. *Construction and Building Materials, 229*, 116876. https://doi.org/https://doi.org/10.1016/j.conbuildmat.2019.116876

Hu, W., Jia, X., Zhu, X., Su, A., Du, Y., and Huang, B. (2020) Influence of moisture content on intelligent soil compaction. *Automation in Construction, 113*, 103141. https://doi.org/https://doi.org/10.1016/j.autcon.2020.103141

Hu, W., Shu, X., Jia, X., and Huang, B. (2018) Geostatistical analysis of intelligent compaction measurements for asphalt pavement compaction. *Automation in Construction, 89*, 162-169. https://doi.org/https://doi.org/10.1016/j.autcon.2018.01.012

Jia, X., Hu, W., Polaczyk, P., Gong, H., and Huang, B. (2019) Comparative Evaluation of Compacting Process for Base Materials using Lab Compaction Methods. *Transportation Research Record, 2673*(4), 558-567. https://doi.org/10.1177/0361198119837953

Jiang, Y., Deng, C., Li, Q., and Liu, H. (2019) Effect of Compaction Methods on Physical and Mechanical Properties of Asphalt Mixture. *Journal of Materials in Civil Engineering, 31*(6), 04019075. https://doi.org/10.1061/(ASCE)MT.1943-5533.0002732

Jianlong Zheng, X. C., Qingrui Li. (2007). Analysis research on vibratory compacting process of hot asohalt mixture pavement. *Engineering Mechanics, 25*(10), 200-207.

Kaya, O., Garg, N., Ceylan, H., and Kim, S. (2018). *Development of Artificial Neural Networks Based Predictive Models for Dynamic Modulus of Airfield Pavement Asphalt Mixtures*. https://doi.org/10.1061/9780784481554.001

Kim, H., Wagoner, M. P., and Buttlar, W. G. (2008). Simulation of Fracture Behavior in Asphalt Concrete Using a Heterogeneous Cohesive Zone Discrete Element Model. *Journal of Materials in Civil Engineering, 20*(8), 552-563. https://doi.org/doi:10.1061/(ASCE)0899-1561(2008)20:8(552)

Li, X., Wang, H., Zhang, C., Diab, A., and You, Z. (2016) Characteristics of a Surfactant Produced Warm Mix Asphalt Binder and Workability of the Mixture. *Journal of Testing and Evaluation, 44*(6), 2219-2230. https://doi.org/10.1520/JTE20140447

Linden, R. N., Mahoney, J. P., and Jackson, N. C. (1989). Effect of Compaction on Asphalt Concrete Performance. *Transportation Research Record*. https://onlinepubs.trb.org/Onlinepubs/trr/1989/1217/1217-003.pdf

Ling, J., Lin, S., Qian, J., Zhang, J., Han, B., and Liu, M. (2018). Continuous Compaction Control Technology for Granite Residual Subgrade Compaction. *Journal of Materials in Civil Engineering, 30*(12), 04018316. https://doi.org/doi:10.1061/(ASCE)MT.1943-5533.0002522

Liu, D., Li, Z., and Lian, Z. (2014) Compaction quality assessment of earth-rock dam materials using roller-integrated compaction monitoring technology. *Automation in Construction, 44*, 234-246. https://doi.org/https://doi.org/10.1016/j.autcon.2014.04.016

Liu, D., Li, Z., and Liu, J. (2015) Experimental study on real-time control of roller compacted concrete dam compaction quality using unit compaction energy indices. *Construction and Building Materials, 96*, 567-575. https://doi.org/https://doi.org/10.1016/j.conbuildmat.2015.08.048

Liu, D., Lin, M., and Li, S. (2016) Real-Time Quality Monitoring and Control of Highway Compaction. *Automation in Construction, 62*, 114-123. https://doi.org/https://doi.org/10.1016/j.autcon.2015.11.007

Liu, S., Huang, H., Qiu, T., and Gao, L. (2017) Comparison of Laboratory Testing Using SmartRock and Discrete Element Modeling of Ballast Particle Movement. *Journal of Materials in Civil Engineering, 29*(3), D6016001. https://doi.org/10.1061/(ASCE)MT.1943-5533.0001540

Liu, S., Huang, H., Qiu, T., and Kwon, J. (2016) Effect of geogrid on railroad ballast particle movement. *Transportation Geotechnics, 9*, 110-122. https://doi.org/https://doi.org/10.1016/j.trgeo.2016.08.003

Liu, Y., Dai, Q., and You, Z. (2009) Viscoelastic Model for Discrete Element Simulation of Asphalt Mixtures. *Journal of Engineering Mechanics-asce - J ENG MECH-ASCE, 135*.

https://doi.org/10.1061/(ASCE)0733-9399(2009)135:4(324)

Liu, Y., You, Z., and Zhao, Y. (2012 Three-dimensional discrete element modeling of asphalt concrete: Size effects of elements. *Construction and Building Materials, 37*, 775-782. https://doi.org/https://doi.org/10.1016/j.conbuildmat.2012.08.007

Liu, Y., Zhou, X., You, Z., Yao, S., Gong, F., and Wang, H. Discrete element modeling of realistic particle shapes in stone-based mixtures through MATLAB-based imaging process. *Construction and Building Materials, 143*, 169-178. https://doi.org/https://doi.org/10.1016/j.conbuildmat.2017.03.037

Lugeiyamu, L., Kunlin, M., Mensahn, E. S. K., and Faraz, A. Utilization of waste polyethylene terephthalate (PET) as partial replacement of bitumen in stone mastic asphalt. *Construction and Building Materials, 309*, 125176. https://doi.org/https://doi.org/10.1016/j.conbuildmat.2021.125176

Ma, Y., Chen, F., Ma, T., Huang, X., and Zhang, Y. (2022). Intelligent Compaction: An Improved Quality Monitoring and Control of Asphalt Pavement Construction Technology. *IEEE Transactions on Intelligent Transportation Systems, 23*(9), 14875-14882. https://doi.org/10.1109/TITS.2021.3134699

Malekian, A., and Chitsaz, N. (2021). Concepts, procedures, and applications of artificial neural network models in streamflow forecasting. *Advances in Streamflow Forecasting: From Traditional to Modern Approaches*(25), 115-147. https://doi.org/https://doi.org/10.1016/B978-0-12-820673-7.00003-2

Manzi, S., Mazzotti, C., and Chiara Bignozzi, M. (2017 Self-compacting concrete with recycled concrete aggregate: Study of the long-term properties. *Construction and Building Materials, 157*, 582-590. https://doi.org/https://doi.org/10.1016/j.conbuildmat.2017.09.129

Marcelino, P., de Lurdes Antunes, M., Fortunato, E., and Gomes, M. C. (2021). Machine learning approach for pavement performance prediction. *International Journal of Pavement Engineering, 22*(3), 341-354. https://doi.org/10.1080/10298436.2019.1609673

Masad, E., Kassem, E., and Chowdhury, A. (2009). Application of imaging technology to improve the laboratory and field compaction of HMA https://rosap.ntl.bts.gov/view/dot/16838

Masad, E., Muhunthan, B., Shashidhar, N., and Harman, T. (1999) Internal Structure Characterization of Asphalt Concrete Using Image Analysis. *Journal of Computing in Civil Engineering, 13*(2), 88-95. https://doi.org/10.1061/(ASCE)0887-

3801(1999)13:2(88)

Masad, E., Muhunthan, B., Shashidhar, N., and Harman, T. (1999 Quantifying Laboratory Compaction Effects on the Internal Structure of Asphalt Concrete. *Transportation Research Record, 1681*(1), 179-185. https://doi.org/10.3141/1681-21

Meehan, C. L., Cacciola, D. V., Tehrani, F. S., and Baker, W. J. Assessing soil compaction using continuous compaction control and location-specific in situ tests. *Automation in Construction, 73*, 31-44. https://doi.org/https://doi.org/10.1016/j.autcon.2016.08.017

Moayedi, H., Mosallanezhad, M., A Rashid, A. S., Wan Jusoh, W., and Mu'azu, M. (2020). A systematic review and meta-analysis of artificial neural network application in geotechnical engineering: theory and applications. *Neural Computing and Applications, 32*. https://doi.org/10.1007/s00521-019-04109-9

Moayedi, H., Mosallanezhad, M., Rashid, A. S. A., Jusoh, W. A. W., and Muazu, M. A. (2019). A systematic review and meta-analysis of artificial neural network application in geotechnical engineering: theory and applications. *Neural Computing and Applications, 32*, 495 - 518. https://doi.org/10.1007/s00521-019-04109-9

Mokwa, R., and Cuelho, E. (2008). *Laboratory Testing of Soil Using the Superpave Gyratory Compactor,* Transportation Research Board 87th Annual Meeting,

Moussa, G., and Owais, M. (2020). Pre-trained deep learning for hot-mix asphalt dynamic modulus prediction with laboratory effort reduction. *Construction and Building Materials, 265*. https://doi.org/10.1016/j.conbuildmat.2020.120239

Movilla-Quesada, D., Raposeiras, A. C., Silva-Klein, L. T., Lastra-González, P., and Castro-Fresno, D. Use of plastic scrap in asphalt mixtures added by dry method as a partial substitute for bitumen. *Waste Management, 87*, 751-760. https://doi.org/https://doi.org/10.1016/j.wasman.2019.03.018

Mushtaq, F., Huang, Z., Shah, S. A., Zhang, Y., Gao, Y., Azab, M., Hussain, S., and Anwar, M. K. (2022). Performance Optimization Approach of Polymer Modified Asphalt Mixtures with PET and PE Wastes: A Safety Study for Utilizing Eco-Friendly Circular Economy-Based SDGs Concepts. *Polymers, 14*(12). https://doi.org/10.3390/polym14122493

Nabipour, N., Karballaeezadeh, N., Dineva, A., Mosavi, A., Mohammadzadeh S., D., and Shamshirband, S. (2019). Comparative Analysis of Machine Learning Models for Prediction of Remaining Service Life of Flexible Pavement. *Mathematics, 7*(1198). https://doi.org/doi:10.3390/math7121198

Nieves, A. (2014). Intelligent Compaction: Summary of Intelligent Compaction for HMA/WMA

Paving. https://www.fhwa.dot.gov/construction/ictssc/pubs/hif13053.pdf

Nohse, Y., Uchiyama, K., Kanamori, Y., Kase, J., Kawai, Y., Masumura, K., and Tateyama, K. (1999). *An attempt applying a new control system for the vibratory compaction using GPS and CMV in the embankment construction* 13th Int. Conf. of the ISTVS, International Society of Terrain-Vehicle Systems, Hanover, NH.

Nunn, M. E. (1978). Deformation testing of dense coated macadam: effect of method of specimen compaction. *Transport Research Laboratory, 21p*. https://doi.org/https://trid.trb.org/view/87015

Oliviero Rossi, C., Caputo, P., Baldino, N., Lupi, F. R., Miriello, D., and Angelico, R. Effects of adhesion promoters on the contact angle of bitumen-aggregate interface. *International Journal of Adhesion and Adhesives, 70*, 297-303. https://doi.org/https://doi.org/10.1016/j.ijadhadh.2016.07.013

Partl, M. N., Flisch, A., and Jönsson, M. (2003) Gyratory Compaction Analysis with Computer Tomography. *Road Materials and Pavement Design, 4*(4), 401-422. https://doi.org/10.1080/14680629.2003.9689956

Partl, M. N., Flisch, A., and Jönsson, M. (2007) Comparison of Laboratory Compaction Methods using X-ray Computer Tomography. *Road Materials and Pavement Design, 8*(2), 139-164. https://doi.org/10.1080/14680629.2007.9690071

Peterson Robert, L., Mahboub Kamyar, C., Anderson, R. M., Masad, E., and Tashman, L. (2004). Comparing Superpave Gyratory Compactor Data to Field Cores. *Journal of Materials in Civil Engineering, 16*(1), 78-83. https://doi.org/10.1061/(ASCE)0899-1561(2004)16:1(78)

Polaczyk, P., Han, B., Huang, B., Jia, X., and Shu, X. (2018) Evaluation of the hot mix asphalt compactability utilizing the impact compaction method. *Construction and Building Materials, 187*, 131-137. https://doi.org/https://doi.org/10.1016/j.conbuildmat.2018.07.117

Robert N. Linden, Joe P. Manoney, and Jackson, N. C. (1999). Effect of Compaction on Asphalt Concrete Performance *Transportation Research Record, 1217*, 20-28.

Roberts Freddy, L., Mohammad Louay, N., and Wang, L. B. (2002). History of Hot Mix Asphalt Mixture Design in the United States. *Journal of Materials in Civil Engineering, 14*(4), 279-293. https://doi.org/10.1061/(ASCE)0899-1561(2002)14:4(279)

Sawan, A. (2018). *Finite Elements Performance Analysis of Asphalt Pavement Mixtures Modified Using Nano Additives*

Schmidhuber, J. (2014). Deep Learning in Neural Networks: An Overview. *Neural Networks, 61*. https://doi.org/10.1016/j.neunet.2014.09.003

Schuirmann, D. J. (1987). A comparison of the two one-sided tests procedure and the power approach for assessing the equivalence of average bioavailability. *Journal of Pharmacokinetics and Biopharmaceutics, 15*(6), 657-680. https://doi.org/https://doi.org/10.1007/bf01068419

Seitllari, A., Kumbargeri, Y., Biligiri, K., and Boz, I. (2019 A soft computing approach to predict and evaluate asphalt mixture aging characteristics using asphaltene as a performance indicator. *Materials and Structures, 52*. https://doi.org/10.1617/s11527-019-1402-5

Song, W., Xu, F., Wu, H., and Xu, Z. (2021 Investigating the skeleton behaviors of open-graded friction course using discrete element method. *Powder Technology, 385*, 528-536. https://doi.org/https://doi.org/10.1016/j.powtec.2021.03.012

Souza, V. M. A., Giusti, R., and Batista, A. J. L. (2018) Asfault: A low-cost system to evaluate pavement conditions in real-time using smartphones and machine learning. *Pervasive and Mobile Computing, 51*, 121-137. https://doi.org/https://doi.org/10.1016/j.pmcj.2018.10.008

Stakston, A. D., Bahia, H. U., and Bushek, J. J. (2002 Effect of Fine Aggregate Angularity on Compaction and Shearing Resistance of Asphalt Mixtures. *Transportation Research Record, 1789*(1), 14-24. https://doi.org/10.3141/1789-02

Tashman, L., Masad, E., D'Angelo, J., Bukowski, J., and Harman, T. (2002). X-ray Tomography to Characterize Air Void Distribution in Superpave Gyratory Compacted Specimens. *International Journal of Pavement Engineering, 3*(1), 19-28. https://doi.org/10.1080/10298430290029902a

Tashman, L., Masad, E., Peterson, B., and Saleh, H. (2001 Internal structure analysis of asphalt mixes to improve the simulation of Superpave gyratory compaction to field conditions. *Proceedings of the Association of Asphalt Paving Technologists, 70*, 605-645.

Taunk, K., De, S., Verma, S., and Swetapadma, A. A Brief Review of Nearest Neighbor Algorithm for Learning and Classification. 2019 International Conference on Intelligent Computing and Control Systems, https://doi.org/10.1109/ICCS45141.2019.9065747

Thurner, H., and Sandström. (1980). *A new device for instant compaction control,* International Conference on Compaction, 1980, Vol.2 .

U.S. Department of Transportation, and Federal Highway Administration. (2013). Intelligent Compaction. *TechBrief, FHWA-HIF-13-051*.

https://www.fhwa.dot.gov/construction/pubs/hif13051.pdf

Vavrik, W. R., Pine, W. J., and Carpenter, S. H. (2002). Aggregate Blending for Asphalt Mix Design: Bailey Method. *Transportation Research Record, 1789*(1), 146-153. https://doi.org/10.3141/1789-16

Wang, X., Shen, S., and Huang, H. (2021) Meso-Scale Kinematic Responses of Asphalt Mixture in Both Field and Laboratory Compaction. *Transportation Research Record: Journal of the Transportation Research Board, 2675*, 036119812110092. https://doi.org/10.1177/03611981211009222

Wang, X., Shen, S., Huang, H., and Almeida, L. (2018) Characterization of particle movement in Superpave gyratory compactor at mesoscale using SmartRock sensors. *Construction and Building Materials, 175*, 206-214. https://doi.org/10.1016/j.conbuildmat.2018.04.146 https://doi.org/https://doi.org/10.1016/j.conbuildmat.2018.04.146

Wang, X., Shen, S., Huang, H., and Yu, S. (2023) Understanding the role of particle rotation in asphalt mixture compaction by tracking coarse aggregate movement. *Construction and Building Materials, 395*, 132325. https://doi.org/https://doi.org/10.1016/j.conbuildmat.2023.132325

Wang, X., Shen, S., Huang, H., and Zhang, Z. (2019) Towards smart compaction: Particle movement characteristics from laboratory to the field. *Construction and Building Materials, 218*, 323-332. https://doi.org/https://doi.org/10.1016/j.conbuildmat.2019.05.122

White, D. J., Thompson, M. J., Vennapusa, P., and Siekmeier, J. (2008). Implementing Intelligent Compaction Specification on Minnesota TH-64: Synopsis of Measurement Values, Data Management, and Geostatistical Analysis. *Transportation Research Record, 2045*(1), 1-9. https://doi.org/10.3141/2045-01

Xinjun, L. I., and Gibson, N. (2011) Mechanistic characterization of aggregate packing to assess gyration levels during HMA mix design. *Asphalt Paving Technology, AAPT, 80*, 33-64.

Xu, F., Zhao, Y., and Li, K. (2021). Using Waste Plastics as Asphalt Modifier: A Review. *Materials (Basel), 15*(1). https://doi.org/10.3390/ma15010110

Xu, G., and Chang, G. K. (2019). Continuous Compaction Control–Mathematical Models and Parameter Identification. International Conference on Inforatmion technology in Geo-Engineering, https://doi.org/10.1007/978-3-030-32029-4_49

Xu, G., Chang, G. K., and Correia, A. G. (2018). Intelligent Compaction Measurement Values Classification. Supplement to the Proceedings of the International Society for Intelligent

Construction 2022 Conference (ISIC 2022),

Xu, G., Chang, G. K., Wang, D., Correia, A. G., and Nazarian, S. (2022) The pioneer of intelligent construction—An overview of the development of intelligent compaction. *Journal of Road Engineering, 2*(4), 348-356. https://doi.org/https://doi.org/10.1016/j.jreng.2022.12.001

Xu, M., Fralick, D., Zheng, J. Z., Wang, B., Tu, X. M., and Feng, C. (2017). The Differences and Similarities Between Two-Sample T-Test and Paired T-Test. *Shanghai Arch Psychiatry, 29*(3), 184-188. https://doi.org/10.11919/j.issn.1002-0829.217070

Xu, Q., and Chang, G. K. (2013 Evaluation of intelligent compaction for asphalt materials. *Automation in Construction, 30*, 104-112. https://doi.org/https://doi.org/10.1016/j.autcon.2012.11.015

Yang, X., Guan, J., Ding, L., You, Z., Lee, V. C. S., Mohd Hasan, M. R., and Cheng, X. (2021) Research and applications of artificial neural network in pavement engineering: A state-of-the-art review. *Journal of Traffic and Transportation Engineering (English Edition), 8*(6), 1000-1021. https://doi.org/https://doi.org/10.1016/j.jtte.2021.03.005

Yao, H., Xu, M., Liu, J., Liu, Y., Ji, J., and You, Z. (2022 Literature Review on the Discrete Element Method in Asphalt Mixtures *Frontiers in Materials, 9*. https://doi.org/10.3389/fmats.2022.879245

You, Z., and Buttlar, W. (2005). Application of Discrete Element Modeling Techniques to Predict the Complex Modulus of Asphal" Aggregate Hollow Cylinders Subjected to Internal Pressure. *Transportation Research Record, 1929*, 218 - 226.

You, Z., and Liu, Y. (2010). Three-Dimensional Discrete Element Simulation of Asphalt Concrete Subjected to Haversine Loading. *Road Materials and Pavement Design, 11*(2), 273-290. https://doi.org/10.1080/14680629.2010.9690276

You, Z., Liu, Y., and Dai, Q. (2011) Three-Dimensional Microstructural-Based Discrete Element Viscoelastic Modeling of Creep Compliance Tests for Asphalt Mixtures. *Journal of Materials in Civil Engineering, 23*(1), 79-87. https://doi.org/10.1061/(ASCE)MT.1943-5533.0000038

Yu, H., and Shen, S. (2012) Impact of aggregate packing on dynamic modulus of hot mix asphalt mixtures using three-dimensional discrete element method. *Construction and Building Materials, 26*(1), 302-309. https://doi.org/https://doi.org/10.1016/j.conbuildmat.2011.06.025

Yu, H., and Shen, S. (2013) A micromechanical based three-dimensional DEM approach to

characterize the complex modulus of asphalt mixtures. *Construction and Building Materials, 38*, 1089-1096. https://doi.org/https://doi.org/10.1016/j.conbuildmat.2012.09.036

Yu, Q. M., Liu, J. K., and Tian, Y. H. (2014). Analysis of Application Situation of Continuous Compaction Control (CCC). *Applied Mechanics and Materials, 501-504*, 983-992. https://doi.org/10.4028/www.scientific.net/AMM.501-504.983

Yu, S., and Shen, S. (2023). Compaction Prediction for Asphalt Mixtures Using Wireless Sensor and Machine Learning Algorithms. *IEEE Transactions on Intelligent Transportation Systems, 24*(1), 778-786. https://doi.org/10.1109/TITS.2022.3218692

Yu, S., Shen, S., and Lu, M. (2023) Data sensing and compaction condition modeling for asphalt pavements. *Automation in Construction, 154*, 105021. https://doi.org/https://doi.org/10.1016/j.autcon.2023.105021

Zhang, C., Shen, S., Huang, H., and Wang, L. (2021) Estimation of the Vehicle Speed Using Cross-Correlation Algorithms and MEMS Wireless Sensors. *Sensors (Basel, Switzerland), 21*. https://doi.org/10.3390/s21051721

Zhang, D., Cheng, Z., Geng, D., Xie, S., and Wang, T. (2022). Experimental and Numerical Analysis on Mesoscale Mechanical Behavior of Coarse Aggregates in the Asphalt Mixture during Gyratory Compaction. *Processes, 10*(1), 47. https://www.mdpi.com/2227-9717/10/1/47

Zhang, W., Raza Khan, A., Yoon, S., Lee, J., Zhang, R., and Zeng, K. (2021) Investigation of the correlations between the field pavement in-place density and the intelligent compaction measure value (ICMV) of asphalt layers. *Construction and Building Materials, 292*, 123439. https://doi.org/https://doi.org/10.1016/j.conbuildmat.2021.123439

Zhao, Y., Xie, S., Gao, Y., Zhang, Y., and Zhang, K. (2021) Prediction of the number of roller passes and degree of compaction of asphalt layer based on compaction energy. *Construction and Building Materials, 277*, 122274. https://doi.org/https://doi.org/10.1016/j.conbuildmat.2021.122274

Zhou, X., Chen, S., Ge, D., Jin, D., and You, Z. (2020) Investigation of asphalt mixture internal structure consistency in accelerated discrete element models. *Construction and Building Materials, 244*, 118272. https://doi.org/https://doi.org/10.1016/j.conbuildmat.2020.118272

Zhu, H., and Nodes, J. E. (2000) Contact based analysis of asphalt pavement with the effect of aggregate angularity. *Mechanics of Materials, 32*(3), 193-202.

https://doi.org/https://doi.org/10.1016/S0167-6636(99)00054-X

Zhu, X., Qian, G., Yu, H., Yao, D., Shi, C., and Zhang, C. (2022) Evaluation of coarse aggregate movement and contact unbalanced force during asphalt mixture compaction process based on discrete element method. *Construction and Building Materials, 328*, 127004. https://doi.org/https://doi.org/10.1016/j.conbuildmat.2022.127004

Ziari, H., Sobhani, J., Ayoubinejad, J., and Hartmann, T. (2015) Prediction of IRI in short and long terms for flexible pavements: ANN and GMDH methods. *International Journal of Pavement Engineering, 17*, 1-13. https://doi.org/10.1080/10298436.2015.1019498

VITA

Shuai Yu

EDUCATION

Doctor of Philosophy (Ph.D.) in Civil Engineering	Pennsylvania State University
Master of Science (M.Sc.) in Transportation Engineering	Tongji University
Bachelor of Science (B.Sc.) in Transportation Engineering	Harbin Institute of Technology

PROFESSIONAL EXPERIENCES

2018-2019, Civil Engineer	Tianjin Municipal Engineering Design and Research Institute
2022-2023, Teaching Assistant	Pennsylvania State University

SELECTED PUBLICATIONS

ASTM D8541-23 Standard Test Method for Determination of Relative Rotation to Evaluate the Workability of Asphalt Mixture Using Wireless Particle-Size Sensors.

Yu, S., Shen, S, Lu, M (2023), Data Sensing and Compaction Condition Modeling for Asphalt Pavements, *Automation in Construction.*

Yu, S., Shen, S. (2023). Compaction Prediction for Asphalt Mixtures Using Wireless Sensor and Machine Learning Algorithm. *IEEE Transactions on Intelligent Transportation Systems*.

Zhang, C., Shen S., Yu, S., (2023), In-Situ Dynamic Modulus Prediction for Asphalt Pavement Combining Machine Learning Algorithm and Sensing Technology, *IEEE Transactions on Intelligent Transportation Systems*.

Wang, X., Shen S., Huang H, Yu, S., (2023), Understanding the Role of Particle Rotation in Asphalt Mixture Compaction by Tracking Coarse Aggregate Movement, *Construction and Building Materials.*

Yu, S., Shen, S., et al. (2022). Effect of warm mix asphalt additive on the workability of asphalt mixture: From particle perspective. *Construction and Building Materials.*

Yu, S., Li, P., Zhang, Z., et al. (2021). Virgin Binder Determination for High RAP Content Mixture Design. *Journal of Materials in Civil Engineering.*

Yu, S., Shen, S., et al. (2021) Engineered Semi-Flexible Composite Mixture Design and Its Implementation Method at Railroad Bridge Approach. *Transportation Research Record,*

Yu, S., Shen, S., et al. (2018). Effect of Partial Blending on High Content Reclaimed Asphalt Pavement (RAP) Mix Design and Mixture Properties. *Transportation Research Record.*

Yu, S., Shen, S., et al. (2017). Evaluation of the Blending Effectiveness of Reclaimed Asphalt Pavement Binder. *Journal of Materials in Civil Engineering.*

AWARDS

- Leo Russell Graduate Fellowship 2022
- 1st prize in Poster Competition in AJE35 Standing Committee 2023
- Outstanding Graduate Student Award at IACIP 2023
- 3rd prize in the Poster Competition at IACIP Meeting 2022 & 2023